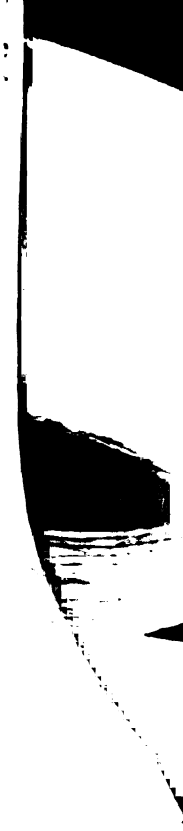

LYAPUNOV STABILITY BASED NETWORK CONDITIONS FOR CHARACTERIZING RETENTION AND LOSS OF POWER SYSTEM TRANSIENT STABILITY

By

Gholamhossein Sigari

A DISSERTATION

Submitted to
Michigan State University
in partial fulfillment of the requirements
for the degree of

DOCTOR OF PHILOSOPHY

Department of Electrical Engineering
and Systems Science

1985

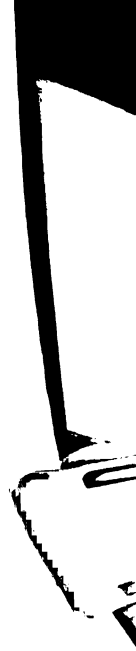

ABSTRACT

LYAPUNOV STABILITY BASED NETWORK CONDITIONS
FOR CHARACTERIZING RETENTION AND
LOSS OF POWER SYSTEM TRANSIENT STABILITY

By

Gholamhossein Sigari

A topological energy function has been derived from the first principles that retain the network without aggregation back to generator internal buses and includes a general description of real and reactive power load models as a function of voltage. For the special case of a constant real power, constant current reactive load model and the one axis generator model a topological Lyapunov energy function has been derived.

Based on the Popov stability criterion a characterization of the region of stability and a definition of loss of transient stability have been presented. Then three different theorems stating necessary and sufficient conditions for the loss of transient stability have been established. The conditions stated in these theorems describe an estimate of the region of instability. Although a precise boundary between the region of stability and the region of instability is not established a relationship between the regions of stability and instability has been established.

Th
th
occ
eas
whi
int
nec
sta
tha
par
a g

sta
cond
are
mach
outs

New
the
stab
the
the
were

The necessary condition for instability provides a condition that if satisfied, will ensure that a loss of stability will occur. Thus the necessary and sufficient conditions provide easily tested conditions on the entire states of the system which can be clearly identified with the loss of synchronism inherent in the loss of transient stability. These necessary and sufficient conditions for loss of transient stability permit the proper definition of stability margin that measures the relative security of the system for a particular fault cleared at a particular clearing time with a given fault clearing action.

Stability criteria are proposed based on the Popov stability criterion and these necessary and sufficient conditions for loss of stability. These stability criteria are then related to the PEBS method developed for the single machine energy function and the PEBS method based on the cutset energy function.

The above theoretical results were tested on the 39 bus New England system. These tests confirmed the properties of the energy function and Lyapunov energy functions. The stability criteria tested clearly and accurately determined the critical cutset and critical clearing time and verified the accuracy and validity on the stability criteria that were developed based on the theory developed.

To Mojtaba and Horiyeh

advis

cours

only

never

S

of Drs

Shanbl

is als

D

are th

two ye

S

Words

Mo

encoura

Graduat

ACKNOWLEDGEMENTS

I would like to express my appreciation to my thesis advisor, Dr. R.A. Schlueter, for his guidance throughout the course of my doctoral program. Dr. Schlueter served not only as advisor but also a friend and his friendship will never be forgotten.

Special acknowledgement is made for the contributions of Drs. G. Park and H. Khalil. The participation of Drs. M. Shanblatt and D. Yen and N. Guven on my guidance committee is also appreciated and acknowledged.

Dr. Schlueter and the Division of Engineering research are thanked for providing financial support over the final two years of my doctoral program.

Special thanks to "Sam" Miller with the Wizards of Words for her word processing talents.

Most of all, I would like to thank my father, for his encouragement and financial support during the course of my graduate studies.

TABLE OF CONTENTS

LIST OF FIGURES

Fi

Fi

Fig

Fig

Fig

Fig.

Fig.

Fig.

Fig.

Fig

Fig

Fig

Fig.

Fig.

Fig.

Fig.

Fig.

CHAPTER 1

INTRODUCTION

The present method of determining retention or loss of stability due to transients caused by electrical faults or loss of generation contingencies is time-step integration of the differential equations. The transient stability programs that perform the time step integration can take as long as 15 CPU minutes on the largest and fastest computers to determine retention or loss of stability for a single fault, cleared at a specific time with a specific line switching action, on a specific system* with a particular network configuration; load level, type and distribution; unit commitment, generation dispatch, and base case load flow. To determine the transfer capabilities from the Northwest (Oregon, Washington) and the East (Utah, Nevada, Arizona) to southern California for each season (summer, winter, spring, fall) requires solutions of hundreds of fault cases that keep a VAX 785 running continuously for three months. Although not all utilities must be as concerned with limiting power transfers to maintain

*The computation time depends on the model and the complexity and size of the system. The CPU time reported above is obtained from results on the WSCC system.

transient stability over a wide range of operating conditions and fault cases; all utilities perform transient stability simulations and set transfer limits on generating units and across interfaces that are based on transient stability simulations for the operating conditions expected over each season or year.

Transient stability simulations are performed daily on the Ontario Hydro System in order to adjust the seasonal transfers based on changes in network configuration, unit commitment, load level and distribution, voltage profile, and load flow conditions expected over the next day.

Operators at the control center desire the ability to perform transient stability simulations to assess the stability margin of the system for a current operating condition that was not anticipated by operation planners in their seasonal or daily assessments. The capability of performing transient stability simulations on line is completely impractical at present based on the very large computation time required even for the fastest computers using the simplest of power system models. Thus, the operator cannot adjust transfer limits on-line based on transient stability simulations for faults given the operation condition presently experienced or anticipated to occur over the next few hours.

Adaptive protection schemes that would only trip generators when a loss of transient stability would be imminent for a particular operating condition, given occurrences

of a particular fault, would be feasible if transient stability simulation could be performed with computational requirements equal to load flow (steady state solution of the network equations). The tripping of large radially connected generators can cost a utility $20,000 an hour in increased fuel costs. The generator tripping may require the generator boiler to be shut down and restarted, which can take up to a week in some cases. A utility could save fuel costs by not tripping a particular generator for every possible contingency but only for those that would cause a possible loss of transient stability.

The time step integration of the transient stability model, includes

1) 2N nonlinear algebraic equations that represent the N bus transmission network;

2) the kM differential equations that describe the synchronous generator, exciter, power system stabilizer, and turbine energy system for the M generating units in the model. The order of the model k can be as low as 2 for a classical machine model and as high ten for a more sophisticated model that requires tremendous CPU, I/O and memory.

A fast transient stability method has long been desired that could determine retention or loss of stability with the computation requirements of a load flow. Two developments are necessary to make such a development a reality:

1) the determination of a Lyapunov function and a characterization of the region of stability for the particular system and fault case;

2) a method for predicting whether the system fault trajectory will remain within the region of stability and remain stable or else enter the region of instability and thus lose stability.

Significant research effort has been expended on developing the energy function and characterizing the region of stability. Up to now, these efforts have been only marginally successful at best. The research reported in this thesis is directed at developing Lyapunov functions or energy functions for much more detailed transient stability models than have been previously developed. A characterization of the region of stability and region of instability is then established that greatly extends previous results. This characterization of the region of stability is then used to justify a stability criterion that is related to the potential energy boundary surface (PEBS) methods developed for the single machine energy function.

It should be noted that no effort will be made to develop a method for predicting whether a fault trajectory will remain within the region of stability or enter the region of instability given a particular fault, fault clearing time and clearing action, and a particular system and its operating condition. Such a method was developed in a previous thesis for the classical power system model and could be extended to the more complex models. [21]

The ultimate development of a fast transient stability assessment method can

1) greatly reduce the computational requirements for determining transfer limits in seasonal transmission performance assessments;

2) permit daily transfer limit adjustments based on hundreds of transient stability simulations at modest computational requirements and costs. At present, only a few transient

stability simulations can be performed to adjust transfer limits based on the expected operating condition over the next day;

3) permit on-line transient stability simulation and transfer limit adjustment by operators. At present, the capability to simulate faults on-line is impossible;

4) permit adaptive generator tripping, that would only trip a generator when the particular contingency that occurred on a system with a given operating condition would cause loss of transient stability.

Power System Stability Models Considered in This Thesis

A review of the literature on the development of Lyapunov functions and energy functions is given in Chapter 2 along with discussion of the equal area and PEBS methods for determining retention or loss of stability. In Chapter 3, a topological energy function is derived from first principles which retains the network without aggregation back to generator internal buses and which includes a description of real and reactive power load models as a function of voltage. Similar models have been hypothesized [9, 16] but never derived from first principles.

A Lyapunov function is derived for a model that

1) retains the network and does not aggregate the network back to internal buses;

2) models the real power load as constant power and the reactive power load as constant current;

3) models the flux linkage decay in the synchronous machine as well as the electromechanical component of the machine model.

This Lyapunov function is derived using the Popov Criterion of the Moore Anderson [10] and the construction method of Willems [3].

In Chapter 5, a discussion of the region of stability based on the Popov stability criterion and the definition of the loss of transient stability is presented. Three different theorems stating necessary and sufficient conditions for loss of transient stability are established. A stability criteria; based on the region of stability and the region of instability is proposed for determining the critical cutset and critical clearing time. A second stability criterion is proposed that based on a performance measure determines the critical clearing time.

The stability criteria developed in Chapter 5 are reviewed and then applied to four fault cases. The results indicate that both stability criteria can determine the critical clearing time with no detectable error. These results confirm the theory developed in Chapter 5, upon which they were proposed. Chapter 7 reviews the research performed in the thesis and its contribution. A discussion of extensions of the research is also given.

CHAPTER 2

REVIEW OF LYAPUNOV STABILITY THEORY APPLIED TO POWER SYSTEMS

The objectives of this chapter are

1) to introduce and review the simplified single machine infinite bus power system transient stability model;

2) to discuss the equal area and potential energy boundary surface methods for determining retention or loss of stability for this single machine infinite bus model. This discussion provides understanding and motivation for the analysis that derives the region of stability and the region of instability for multimachine transient stability models in Chapter 5;

3) to review Lyapunov stability theory;

4) to review the literature in [3, 9, 17] and developing Lyapunov based and integral based energy functions for various power system transient stability models;

5) to present the form of the energy functions derived for different power system transient stability models.

2.1 Equal Area Criterion for the Single Machine Infinite Bus Model

The simple single machine infinite bus power system transient stability model is introduced to indicate the general form of the multimachine transient stability model which will be presented and discussed later. The equal area criterion is presented in order to indicate the energy

transfers during a fault and during the post fault period after the fault is cleared. The fault is cleared by an appropriate line switching action that isolates the faulted branch.

The single machine infinite bus transient stability model has the form:

$$M\ddot{\delta} = P_m - C \sin\delta \qquad (W) \qquad (2.1)$$

where

M: generator inertia constant,(J.s)

δ: generator angle, (Radians)

P_m: mechanical input, (W)

C: $\frac{E\ V\infty}{x}$ where E is generator's internal voltage, $V\infty$ is infinite bus voltage and x is the equivalent transmission line reactance connecting the generator internal bus and the infinite bus.

The prefault model and the prefault stable equilibrium point δ^{s1} are defined by

$$M\ddot{\delta} = o = P_m - C_o \sin\delta^{s1} \qquad (2.2)$$

where P_m, the prefault power angle curve $C_o \sin\delta$, and δ^{s1} are shown in Figure 1.a.

The faulted system model is defined as:

$$M\ddot{\delta} = P_m - C_1 \sin\delta \qquad (2.3)$$

where the faulted power angle curve $C_1 \sin\delta_1$ is shown in Figure 1.a. The post fault system is defined as:

$$M\ddot{\delta} = P_m - C_2 \sin\delta \qquad (2.4)$$

where the post fault power angle $C_2 \sin\delta_1$ is shown in Figure 1.a. The post fault stable equilibrium point δ^{s2} is defined as:

Fig. (1.a) Power-angle curves showing the critical clearing angles δ_c and areas A_1 and A_3.

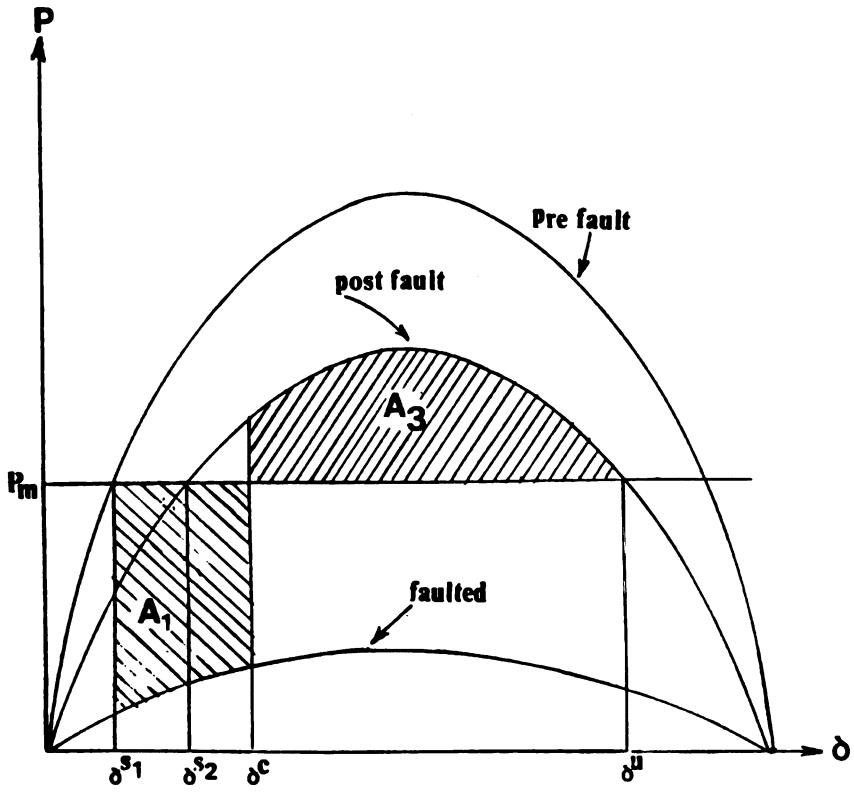

$$P_m - C_2 \sin \delta^{s2} = 0 \qquad (2.5)$$

and the unstable equilibrium point δ^u is defined as:

$$P_m - C_2 \sin \delta^u = 0 \qquad (2.6)$$

The system is assumed to remain at the prefault stable equilibrium point δ^{s1} until the fault occurs at t=0. At $t=0^+$ and until the fault is cleared at $t-t_c$, the mechanical power P_m is larger than the electrical power $C_1 \sin\delta(t)$ causing the machine to accelerate. The energy

$$V_{pe}(t) = P_m (\delta(t)-\delta^{s1}) + C_1 (\cos\delta(t)-\cos\delta^{s1}) \qquad (2.7)$$

increases until the fault is cleared at $t=t_c$. The acceleration energy, which is the kinetic energy increase on the inertia of machine, is:

$$A_1(t_c) = V_{pe}(t_c) = P_m(\delta^c-\delta^{s1}) + C_1 (\cos\delta^c-\cos\delta^{s1}) \qquad (2.8)$$

where $\delta^c=\delta_i(t_c)$. At t_c, the fault is cleared and kinetic energy $A_1(t_c)$ must be absorbed by the post fault network for the accelerated generator to reverse direction and return to the stable equilibrium point δ^{s2}. The acceleration energy absorbed by the post fault network at time t is:

$$A_3(t,t_c) = V_{pe}(t, t_c) = P_m(\delta(t)-\delta^c) + C_2(\cos\delta(t)-\cos\delta^c) \qquad (2.9)$$

This value of $A_3(t,t_c)$ is negative and its absolute value reaches a maximum at $t=t_B(t_c)$ when the system is stable where:

$$A_1(t_c) + A_3 (t_B(t_c),t_c) = 0 \qquad (2.10)$$

At $t=t_B(t_c)$, the angle $\delta(t_B(t_c))$ reaches its maximum excursion as shown in Figure 1.a and the accelerating kinetic

Fig. (1.b) Equal area criterion net acceleration energy E(t) versus time.

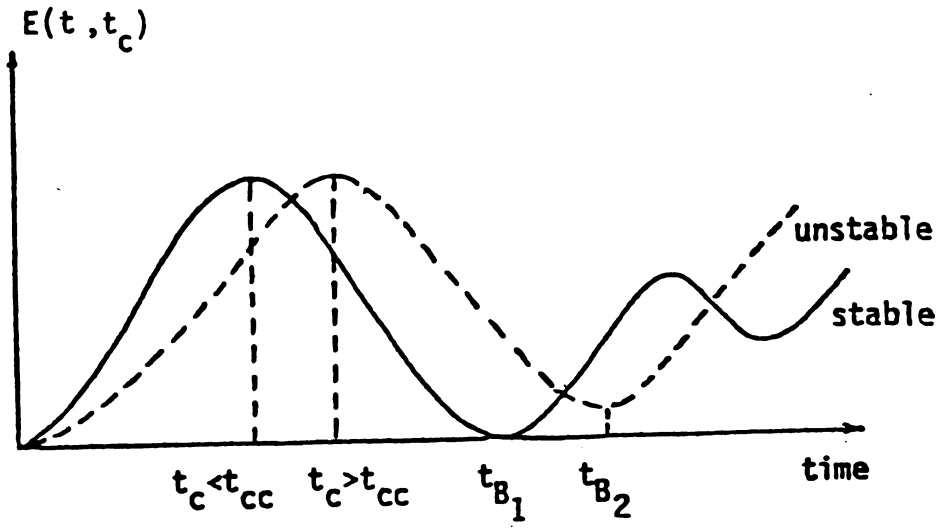

energy is totally absorbed by the network and the area $A_1(t_c)$ and $A_3(t_B(t_c))$ in Figure 1.a are equal reflecting the condition given by (2.10). If the fault is cleared at the critical clearing time t_{cc} condition (2.10) still holds but $\delta(t_B(t_c))=\delta^u$. If $t_c>t_{cc}$, the area $A_3(t,t_c)$ is less than $A_1(t_c)$ for all $t>t_c$ and thus the velocity of the machine angle $\dot{\delta}(t)$ never reaches zero and $\delta(t)$ passes the unstable equilibrium point δ^u. For $\delta(t)>\delta^u$, $A_3(t,t_c)$ increases and $A_1(t_c) + A_3(t,t_c)$ increases.

The net acceleration energy, defined as:

$$E(t,t_c) = \begin{cases} A_1(t) & 0\leq t<t_c \\ A_1(t_c) + A_3(t,t_c) & t>t_c \end{cases} \qquad (2.11)$$

increases during the fault $0\leq t\leq t_c$ and decreases immediately after t_c when the fault is cleared. If the system is stable, the net acceleration energy satisfies

$$E(t_B(t_c),t_c) = 0 \qquad (2.12)$$

when the angle $\delta(t)$ reaches its peak excursion $\delta(t_B(t_c))$ where both $t_B(t_c)$ and $\delta(t_B(t_c))$ depend on t_c. If $t_c>t_{cc}$, $E(t,t_c)$ never reaches zero for $t>t_c$, as shown in Figure 1.b. Thus if $E(t,t_c)$ determines the minimum as a function of t and defines the value as:

$$E^*(t_c) = \min_t E(t,t_c) \qquad (2.13)$$

then $E^*(t_c)$ should equal zero for all $t_c<t_{cc}$ and should be an increasing function of t_c for $t_c>t_{cc}$.

2.2 Potential Energy Boundary Surface, (PEBS) Method

The potential energy boundary surface method is now introduced for single machine infinite bus system model. The PEBS method assumes that there is a maximum potential energy absorption capability of the post fault network. This maximum potential energy absorption capability is never approaches for $t_c<t_{cc}$ but is utilized in an attempt to decelerate the accelerated machines for $t_c>t_{cc}$. Figure 2.a shows the change of generator's angle for different clearing times. The system remains at δ^{sl} until t=0 and reaches a maximum angle $\delta(t_B(t_c))$ at $t_B=t_B(t_c)$ for a clearing time t_c. A measure of the energy absorbed by the post fault network is

$$V^*(t_c) = P_m(\delta(tB)-\delta^{sl}) + C_2[Cos\delta(t_B)-Cos\delta^{sl})] \qquad (2.14)$$

as shown by the area in Figure 2.b. The value of $V^*(t_c)$ increases for $t_c<t_{cc}$ and remains constant for $t_c>t_{cc}$ for a single machine infinite bus model. The energy $V^*(t_c)$ actually decreases for $t_c>t_{cc}$ in the multimachine model making the function $V^*(t_c)$ reach a sharp maximum at t_{cc}. In the multimachine system the function $V^*(t_c)$ is evaluated based on the potential energy component of the single machine energy function given in equation (2.24). This potential energy boundary surface method for multimachine power systems will be shown to be related to the integral criterion method developed in Chapter 5 to determine when

Fig. (2.a) Maximum values of generator angles for different clearing times.

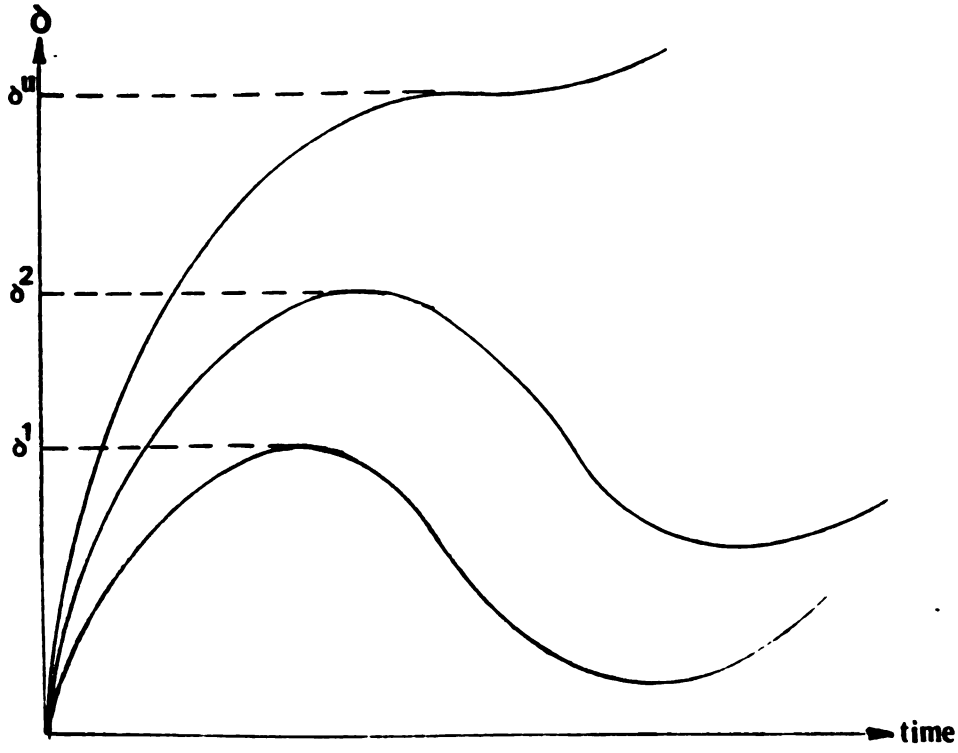

Fig. (2.b) The potential energy stored in the system for different clearing times.

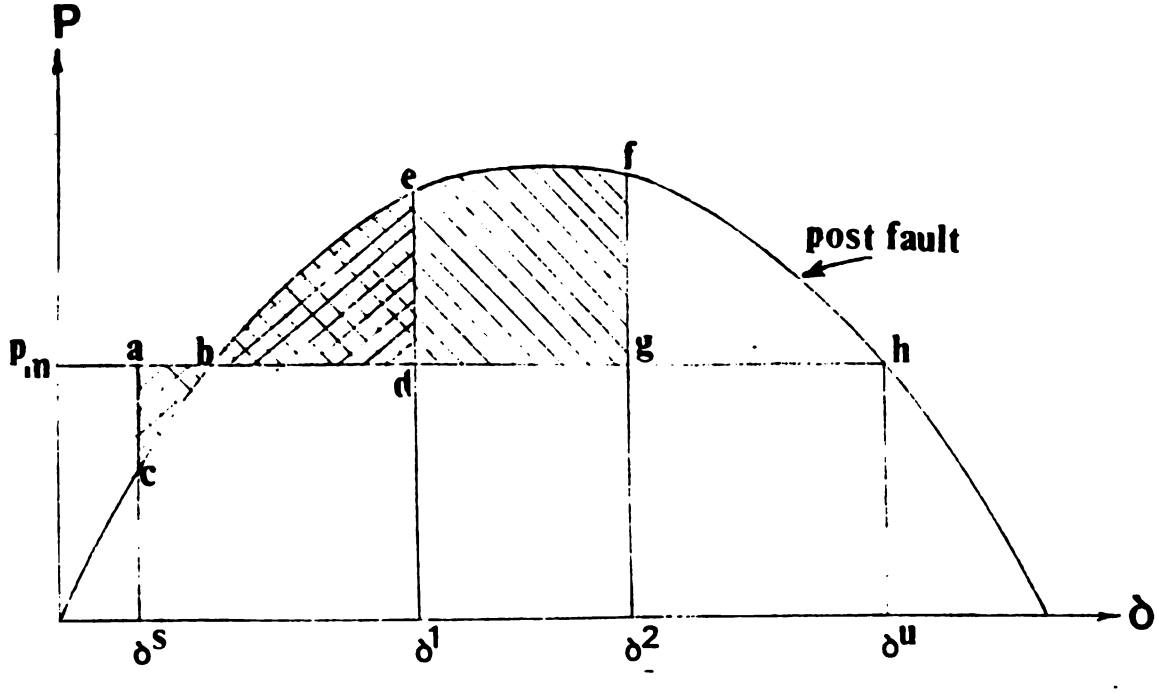

loss of transient stability based on the region of stability defined in that chapter.

2.3 Review of Literature on Energy and Lyapunov Functions

The two methods discussed in Sections 2.1 and 2.2 of this chapter present a physical understanding of how the single machine infinite bus system retains or loses stability. The practical power system model includes hundreds of generators. In order to apply the stability assessment methods developed in sections (2.1) and (2.2) to a multimachine power system, Lyapunov's direct method has been used. The initial research focused on development of energy functions that could be used in this method.

The first energy functions for classical transient stability model were derived by Magnuson and Aylett [1, 2] via the energy integral method. Later on, the systematic construction of Lure type Lyapunov energy functions for power system was proposed by Willems [3]. This Lyapunov function did not contain transfer conductances and it was realized that these terms were not small and could not be neglected since they accounted for the load impedances.

There has been an attempt to prove that the energy function which includes the transfer conductances is a Lyapunov energy function [4], and another attempt to approximate this energy function with a Lyapunov type energy function [5], but none of these efforts have been successful. Moreover, this energy function has several

drawbacks in addition to the fact that it has not been proven to be a Lyapunov function. The first of these drawbacks is that this energy function is not topological, which means that the transmission network has been aggregated back to internal generator buses. Thus all load buses have been eliminated and all the elements in the resulting transmission network do not represent the actual components. The aggregation masks the effects of operating conditions (load level and distribution, unit commitment, generation dispatch, network configuration, and load flow) on stability because aggregation does not leave the network and its operating conditions intact and reflects the actual network operating conditions throughout the aggregated network. It is thus difficult to access the specific operating conditions that directly contribute to loss of stability for a specific fault.

The second drawback is that the load at each bus is assumed to be constant impedance since this assumption must be made to eliminate the load buses. It would be desirable to allow real power and reactive power load models to be selected separately and independently at each load bus. The real and reactive load should be either constant impedance, constant current, constant power or a combination of these or some polynomial function of voltage and frequency.

The third drawback is that in most cases the generator model does not include flux decay effects.

Kakimoto [6], developed a Lure type function for a nontopological transient stability model with flux decay using the generalized Popov criterion developed by Moore and Anderson and a construction method developed by Willems. The energy function presented in [6] is global and has all the drawbacks previously mentioned.

Rastgoufard [17], developed a single machine energy function for the nontopological model of multimachine power systems. This energy function describes the kinetic and potential energies for a single critical generator, but since it is derived for an aggregated model it masks the effects of operating conditions in the transmission network. The region of stability determined based on the single machine energy function is more accurate than can be obtained based on the global energy function since the single machine energy function contains all the information required to predict retention or loss of stability if the critical generator for which the energy function is written can be properly identified [17].

Bergen and Hill [7], developed a topological Lyapunov energy function by assuming that the loads were small generators with small inertias which disappear after the energy function is constructed. The resulting energy function when load bus generator inertias are set to zero is a constant real power load model (with a term that depends on frequency). Voltage at both generator and load buses is assumed to be constant.

Athay [8], constructed a topological energy function by attempting to account for kinetic energy in the generators and the potential and magnetic energies of the transmission grid and loads. Real load power was permitted to be a function of voltage and thus the load bus voltage was allowed to change. The reactive load energy was ignored and thus the resulting energy function was not complete.

Mussavi [9], developed an energy function by hypothesis. He did not attempt to derive kinetic energy, position energy and magnetic energy of the transmission grid, from the first principles and thus the kinetic energy term given is with respect to a synchronous reference and position and magnetic energies are based on an inertial center reference. A very important insight of this paper is the inclusion of the reactive energy of the load which has never before been included. This term is necessary as indicated by the analysis in [9] that shows the resultant energy function is conservative. The drawback in this energy function is that the kinetic energy is based on a different reference than the other energy terms.

Sastry [16], gives a hypothesized topological energy function for a model where flux linkage and saliency effects of generators have been considered. The load modeling in [11] is very practical. There has again been no effort to derive a Lyapunov topological energy function for the recommended modeling.

This thesis extends the energy function of Mussavi by deriving the energy function from first principles rather than hypothesizing that form. The kinetic energy term is thus based on the same inertial center reference as the potential energy terms. The load model at every bus allows real power to depend on voltage which was not true in [7]. Finally the real and reactive loads are derived for the case where both real and reactive loads at each bus can be unique percentage of constant power, constant current, and constant impedance load models. The energy function for the special case where reactive load is constant current and real power load at every bus is constant, is derived as a Lure type Lyapunov function using the Popov criterion of Moore-Anderson [12] and the construction method of Willems [3].

2.4 Lyapunov's Direct Method and Present Energy Functions

Since the function of this chapter is to facilitate the understanding of the development in the following chapters, the Lyapunov's direct method is reviewed:

The equilibrium point $\underline{0}$ of a system with model

$$\dot{\underline{x}} = \underline{f}(\underline{x}) \tag{2.15}$$

is asymptotically stable if there exists a continuously differentiable function $V(\underline{x})$ which is locally positive definite and for some real $s>0$ satisfies:

$$\dot{V}(\underline{x})<0 \tag{2.16}$$

for all

$$||x||<s \tag{2.17}$$

This method could be applied to power systems, but the problem is to identify the equations of system as (2.15) and then be able to construct an energy function with properties (i) and (ii). Based on specific models used, several Lyapunov energy functions have been derived for power systems as indicated in the previous section. There are two kinds of power system stability models for which Lyapunov functions have been derived:

1) an aggregated network model
2) topological model.

2.4.1. Lyapunov Energy Function for the Aggregated Network Model

In the classical power system model, all of the network and load buses are aggregated and only the internal generator buses are retained as shown in Figure 3. The buses and branches in the dotted box in this figure are aggregated based on the assumption of constant impedance load at these buses. A constant voltage behind transient reactance generator model is also assumed in the classical model. Willems [3] derived the Lyapunov energy function for the classical model. Kakimoto's Lyapunov energy function [6] is an extension of this work and assumes that the generators are modeled by a single axis generator model. The network is aggregated back to internal generator buses as in the classical model. The power system transient stability model used in [6] is

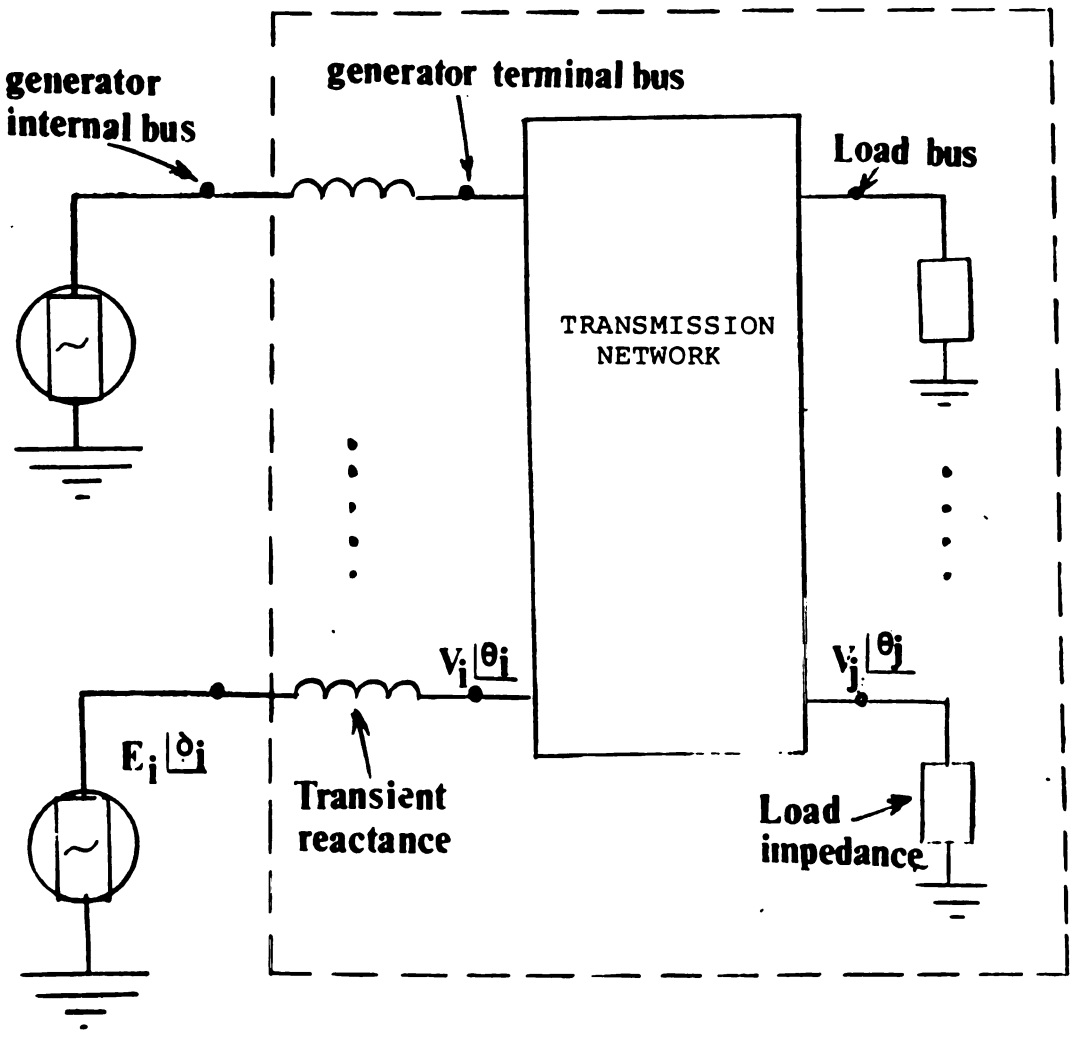

Fig. (3) Power system model for: the classical model all the elements inside the doted box are aggregated.

$$M_i\ddot{\delta}_i + d_i\dot{\delta}_i = P_{mi} - \sum_{j=1}^{N} Y_{ij}E_iE_j \text{ Sin } (\delta_{ij}+\theta_{ij}) \qquad (2.18)$$

and

$$T'_{doi}\frac{dE_i}{dt} = -(E_i-E_i^o)-(x_{di}-x'_{di})\sum_{j=1}^{m} B_{ij}(Ej^o \text{ Cos } \delta^o_{ij} - E_j \text{ Cos } \delta_{ij}) \quad \text{for } i=1,\ldots,N \qquad (2.19)$$

where for each generator i:

P_{mi}: mechanical power input

$Y_{ij}\,\underline{|\phi_{ij}}$: Post fault admittance between the ith and jth internal generator buses of the aggregated network

θ_{ij}: compliment of ϕ_{ij}

$E_i\,\underline{|\delta_i}$: internal voltage

δ_{ij}: $\delta_i-\delta_j$

$E'_{qi}\,\underline{|\delta_i}$: voltage magnitude and angle at the internal generator bus, δ_i is referenced to

For the modeling given by (2.19), Kakimoto derived the following Lyapunov energy function using the Moore-Anderson theorem and the construction method of Willems [3].

$$V = \left(\frac{1}{2\Sigma M_i}\right)\sum_{i=1}^{N}\sum_{j=1}^{N} M_iM_j\,(\omega_i-\omega_j)^2 +$$

$$\sum_{i=1}^{N}\sum_{j=1}^{N} B_{ij}[E_iE_j(\text{Cos}\delta^o_{ij}-\text{Cos}\delta_{ij} - (\delta_{ij}-\delta^o_{ij})E^o_iE^o_j$$

$$\text{Sin } \delta^o_{ij} - (E_i-E^o_i)(E_j-E^o_j) \text{ Cos } \delta^o_{ij}] +$$

$$\sum_{i=1}^{N} (E_i-E^o_i)^2\,(x_{di}-x'_{di}) \qquad (2.20)$$

The superscript "o" denotes the stable equilibrium point of the post fault system.

In order to obtain his Lyapunov function Kakimoto assumed that each internal voltage lags behind the q axis of each generator by a constant angle ϕ, and the transfer conductances in the reduced admittance matrix are negligible. Despite the significant contribution of this research, it has the following deficiences:

a) assumes that the real power load can be modeled as constant impedance in order to aggregate the network and then assumes the load is constant real power which is incorporated in P_{mi}. Aggregating the load back to external buses and assuming it to be a constant power load model, significantly modifies the model and the critical clearing times obtained;

b) aggregates the network and thus loses the ability to determine or understand the fundamental cause of the loss of stability and the operating condition changes that would improve the stability margin for that particular fault;

c) ignores the reactive load and the magnetic energy stored in the loads that can influence the stability of the system as voltage changes occur;

d) neglects the transfer conductances of the equivalent branches in the network.

2.4.2 Individual Machine Energy Function

Another type of energy function derived based on the classical model of power system is the single machine energy function. The single machine energy function has been derived in Michigan State University by Rastgoufard [17] for a synchronous reference frame model and by Fouad [18] using

a center of angle reference transient stability model. The model used for this single energy function is identical to that used by Willems [3] and neglects the flux decay in (2.19). The voltages at generator internal buses are thus constant and the model has the form

$$M_i\dot{\omega}_i = P_i - P_{ei} \tag{2.21}$$

and

$$\dot{\delta}_i = \omega_i \tag{2.22}$$

where:

$$P_{ei} = \sum_{\substack{j=1 \\ j\neq i}}^{N} [C_{ij} \text{ Sin } (\delta_i-\delta_j) + D_{ij} \text{ Cos } (\delta_i-\delta_j)] \tag{2.23}$$

$$P_i = P_{mi} - E_i{}^2 G_{ii}$$

$$C_{ij} = E_i E_j B_{ij}$$

$$D_{ij} = E_i E_j G_{ij}$$

P_{mi} = mechanical input power

E_i = constant voltage behind transient reactance

δ_i = rotor angle

ω_i = rotor speed

M_i = moment of inertia

The energy function derived in [17] has the form

$$V_i = \frac{1}{M_T} \sum_{j=1}^{N} M_j (\omega_i-\omega_j)^2 - \frac{1}{M_T} \sum_{j=1}^{N} [P_i M_j - P_j M_i]$$

$$[\delta_{ij}-\delta_{ij}^{sl}] - C_{ij}[\cos\delta_{ij}-\cos\delta_{ij}] + \int_{\delta_i^{sl}+\delta_j^{sl}-\delta_o^{sl}}^{\delta_i=\delta_j+\delta_o} D_{ij}\cos\delta_{ij}\, d(\delta_i+\delta_j-\delta_o)$$

where

$$\delta_o = \frac{1}{M_T} \sum_{i=1}^{N} M_i\delta_i \quad \text{and} \quad M_T = \sum_{i=1}^{N} M_i$$

An equal area method and a potential energy boundary surface method [21] were derived based on this energy function. These methods are similar to those described in Section 2.1 for the single machine infinite bus model. These methods have no detectable error in determining the critical clearing time once the proper critical generator is identified in order to write the energy function and then apply these methods. The theoretical development of a region of stability and the region of instability for this model, based on the research performed in Chapter 5, is underway, which would hopefully provide a theoretical justification for the equal area and potential energy boundary surface methods developed for this individual machine energy function.

2.4.3 A Topological Lyapunov Energy Function

A Lyapunov energy function for a topological power system model, where the network is not aggregated back to

internal generator buses, was derived by Bergen and Hill [7]. The power system model has the form given below:

$$M_i \ddot{\delta}_i + D_i \dot{\delta}_i + \sum_{\substack{j=1 \\ j\neq i}}^{N} b_{ij} \text{ Sin } (\delta_i - \delta_j) = P^o_{mi} \qquad \text{for } i=1,\ldots, N_g \qquad (2.25)$$

and for each load bus i:

$$D_i \dot{\delta}_i + \sum_{\substack{j=1 \\ j\neq i}}^{N} b_{ij} \text{ Sin } (\delta_i - \delta_j) = -P^o_{Di} \qquad \text{for } i=N_{g+1},\ldots,N \qquad (2.26)$$

where $P_{Di} = P^o_{Di} + D_i \dot{\delta}_i$ (2.27)

and

M_i: generator inertia constant

δ_i: generator internal angle or angle of voltage of bus i

D_i: damping ratio

b_{ij}: $B_{ij} V_i V_j$

P_{mi}: mechanical input of generator i

P_{Di}: electrical real power of bus i

Bergen and Hill [7], obtained the following Lyapunov function based on their topological model of power system:

$$V = \frac{1}{2} \sum_{k=1}^{N_g} M_k \omega^2_k + \sum_{k=1}^{L} b_k \int_{\sigma^o_k}^{\sigma_k} (\text{Sin } u - \text{Sin}\delta^o_k)\, du \qquad (2.28)$$

where L is the number of the lines and N_g is the number of generators.

Bergen and Hill [7], derived their Lyapunov energy function using this model. This work is a significant contribution especially in giving the opportunity to understand the reason of lack of synchronism in the power system in the case of instability. However, it has some deficiencies:

a) Real load power is not a function of voltage. The real power for the sake of derivation has been assumed to be a function of frequency but it doesn't have any dependence on voltages. This assumption significantly affects the critical clearing time predicted.

b) The flux linkage and field effects of generator model have been completely ignored. This will cause an error in kinetic and potential energy terms.

c) Load bus voltages are kept constant. This assumption is inconsistent with any transient stability simulation model and would cause a conservative critical clearing time since load would not decrease during the fault.

d) The reactive load power has been ignored in this model so the magnetic energy due to generators and reactive power load is missing in the potential energy term.

2.5 Summary

The literature on the application of Lyapunov's direct method to power systems has been reviewed. The focus of this literature review has been on the development of Lyapunov energy functions in order to make apparent

1) the contribution made in the derivation of energy functions for a topological network model that permits a general real and reactive load model in Chapter 3;

2) the contribution of deriving the Lyapunov energy function for a topological network model, constant real power load model, constant current reactive load model, and a single axis generator model in Chapter 4;

3) the contribution made in Chapter 5 in deriving the region of stability and region of instability for a power system based on the Popov stability criterion assumed to be satisfied in the derivation of the Lyapunov energy function for the topological model in Chapter 4.

CHAPTER 3

TOPOLOGICAL ENERGY FUNCTION

A topological energy function is derived in this section that

1) retains the actual network and thus does not aggregate the network back to internal generator buses;

2) allows a general real power load model that can include constant impedance, constant current and constant power components;

3) allows a general reactive load model that can include constant current, constant impedance and constant power components.

The energy function is constructed using the integral method that associates with each term in the differential equations that describe the system. A term is added to this energy function to account for the reactive load at each bus. The energy function derived based on the integral method for the special case of constant current reactive load and constant power real load can be shown to be a Lyapunov function based on the results of Chapter 4.

Although the form of the energy function has been hypothesized in both [9] and [16], it has never been analytically derived from the integral method, Lyapunov construction methods, or any other procedure. The energy function hypothesized in [9] thus utilizes a kinetic energy term based on the synchronous reference frame but utilizes a

potential energy function based on a center of angle reference frame. This inconsistency could not occur if the energy function were analytically derived. The energy function of Mussavi [9] was the first to successfully model the reactive load energy component and this model is also used in our derivation. A recent unpublished Ph.D. thesis [11] has hypothesized an energy function that is very similar to the one analytically derived in this section. The energy function derived in this thesis and in Sastry [16] permits use of a general reactive load model and specifically itemizes the magnetic energy associated with the transient reactance of the synchronous generator model. A constant impedance load model was used in [9] and no accounting for the magnetic energy associated with the synchronous generator transient was made. The real power load is assumed to be a general load model in this thesis but was restricted to be constant real power in [16].

The energy function is derived in Section 3.2 and then is proved to be conservative in Section 3.3 for the case of constant real power load. The results of a simulation of a 39 bus system for two different fault cases each using a constant current and constant impedance real and reactive load model are presented in Section 3.4. The kinetic potential, and total energy is plotted for the critically stable and unstable simulation runs. The components of the potential energy are also plotted for both stable and unstable simulation runs for each fault case with both the

constant impedance and constant current load models.

3.1 Derivation of the Energy Function

System modeling:

a) Generator model:

It has been assumed that the voltage behind transient reactance in each generator is constant. The swing equations are of the form

$$M_i \ddot{\delta}_i = P_{mi} - P_{ei} \tag{3.1}$$

where

$$E_i = E_i^s \qquad (3.2) \quad \text{for } i = 1,2,\ldots, N_g$$

$$P_{ei} = \frac{E_i V_i}{x'_{d\,i}} \sin(\delta_i - \theta_i) \tag{3.1-a}$$

b) Load model:

The loads include both real and reactive power components which are nonlinear functions of the applied voltage and frequency. However, the constant real power case is considered also. It has been assumed that there are ficticious generators connected to the load buses which are governed by

$$0 = Q_{li} - Q_i$$

$$\varepsilon m_i \ddot{\delta}_i = -P_{li} - P_i \qquad \text{where } i=1,\ldots,N \tag{3.3}$$

c) Transmission system equations:

For the assumed transmission system the power flowing through the i-th bus can be written for load bus i.

$$P_i = \sum_{j=1}^{N} B_{ij}V_iV_j \text{ Sin } (\delta_i-\delta_j) \tag{3.4}$$

$$Q_i = - \sum_{j=1}^{N} B_{ij}V_iV_j \text{ Cos } (\delta_i-\delta_j) \tag{3.5}$$

<u>for generator bus i</u>:

$$P_i = \frac{-E_iV_i}{x'_{di}} \text{ Sin } (\theta_i - \delta_i) + \sum_{j=1}^{N} V_iV_jB_{ij} \text{ Sin } (\theta_i-\theta_j) \tag{3.6}$$

$$Q_i = \frac{V_i^2 - E_iV_i \text{ Cos } (\theta_i-\delta_i)}{x'_{di}} - \sum_{j=1}^{N} B_{ij}V_iV_j \text{ Cos } (\theta_i-\theta_j) \tag{3.7}$$

Derivation of the energy function:

The swing equation with respect to a center of inertia is formulated as

$$M_T\dot{\omega}_o = P_{coA} \tag{3.8}$$

Equations (3.1) and (3.2) could be written in terms of the center of angle reference $\tilde{\omega}_i=\omega_i-\omega_o$ as

$$M_i\dot{\tilde{\omega}}_i = P_{mi}-P_{ci} - \frac{M_i}{M_T}P_{coA} \qquad \text{for } i=1,\ldots, N_g \tag{3.9}$$

$$\varepsilon m_i\dot{\tilde{\omega}}_i = -Pl_i-P_e - \frac{\varepsilon m_i}{M_T} P_{coA} \text{ for } i=1,\ldots, N \tag{3.10}$$

Multiplying both sides of (3.9) and (3.10) by ω_i and then summing both equations and then taking the integral of this sum from t_s to t the new energy function will be

$$VE = \frac{1}{2} \sum_{i=1}^{N_G} M_i (\omega_i-\omega_o)^2 + \frac{1}{2} \sum_{i=}^{N} \varepsilon m_i (\omega_i-\omega_o)^2 - \sum_{i=1}^{N_g} Pm_i (\delta_i-\delta_i^s)$$

$$+ \sum_{i=1}^{N} \int_{\theta(t_s)}^{\theta(t)} Pl_i \, d\theta_i + \sum_{i=1}^{N} \int_{t_s}^{t} \tilde{\omega}_i P_i dt$$

$$+ \sum_{i=1}^{N_g} \int_{t_s}^{t} \omega_i P_i dt + Q_L \qquad (3.11)$$

The term Q_L is added to include the reactive energy in the load that must be included to make this energy function conservative one must utilize the fact that

$$\sum_{i=1}^{N} \varepsilon m_i \tilde{\omega}_i + \sum_{i=1}^{N_g} M_i \tilde{\omega}_i = 0$$

in deriving (3.11).

The first term in (3.11) represents the kinetic energy of generators and the second term represents the kinetic energy at the load buses. By setting $\varepsilon \rightarrow 0$ the second term will vanish. Setting $\varepsilon \rightarrow 0$ eliminates the ficticious generators at load buses that have been included here solely because they must be included to derive the Lyapunov energy functions in Chapter 4. The third term in (3.11) represents the potential energy component associated with linear displacement of rotor angles and the fourth term is representing the potential energy associated with linear displacement of load bus angles. These two terms are called the position components of potential energy. The fifth term

stands for the magnetic energy stored in the network. This term will be discussed in the next section. The last term represents the change in magnetic energy stored in the load.

Thus when $\varepsilon \longrightarrow 0$ the energy function becomes:

$$VE = \frac{1}{2} \sum_{i=1}^{N_g} M_i(\omega_i-\omega_o)^2 - \sum_{i=1}^{N_g} Pm_i(\delta_i-\delta_i^s) +$$

$$\sum_{i=1}^{N} \int_{\theta_i(t_s)}^{\theta_i(t)} Pl_i d\theta_i + \sum_{i=1}^{N} \int_{t_s}^{t} \tilde{\omega}_i P_i dt + Q_L \qquad (3.12)$$

The term $\sum_{i=1}^{N} \int_{t_s}^{t} \tilde{\omega}_i P_i dt$, represents the magnetic energy stored in the network. The magnetic energy* of each line is:

$$\frac{1}{2} LI^2 = \frac{1}{2\omega} X\, I^2 = \frac{1}{2\tilde{\omega}} X \frac{(V_k-V_j)}{jX} \frac{(V_k-V_j)^*}{jX} =$$

$$\frac{1}{2\omega X} (|V_j|^2 - 2|V_k|\,|V_j| \operatorname{Cos} \theta_{kj}) \qquad (3.13)$$

considering (3.13), (3.4) and (3.6)

$$\sum_{i=1}^{N} \int_{t_s}^{t} \tilde{\omega}_i P_i dt = -\frac{1}{2} \sum_{i=1}^{N} \sum_{j=1}^{N} V_i V_j B_{ij} \operatorname{Cos} \theta_{ij} + V_i^s V_j^s$$

$$B_{ij} \operatorname{Cos} \theta^s{}_{ij} + \sum_{i=1}^{N_g} - [V_i^2 + E_i^{s_2} - 2 E_i^s V_i \operatorname{Cos} (\theta_i-\delta_i) -$$

$$(E_i^{s_2} + V_i^{s\,2} - 2E_i^s V_i^s \operatorname{Cos} (\theta_i^s-\delta_i^s)] \frac{1}{2x'_{di}} \qquad (3.14)$$

---

*The energy stored in an inductor is viewed physically as kinetic energy based on the electron motion, but when interpreted in this model is viewed as potential energy.

where $B_i = -\sum_{j=1}^{N} B_{ij}$ and B_{ii} does not include generator transient reactances for i=1,2,..., N_g or load impedance for i=1,2...,N. The first summation in (3.14) represents the magnetic energy stored in the branches that are connected to nongenerator buses, and the second summation gives the magnetic energy stored in the generator transient reactances.

The last term in (3.12) represents the magnetic energy of the load buses. Letting the reactive power at load bus i to be a nonlinear function of voltage V_i, $f_i(V_i)$, Q_L could be written as:

$$Q_L = \sum_{i=1}^{N} \int_{V_i s}^{V_i} \frac{f_i(x_i)}{x_i} \, dx_i \qquad (3.15)$$

The right side of (3.15) is justified as a measure for load energy since $\frac{f_i(V_i)}{V_i}$ represents current and $\int I_i dV_i$ is a measure of energy.

3.2 Proof of Conservativeness of the Energy Function

By substituting the results of (3.14) and (3.15) in (3.12) the new form of energy function will be:

$$VE = \frac{1}{2}\sum_{i=1}^{N_g} M_i(\omega_i-\omega_o)^2 - \sum_{i=1}^{N_g} P_{mi}\,(\delta_i-\delta_i^s)$$

$$+ \sum_{i=1}^{N} \int_{t_s}^{t} Pl_i \frac{d\theta_i}{dt}\cdot dt + \sum_{i=1}^{N} \int_{V_i^s}^{V_i} \frac{f_i(x_i)}{x_i}\, dx_i$$

$$-\frac{1}{2}\sum_{i=1}^{N}\sum_{j-1}^{N} B_{ij}(V_iV_j \operatorname{Cos}\theta_{ij} - V_i^s V_j^s \operatorname{Cos}\theta_{ij}^s)$$

$$+ \sum_{i=1}^{N_g} ((E_i^{s2} + V_i^2 - 2E_i^sV_i \operatorname{Cos}(\delta_i-\theta_i)) - (E_i^{s2} + V_i^{s2}$$

$$-2E_i^sV_i^s \operatorname{Cos}(\delta_i^s-\theta_i^s))\ \frac{1}{2x'_{di}} \qquad (3.16)$$

The first term in (3.16) is representing the kinetic energy and the rest of the terms represent the potential energy. Thus the potential energy in (2-9) PE, is:

$$PE = -\sum_{i=1}^{N_g} Pm_i\,(\delta_i-\delta_i^s) + \sum_{i=1}^{N} \int_{t_s}^{t} Pl_i \frac{d\theta_i}{dt}\cdot dt$$

$$+ \sum_{i=1}^{N} \int_{V_i^s}^{V_i} \frac{f_i(x_i)dx_i}{x_i} - \frac{1}{2}\sum_{i=1}^{N}\sum_{j=1}^{N} B_{ij}(V_iV_j \operatorname{Cos}\theta_{ij}$$

$$- V_i^sV_j^s \operatorname{Cos}\theta_{ij}^s) + \sum_{i=1}^{N_g} \left[((E_i^{s2}+V_i^2-2E_i^sV_i \operatorname{Cos}(\delta_i-\theta_i))\right.$$

$$\left. - (E_i^{s2}+V_i^{s2} - 2E_i^sV_i^s \operatorname{Cos}(\delta_i^s-\theta_i^s))\right] \cdot \frac{1}{2x'_{di}}$$

(3.17)

The energy function presented in (3.16) is a conservative energy i.e., $\frac{d\ VE}{dt} = 0$. This has been shown in the following discussion:

Differentiating PE in (3.17) with respect to bus voltage V_i:

$$\frac{dPE}{dV_i} = \frac{f_i(V_i)}{V_i} + \frac{V_i}{x'_{di}} - \frac{E_i^s}{x'_{di}} \text{Cos}\ (\delta_i - \theta_i) - \sum_{j=1}^{N} B_{ij}V_j \text{ Cos } \theta_{ij} \qquad (3.18)$$

$$\text{for } i=1,\ldots,\ N_G$$

$$\frac{dPE}{dV_i} = \frac{f_i(V_i)}{V_i} - \sum_{j=1}^{N} B_{ij}V_j \text{ Cos } \delta_{ij} \qquad \text{for } i=N_{+1},\ldots,N \qquad (3.19)$$

Thus

$$\frac{dPE}{dV_i} = (Q_{1i} + Q_i)/V_i \qquad \text{for } i=1,2,\ldots,N \qquad (3.20)$$

since by definition $Q1_i = +f_i(V_i)$ is the reactive load of bus i, and Q_i satisfies (3.5, 3.7). It is clear based on (3.3) that

$$\frac{dPE}{dV_i} = 0 \qquad i=1,2,\ldots,N \qquad (3.21)$$

Now differentiating (3.17) with aspect to θ_i:

$$\frac{dPE}{d\theta_i} = + \sum_{j=1}^{N} B_{ij}V_iV_j \text{ Sin } \theta_{ij} - \frac{E_iV_i}{x'_{di}} \text{ Sin } (\delta_i - \theta_i)$$

$$\text{for } i=1,\ldots,N_g \qquad (3.22)$$

$$\frac{dPE}{d\theta_i} = \sum_{j=1}^{N} B_{ij}V_iV_j \text{ Sin } \theta_{ij}$$

for $i=N_{g+1},....,N$ (3.23)

Considering (3.4) and (3.6), and applying their results to (3.22) and (3.23):

$$\frac{dPE}{d\theta_i} = P_i \qquad i=1,2,3,....,N \quad (3.24)$$

It can also be shown that

$$\frac{dPE}{dt} = \sum_{i=1}^{N} Pl_i \frac{d\theta_i}{dt}$$

$i=1,2,3,....,N$ (3.25)

Combining (3.24) and (3.25), one can show that

$$\sum_{i=1}^{N} \frac{dPE}{d\theta_i} \cdot \frac{d\theta_i}{dt} + \frac{dPE}{dt} = \sum_{i=1}^{N} (P_i+Pl_i) \frac{d\theta_i}{dt} = 0$$

$i=1,2,....,N$ (3.26)

since

$$P_i + P_{ei} = 0 \qquad i=1,2,3,....,N$$

from (3.3).

Now differentiating with respect to δ_i:

$$\frac{dPE}{d\delta_i} = -Pm_i + \frac{E_iV_i}{x_{di}} \text{ Sin } (\delta_i - \theta_i)$$

for $i=1,....,N_g$ (3.27)

Recalling that the kinetic energy is:

$$KE = \frac{1}{2} \sum_{i=1}^{N_g} M_i(\omega_i-\omega_i^o)^2$$

and then differentiating it with respect to ω_i produces

$$\frac{\partial KE}{\partial \tilde{\omega}_i} = M_i(\omega_i - \omega_i^o) \qquad \text{for } i=1,2,\ldots,N_g \tag{3.28}$$

Combining equations (3.27) and (3.28), on i can show that

$$\sum_{i=1}^{N_g} \frac{\partial KE}{\partial \tilde{\omega}_i} \cdot \frac{d\tilde{\omega}_i}{dt} + \frac{\partial PE}{\partial \delta_i} \cdot \frac{d\delta_i}{dt} = \sum_{i=1}^{N_g} (M_i \dot{\tilde{\omega}}_i - Pm_i + P_{ei})\tilde{\omega}_i = 0 \tag{3.29}$$

since

$$M_i \dot{\tilde{\omega}}_i = P_{mi} - P_{ei} \tag{3.30}$$

Considering (3.21), (3.26) and (3.30)

$$\frac{dVE}{dt} = 0 \tag{3.31}$$

and thus the energy function has been shown to be conservative,

3.3 Energy Function with Different Load Models

3.3.1 A General Real Power Load Model

In the case that real load is represented by nonlinear function of applied voltage, the second term in (3.16) could be written as:

$$\sum_{i=N_{g+1}}^{N} \int_{\theta(t_s)}^{\theta(t)} Pl_i d\theta_i = \frac{1}{2} \sum_{i=N_{g+1}}^{N} (\theta(t)-\theta(t_s))(Pl_i(V_i(t_s)) + Pl_i(V_i(t)) \quad (3.32)$$

using the trapezoidal integration rule. Substituting the right hand side of (45) the following generalized function is obtained:

$$VE = \frac{1}{2} \sum_{i=1}^{N_g} M_i \tilde{\omega}_i^2 + \frac{1}{2} \sum_{i=1}^{N} (\theta_i-\theta_i^s)\ (Pl_i^{V(t_s)} + Pl_i^{V(t)})$$

$$- \sum_{i=1}^{N_g} Pm_i(\delta_i-\delta_i^s) + \sum_{i=1}^{N} \int_{V_i(t_s)}^{V_i(t)} \frac{f_i(x_i)}{x_i} dx_i$$

$$-\frac{1}{2} \sum_{j=1}^{N} \sum_{i=1}^{N} B_{ij}(V_iV_j \cos\theta_{ij} - V_i^sV_j^s \cos \theta_{ij}^s)$$

$$+ \sum_{i=1}^{N_g} \left[(E_i+V_i^2-2E_iV_i \cos (\delta_i-\theta_i))-(E_i^2+V_i^{s\,2}\right.$$

$$\left.-2E_iV_i^s \cos (\delta_i^s-\theta_i^s))\right] \cdot \frac{1}{2x'_{di}} \quad (3.33)$$

3.3.2 The Energy Function With Different Reactive Load Models

The reactive power at load buses is assumed to be a general nonlinear function of voltage. Initially the case of constant current reactive load is considered.

a) Constant Current Reactive Load Model

In the case that reactive load is constant current reactive power of the load will be:

$$f_i(x_i) = a_i x_i \quad \text{where} \quad a_i = \frac{-Q_i^s}{V_i^s}$$

and Q_i^s is defined in (3.5) and (3.7). The energy associated with the reactive load Q_L will thus have the form

$$Q_L = \sum_{i=1}^{N} \int_{V_i^s}^{V_i} \frac{f_i(x_i)}{x_i} dx_i = -\sum_{i=1}^{N} Q_i^s \frac{V_i}{V_i^s} + \sum_{i=1}^{N} Q_i^s \qquad (3.34)$$

Substituting (3.34) in (3.33) the following energy function will be obtained:

$$\begin{aligned} VE = {} & \frac{1}{2} \sum_{i=1}^{N_g} M_i(\omega_i-\omega_o)^2 + \frac{1}{2} \sum_{i=1}^{N} (\theta_i-\theta_i^s)\left(Pl_i^{s\,V(t_s)} + Pl_i^{V(t)}\right) \\ & - \sum_{i=1}^{N_g} P_{mi}(\delta_i-\delta_i^s) - \sum_{i=1}^{N} \left(1-\frac{V_i}{V_i^s}\right) \sum_{j=1}^{N} V_i^s V_j^s B_{ij} \cos \theta_{ij}^s \\ & + \sum_{i=1}^{N_g} \left(1-\frac{V_i}{V_i^s}\right)\left(V_i^s E_i^s \cos(\delta_i^s-\theta_i^s) - V_i^{s\,2}\right) \cdot \frac{1}{x'_{di}} \\ & + \sum_{i=1}^{N_g} \Big[(E_i^2+V_i^2-2E_iV_i\cos(\delta_i-\theta_i)) - (E_i^2+V_i^{s\,2} \\ & -2E_iV_i^{s\,2}\cos(\delta_i^s-\theta_i^s))\Big]\frac{1}{2x'_{di}} - \frac{1}{2}\sum_{j=1}^{N}\sum_{i=1}^{N} B_{ij}(V_iV_j\cos(\theta_{ij}) \\ & - V_i^sV_j^s\cos(\theta_{ij}^s)) \end{aligned} \qquad (3.35)$$

b) Constant Impedance Load Model.

In the case of constant impedance reactive load model, the function $f_i(V_i)$ is a quaradic function of voltage:

$$f_i(x_i) = a_i x_i^2 \quad \text{where } a_i = -\frac{Q_i^s}{V_i^{s2}}$$

and the energy associated with the reactive load Q_L has the form

$$Q_L = \sum_{i=1}^{N} \int_{V_i^s}^{V_i} \frac{f_i(x_i)}{x_i}\, dx_i = -\frac{1}{2} \sum_{i=1}^{N} Q_i^s \frac{V_i^2}{V_i^{2s}} + \sum_{i=1}^{N} Q_i^s \tag{3.36}$$

Substituting (3.36) in (3.33) the following energy function will be obtained:

$$\begin{aligned} VE = {} & \frac{1}{2} \sum_{i=1}^{N_g} M_i(\omega_i-\omega_o)^2 + \frac{1}{2} \sum_{i=1}^{N} (\theta_i-\theta_i^s)\,(Pl_i^{s}(t_s) + Pl_i^{V(t)}) \\ & - \sum_{i=1}^{N_g} Pm_i\,(\delta_i-\delta_i^s) + \sum_{i=1}^{N} \left(1-\frac{V_i^2}{V_i^{s2}}\right) \sum_{j=1}^{N} V_i^s V_j^s B_{ij} \cos \theta_{ij}^s \\ & + \sum_{i=1}^{N_g} \left(1-\frac{V_i^2}{V_i^{s2}}\right)(V_i^s E_i^s \cos(\delta_i^s-\theta_i^s) - V_i^2) \cdot \frac{1}{x'_{di}} \\ & + \sum_{i=1}^{N_g} \left[(E_i^2+V_i^2 - 2E_iV_i \cos(\delta_i-\theta_i)) - (E_i^2+V_i^{s2}\right. \\ & \left. - 2E_iV_i^{s2} \cos(\delta_i^s-\theta_i^s))\right] \cdot \frac{1}{2x'_{di}} - \frac{1}{2} \sum_{i=1}^{N} \sum_{j=1}^{N} B_{ij}(V_iV_j \cos \theta_{ij} \\ & - V_i^sV_j^s \cos \theta_{ij}^s) \end{aligned} \tag{3.37}$$

c) Constant Reactive Load Model.

When the reactive power of loads are constant then:

$$f_i(x_i) = a_i \qquad \text{where } a_i = -Q_i^s$$

and the energy associated with the reactive load Q_L has the form

$$Q_L = \sum_{i=1}^{N} \int_{V_i^s}^{V_i} \frac{f_i(x_i)}{x_i}\, dx_i = -\sum_{i=1}^{N} Q_i^s \, \mathrm{Ln}(V_i/V_i^s) \tag{3.38}$$

Consequently the form of energy function will be:

$$\begin{aligned} VE = {} & \frac{1}{2} \sum_{i=1}^{N_g} M_i(\omega_i-\omega_i^o)^2 + \frac{1}{2} \sum_{i=1}^{N} (\theta_i-\theta_i^s)\,(Pl_i^s + Pl_i^v) \\ & - \sum_{i=1}^{N_g} P_{mi}(\delta_i-\delta_i^s) + \sum_{i=1}^{N} \mathrm{Ln}(V_i/V_i^s) \sum_{j=1}^{N} V_i^s V_j^s B_{ij} \cos \delta_{ij}^s \\ & + \sum_{i=1}^{N_g} \mathrm{Ln}(V_i/V_i^s)\,(V_i^s E_i^s \cos(\delta_i^s-\theta_i^s) - V_i^{s2}) \cdot \frac{1}{x'_{di}} \\ & + \sum_{i=1}^{N_g} \left[(E_i^2+V_i^2-2E_iV_i\cos(\delta_i-\theta_i)) - (E_i^2+V_i^{s2}\cos(\delta_i^s-\theta_i^s))\right] \\ & \cdot \frac{1}{2x'_{di}} - \frac{1}{2} \sum_{i=1}^{N} \sum_{j=1}^{N} B_{ij}(V_iV_j\cos\theta_{ij} - V_i^sV_j^s\cos\theta_{ij}^s) \end{aligned} \tag{3.39}$$

d) The Generalized Load Model.

In the case that reactive load is a combination of constant current, constant impedance and constant VAR Model the function $f_i(x_i)$ is of the following form:

$$f_i(x_i) = a_i x_i^2 + b_i x_i + C_i \tag{3.40}$$

where

$$a_i = -\alpha_i \frac{Q_i^s}{V_i^{s2}} \quad b_i = -\beta_i \frac{Q_i^s}{V_i^s} \text{ and } C_i = -\gamma_i Q_i^s$$

This model assumes that a percentage of the load is constant impedance (α_i), constant current (β_i) and constant power (γ_i) such that:

$$\alpha_i + \beta_i + \gamma_i = 1 \tag{3.41}$$

The total energy function in this case has the following form:

$$\begin{aligned} VE = {} & \frac{1}{2}\sum_{i=1}^{N_g} M_i(\omega_i-\omega_i^o)^2 + \frac{1}{2}\sum_{i=1}^{N}(\theta_i-\theta_i^s)(P1_i^s + P1_i^v) \\ & - \sum_{i=1}^{N_g} P_{mi}(\delta_i-\delta_i^s) + \gamma_i\Big[\sum_{i=1}^{N} Ln(V_i/V_i^s)\sum_{j=1}^{N} V_i^s V_j^s B_{ij}\cos\delta_{ij}^s \\ & + \sum_{i=1}^{N_g} Ln(V_i/V_i^s)(V_i^s E_i\cos(\delta_i^s-\theta_i^s) - V_i^{s2})\Big]\cdot\frac{1}{x'_{di}} \\ & + \beta_i\Big[\sum_{i=1}^{N}(1-\frac{V_i}{V_i^s})\sum_{j=1}^{N} V_i^s V_j^s B_{ij}\cos\theta_{ij}^s + \sum_{i=1}^{N_g}(1-\frac{V_i}{V_i^s})(V_i^s E_i\cos\delta_i^s-\theta_i^{s2}) \\ & - V_i^{s2})\Big]\cdot\frac{1}{x'_{di}} + \alpha_i\Big[(\sum_{i=1}^{N}(1-\frac{V_i^2}{V_i^{s2}})\sum_{j=1}^{N} V_i^s V_j^s B_{ij}\cos\theta_{ij}^s) \\ & + \sum_{i=1}^{N_g}(1-\frac{V_i^2}{V_i^{s2}}(V_i^s E_i^s\cos(\delta_i^s-\theta_i^s)-V_i^{s2})\Big]\cdot\frac{1}{x'_{di}} \\ & + \sum_{i=1}^{N_g}\Big[(E_i^2+V_i^2-2E_iV_i\cos(\delta_i-\theta_i))-(E_i^2+V_i^{s2}-2E_iV_i^{s2}\cos(\delta_i^s-\theta_i^s))\Big] \\ & \cdot\frac{1}{2x'_{di}} - \frac{1}{2}\sum_{i=1}^{N}\sum_{j=1}^{N} B_{ij}(V_iV_j\cos\theta_{ij}-V_i^sV_j^s\cos\theta_{ij}^s) \end{aligned} \tag{3.42}$$

3.4 Simulation Results

The components and total energy for the energy functions presented in (3.35) and (3.37) are plotted as a function of time based on transient stability simulations of particular fault on a 39 bus New England system shown in Figure 4. The purpose of computing and plotting the energy functions for both a constant current and a constant impedance reactive load model for two different faults is

1) to indicate that the total energy remains constant after the fault is cleared when the real power load model is constant power confirming that the energy function is conservative when the real power load is constant;

2) to show the relative magnitude of the kinetic and potential energy components and show that since the total energy is conservative that an increase in either kinetic or potential energy results in a decrease in the other energy component;

3) to display the relative magnitude of the position, network magnetic, real power load, and reactive power load components of the potential energy as a function of time. The differences in the potential energy components as well as the swing curves for constant current compared with constant impedance reactive load models will also be shown;

4) to show how a loss of stability causes a sudden sharp drop and oscillations in the various potential energy components as well as a sharp increase in the kinetic energy in the system. The total system energy no longer remains constant once the loss of synchronism occurs and may be due to numerical problems caused by the very large and rapid changes in the system after the loss of synchronism.

The two fault cases considered are a fault on line 26-27 where line 26-27 is removed and a fault on line 21-22 where line 21-22 is removed. It will be observed that the

Fig. (4). New England Study System.

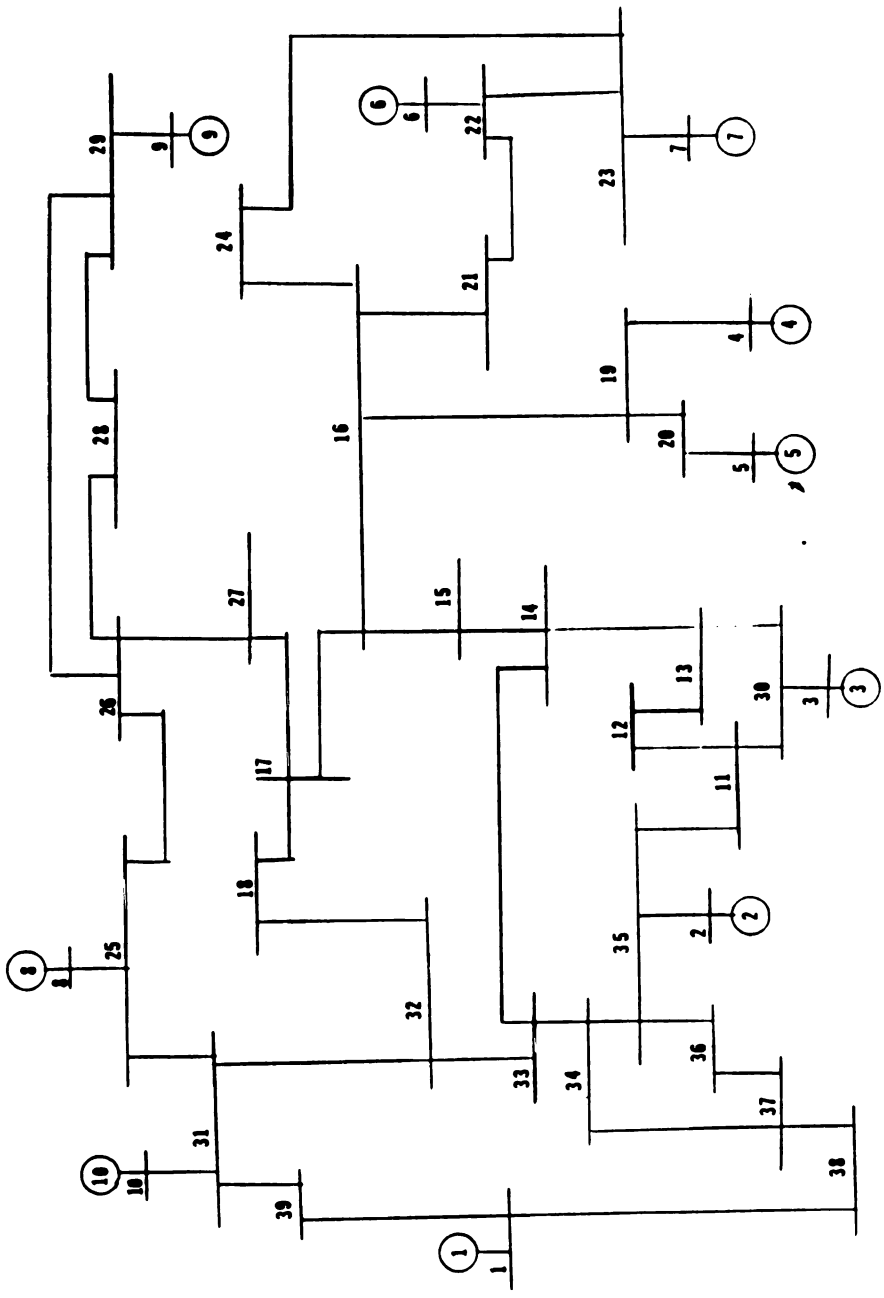

critical clearing time for the fault on line 21-22 is much shorter than for the fault on line 26-27. The results for the simulation of the fault on line 26-27 with that line removed is discussed first for both the constant current and constant impedance load model. The results of the second fault case for both the constant current and constant impedance load models are then discussed. It should be noted that the MVA base used is 10 MVA base due to the fact that the Detroit Edison transient stability program used this MVA base.

i) Fault on Line 26-27 and Constant Current Reactive Load Model.

In this case the fault occurs on line 26-27 and the critical clearing time by simulation has been determined as .36 seconds.

Figure (5.a) shows the variations of angles of generators close to the fault on the stable case. Figure (6.a) shows the variations of the same generator angles for the usntable case. In the stable case the angle of generator No. 9 increases until it reaches 180 degrees and then starts decreasing and continues oscillating until it remains constant. For the unstable case the generator No. 9's angle continues to increase and is the first generator that loses syncronism. Figure (5.b) shows the total, potential and kinetic energies for the stable case; the same kind of energies are shown in Figure (6.b) for the unstable case. In both cases whenever the potential energy is changing the

kinetic energy experiences a negative change of the same magnitude such that the total energy remains constant. The small variations in total energy are due to the computational errors and also the assumption that real power delivered to the load buses is constant. Whenever the potential energy is at its maximum the kinetic energy has its minimum value. This observation supports the PEBS method discussed in Chapter 2. In the unstable case when the system loses synchronism the potential energy experiences a large drastic sudden drop and the kinetic energy starts increasing. Furthermore, there is a sudden drop in total energy which may be due to numerical problems in attempting to accurately simulate the large rapid changes after the point in time when the loss of synchronism occurs.

Figure (5.c) shows three components of potential energy for the stable case. These three components; energy due to real power load, energy stored in the transmission grid, and energy due to the generator's angle displacement, are shown for the unstable case in Figure (6.c). In the stable case the energy due to the generator's angle displacement decreases until minimum is reached and then starts increasing again. In the unstable case, since the generator's angle continues increasing, the position energy component is a monotone decreasing function of time. The other two forms of energy in the stable case increase until a maximum is reached and then decrease smoothly but in the unstable case these energies start oscillating. The sum of

the real load power energy and the magnetic energy stored in the transmission grid is larger as a function of time in the unstable case than in the stable because the system trajectory's peak angle excursion is larger in the unstable case.

Figure (5.d) shows the energy stored in the reactive power loads for the stable case. Figure (5.d) shows the same energy for the unstable case. The amount of this energy is much smaller than the other energies components. Since this energy depends on variation of voltage of the load buses in the stable case, the energy approaches zero as time increases and the system trajectory approaches the SEP. In the unstable case the oscillations of voltages in the load buses cause this energy to experience large oscillations.

ii) Fault on Line 26-27 and Constant Impedance Reactive Load Model

For this case the fault occurs on line 26-27 and the critical clearing time by simulation is determined as .31 seconds. The .05 seconds reduction of critical clearing time due to the change of reactive load modeling is expected because there is a greater reduction in the magnetic energy stored by the reactive load clearing the fault when voltage drops. This reduction in magnetic energy results in increased kinetic energy because the energy function is conservative.

Figure (7.a) shows the changes of angles of generators 7, 8 and 9 which are closer to the fault for the stable case. The variations of the angles of the same generators are shown in Figure (8.a) for the unstable case. In the stable case the angles oscillations die out, but in the unstable case the angle of generator 7 as well as generators 8 and 9 continue increasing. It is important to note that for this kind of load modeling, not only the critical clearing time changes but also the first generator that loses syncronism is different from the constant current load model.

Figure (7.b) shows the changes of total, kinetic and potential energies for the stable case; the same energies for the unstable case are shown in Figure (8.b). In both cases whenever the potential energy has its maximum value the kinetic energy has its minimum value. This observation again supports the PEBS method. In the stable case the total energy is almost constant. The small variations in the total energy over time shown in Figure (7.b) are due to computational error and the assumption that real load at the load buses is constant. For the unstable case as shown in Figure (8.b) the total energy has dropped after the generators have lost synchronism. The potential energy has a sudden drop and the kinetic energy has a sudden increase after the loss of synchronism. This sudden drop occurs because the simulation program is unable to give accurate

solution with the large and sudden changes of voltage magnitudes and the changes in angles.

Figure (7.c) shows the energy due to real loads and energy stored in the transmission grid and energy due to generators angle displacement for the stable case. These three energies are components of potential energy. Figure (8.c) shows the same potential energy components for the unstable case. The energy due to generators angle displacements for the stable case reaches a minimum and then starts increasing but in the unstable case this energy is always decreasing. This continual decrease is because in the unstable case the angles continue increasing. The real load energy and energy stored in the transmission lines for the stable case are smaller and smoother than in the unstable case. In the unstable case these energies have oscillations which are due to large and fast oscillations of voltages and angles.

Figures (7.d) and (8.d) show the energy stored in reactive loads for stable and unstable cases. The reactive power of the load for each bus is a function of the square of the voltage of the corresponding bus. By recalling the equation (3.36) it could be seen that the larger is V_i^2 , the more negative will be the energy due to reactive loads and this explains why this energy in this case is negative compared to constant current load model. In the unstable case, there is an oscillation in this reactive load energy as can be seen in Figure (8.d).

From both cases that fault was on line 26-27, it could be concluded that the total energy stored in the system for the stable case is less than the unstable case.

iii) and iv) For the case that fault has occurred on line 21-22 the same tests of the last two sections were performed, the results have been presented in Figures 9, 10, 11 and 12. These experiments were performed to show that the cases discussed in the preceeding two sections are not special cases. The results of these tests support the conclusions from the tests for the faults on line 26-27.

Fig. (5.a) Variations of angles of generators 7, 8 and 9 for stable case where the fault on line 26-27 is cleared in 0.35 seconds by removing the faulted line.

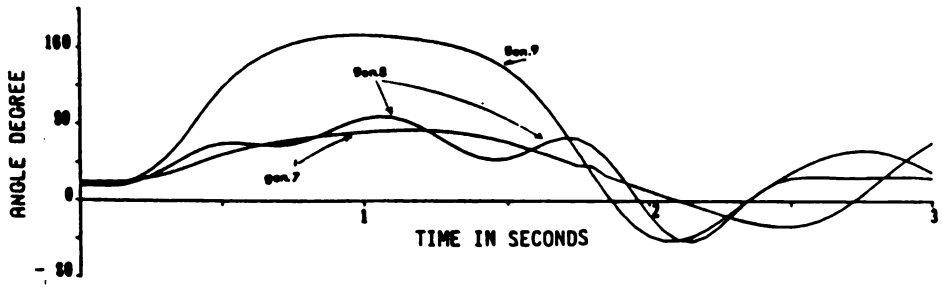

Fig. (5.b) Variations of potential, kinetic and total energy for the stable case where the fault is on line 26-27.

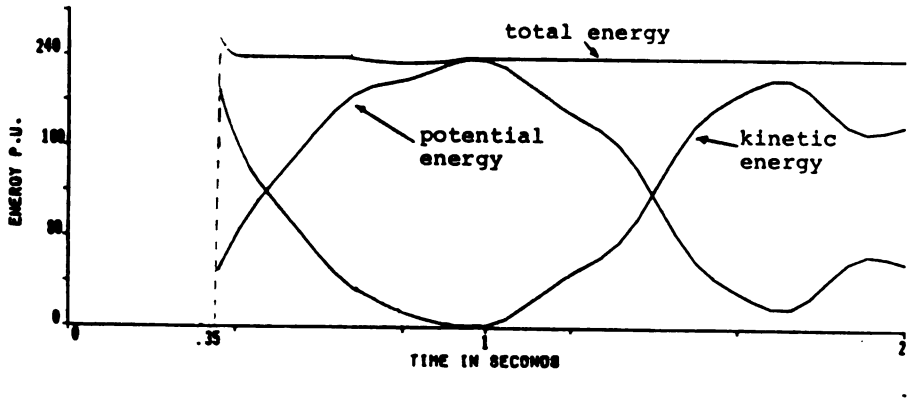

Fig. (5.c) Variations of real load energy and transmission line energy and energy due to angle displacement of generators rotors for the stable case when the fault is on line 26-27.

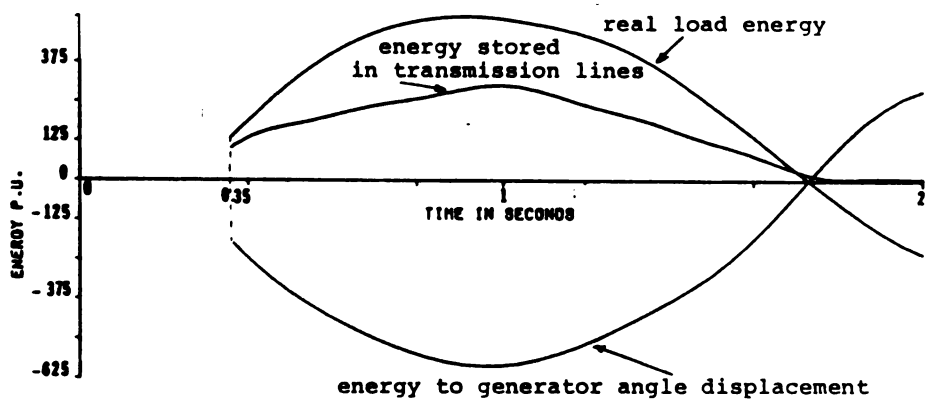

Fig. (5.d) Variation of reactive load energy for the stable case where fault is on line 21-22.

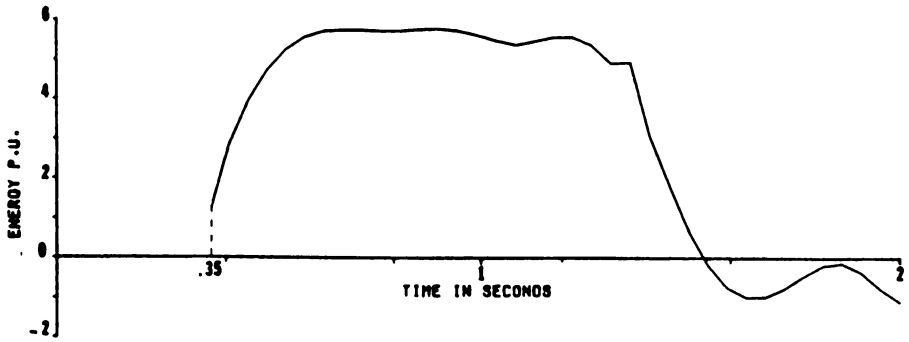

Fig. (6.a) Variation of angles of generators 7, 8 and 9 for unstable case where the fault on line 21-22 is cleared in 0.36 seconds and line 26-27 is removed.

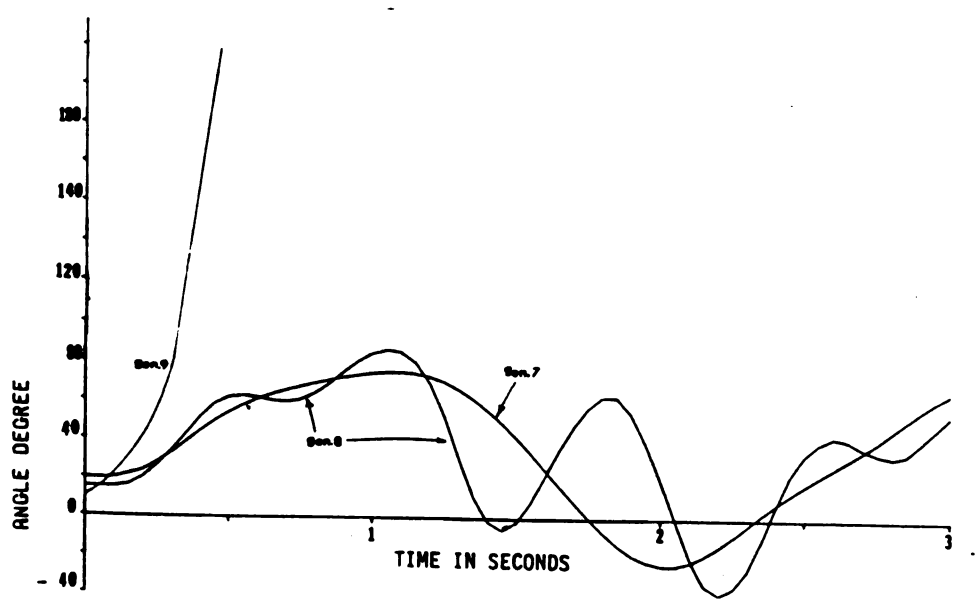

Fig. (6.b) Changes of potential, kinetic and potential energy for the unstable case when the fault is on line 26-27.

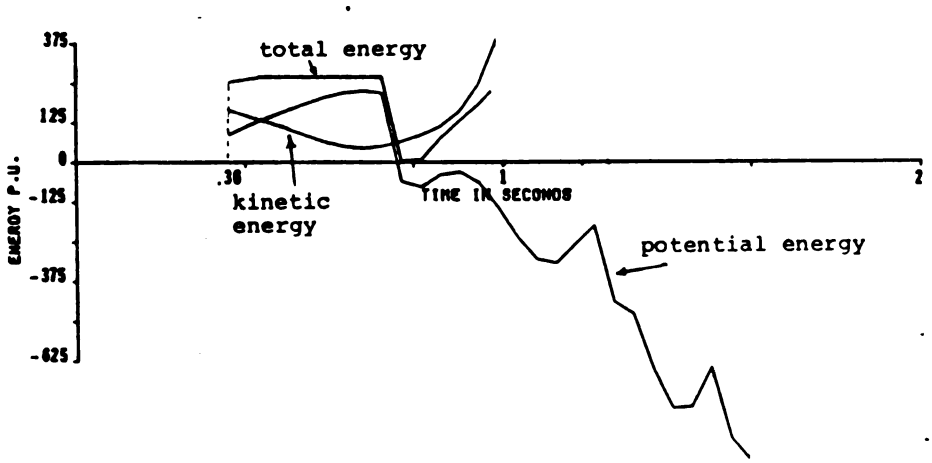

Fig. (6.c) Variation of real load and transmission line energies and energy due to angle displacement of generator rotors for the unstable case when the fault is on line 26-27.

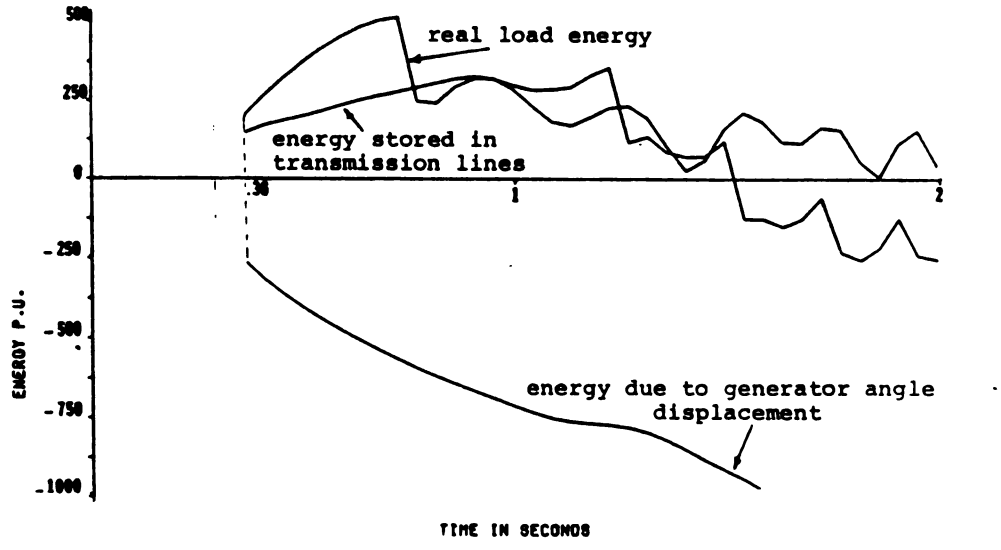

Fig. (6.d) Changes of reactive load energy for the unstable case where fault is on line 26-27.

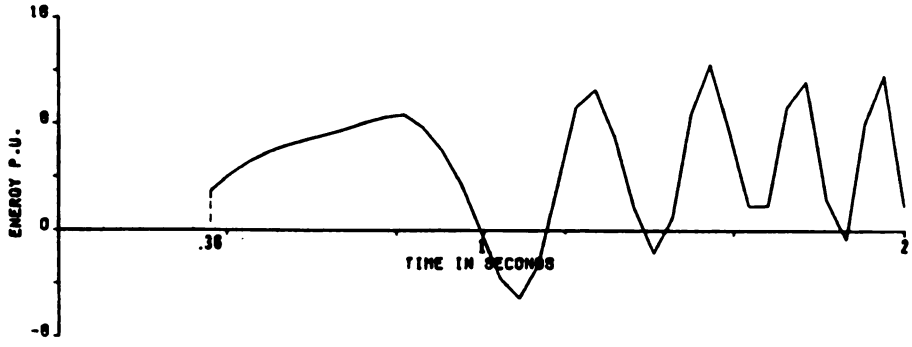

Fig. (7.a) Variation of generators angles for stable case that fault occurs on line 26-27. The fault is cleared at 0.30 seconds and line 26-27 is removed. (Constant impedance load model)

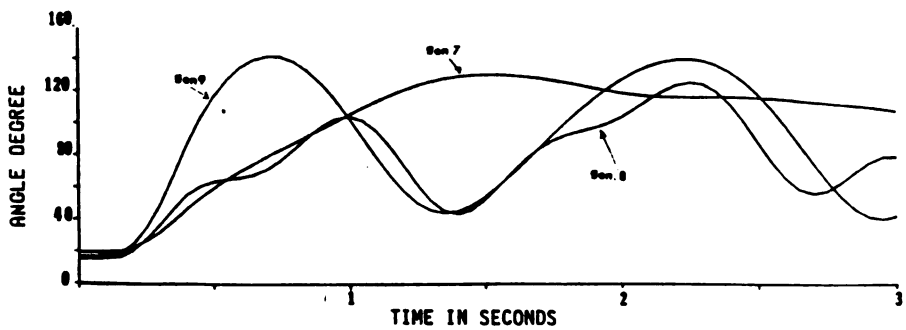

Fig. (7.b) Changes of kinetic, potential and total energies for the stable case when the fault is on line 26-27. (Constant impedance load model)

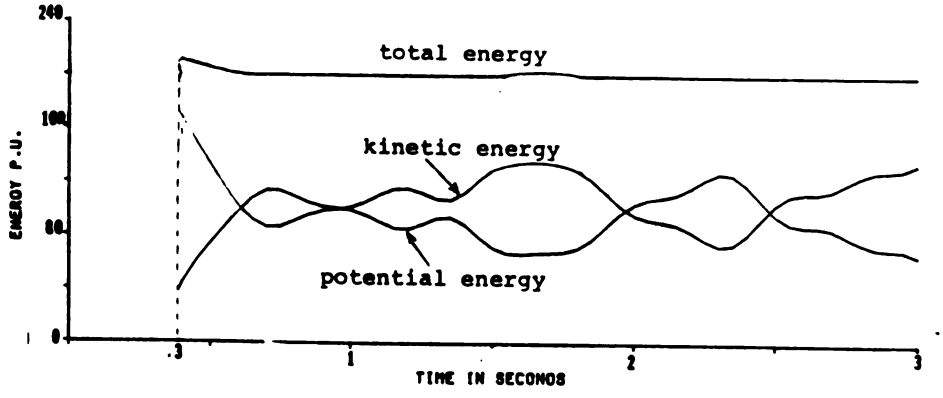

Fig. (7.c) Changes of energy due to generator angle displacement and loads real power energy and energy stored in transmission grid for the stable case where fault on line 26-27 is cleared in 0.3 seconds. (Constant impedance load model)

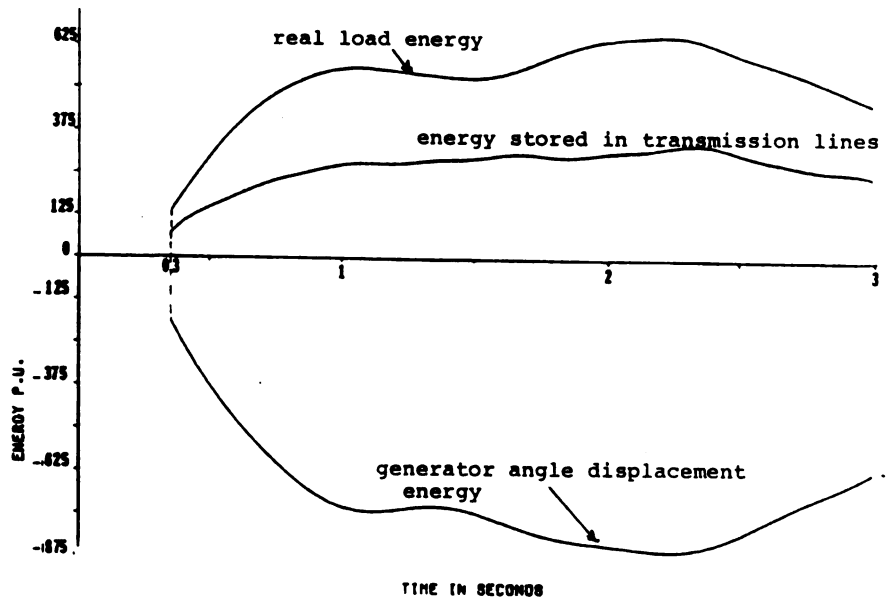

Fig. (7.d) Changes of loads reactive power energy for the stable case when fault is on line 26-27. (Constant impedance load model)

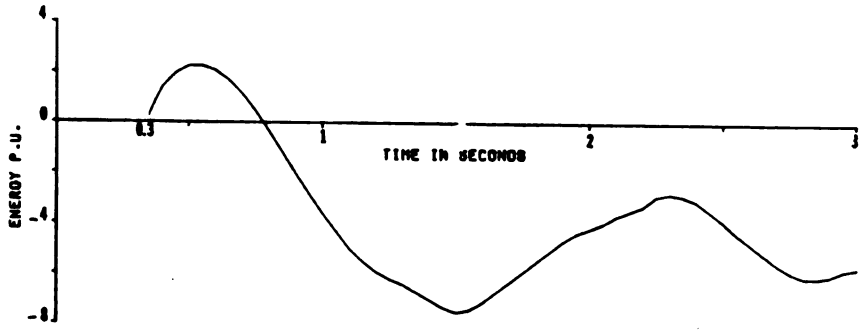

Fig. (8.a) Variation of generators angles for unstable case when the fault occurs on line 26-27. The fault is cleared at 0.31 seconds and line 26-27 is removed. (Constant impedance load model)

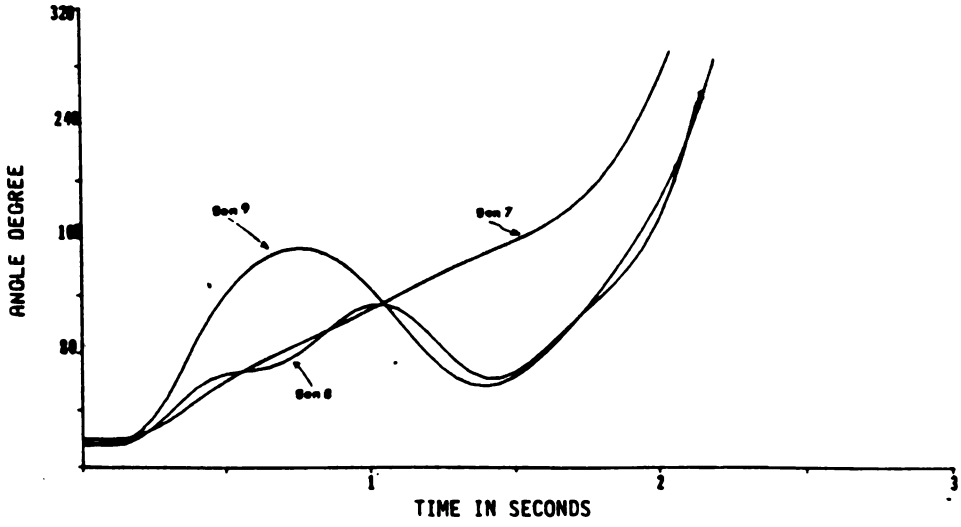

Fig. (8.b) Variations of kinetic, potential and total energies for the unstable case when the fault is on line 26-27. (Constant impedance load model)

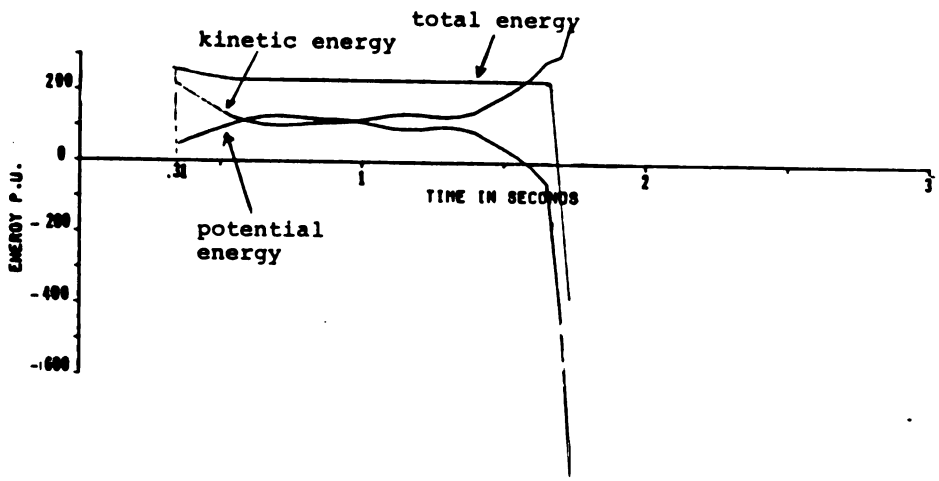

Fig. (8.c) Variations of real load energy, energy due to generator angle displacement and energy stored in transmission line for unstable case when fault is on line 26-27. (Constant impedance load model)

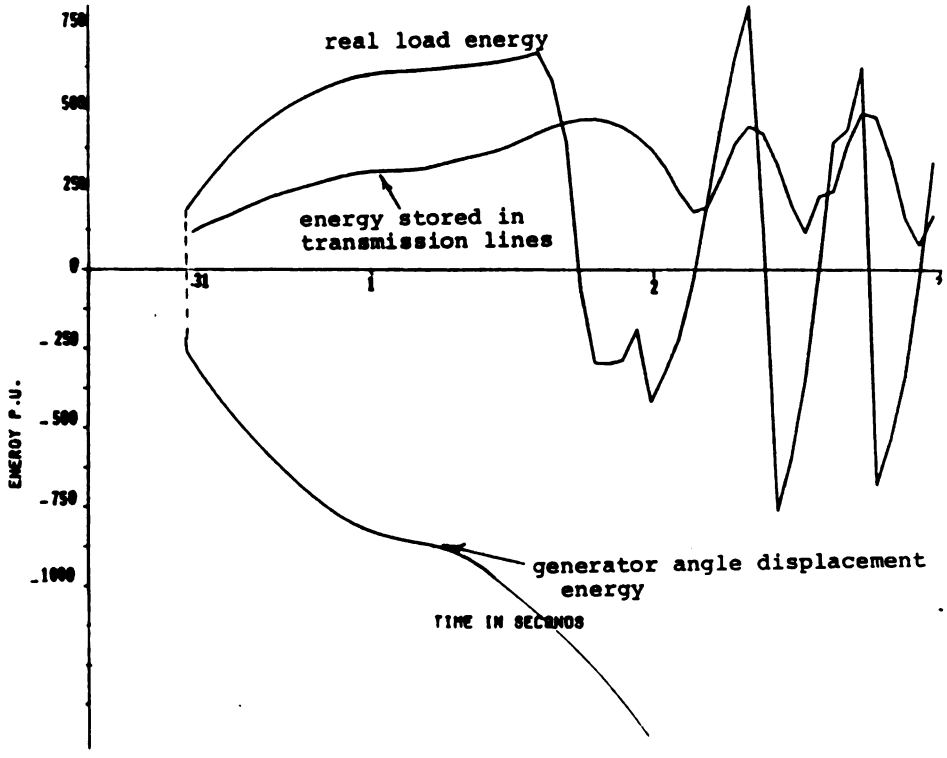

Fig. (8.d) Variations of reactive load energies for the unstable case when the fault is on line 26-27. (Constant impedance load model)

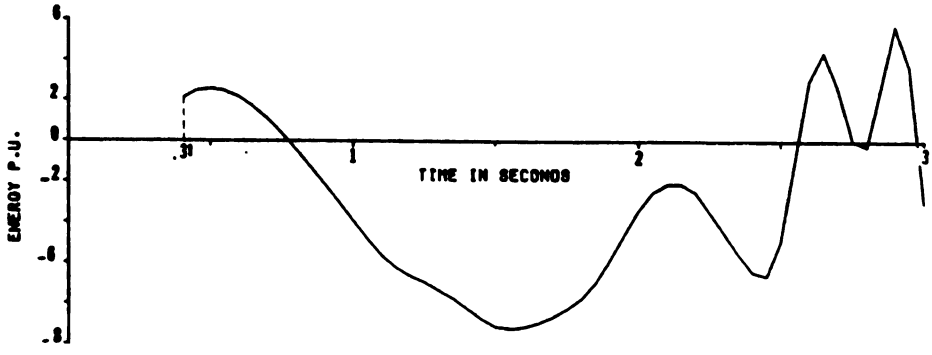

Fig. (9.a) Variation of angles and generators 7, 8 and 6 for the stable case when the fault on line 21-22 is cleared at 0.15 seconds and line 21-22 is removed. (Constant current load model)

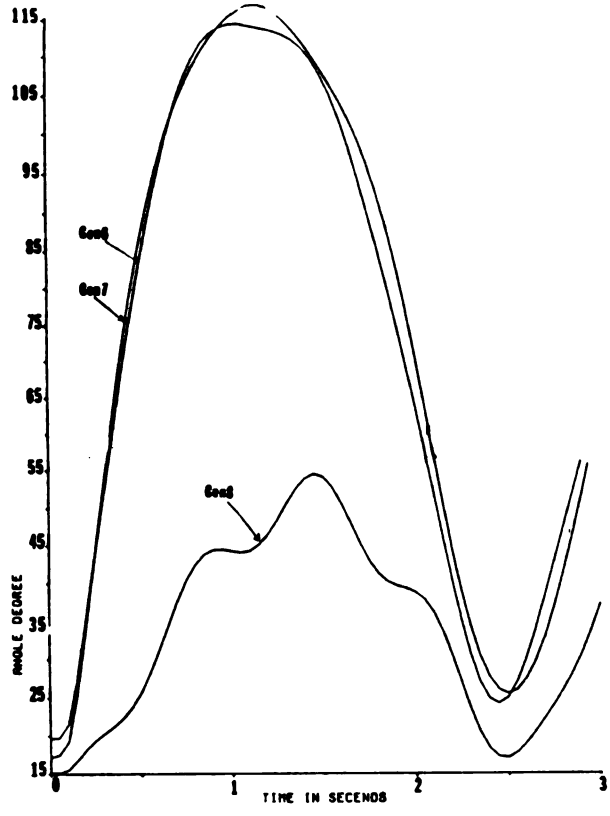

Fig. (9.b) Changes of potential, kinetic and total energies for the stable case where fault was on line 21-22. (Constant current load model)

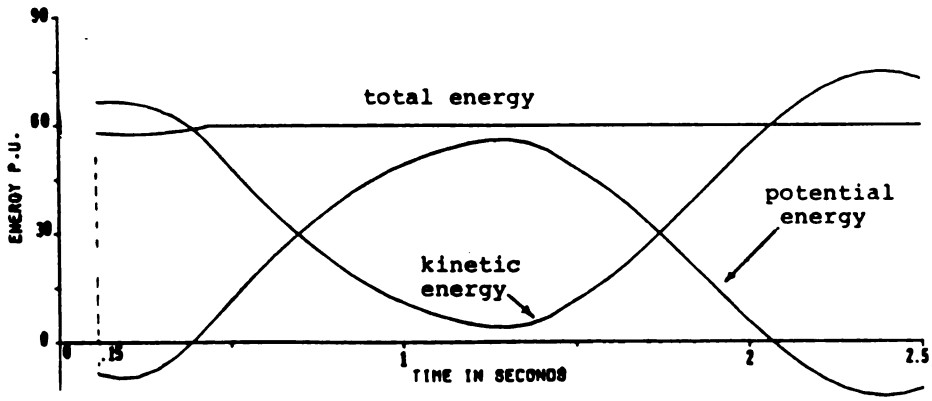

Fig. (9.c) Variations of real power load energy, energy stored in transmission lines and energy due to generator angle displacement for stable case when the fault is on line 21-22. (Constant current load model)

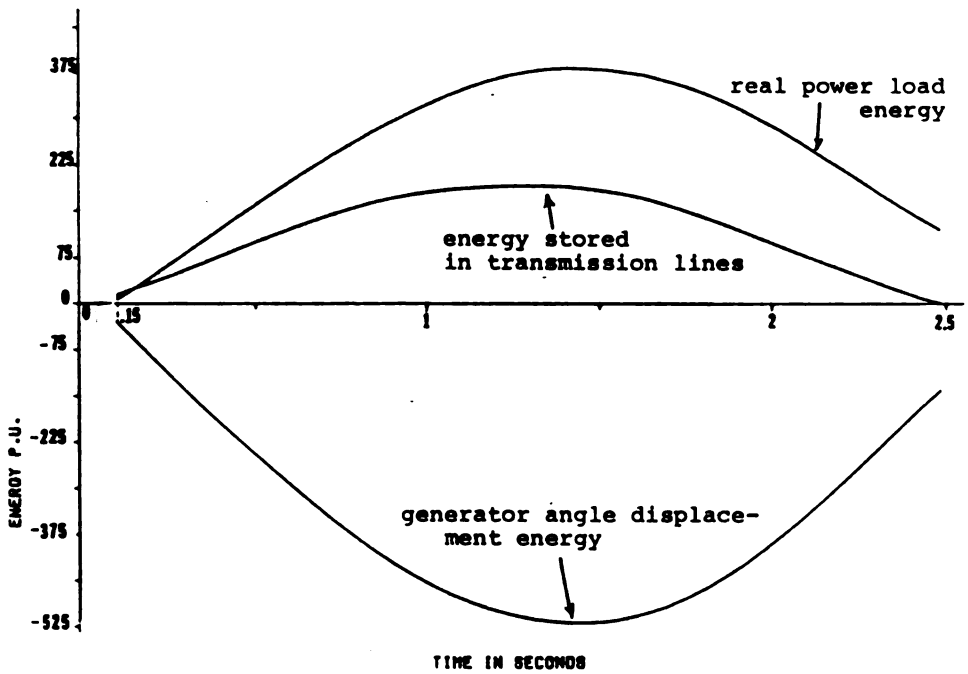

Fig. (9.d) Changes of reactive power load energy for the stable case when the fault is on line 21-22.

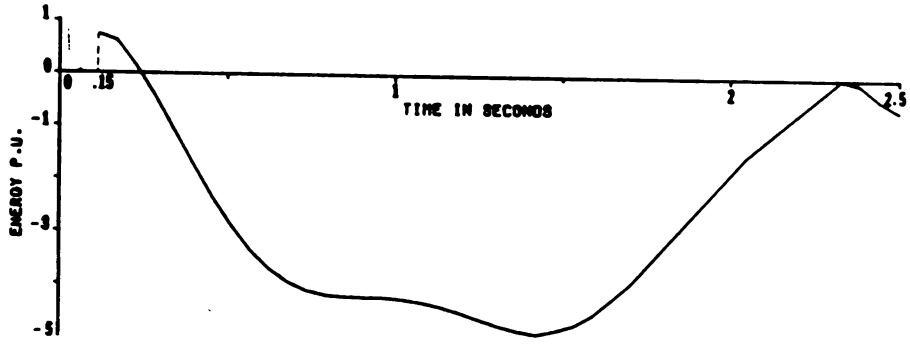

Fig. (10.a) Variation of angles of generator 6, 7 and 8 for unstable case where fault on line 21-22 is cleared in 0.36 seconds and the faulted line is cleared.

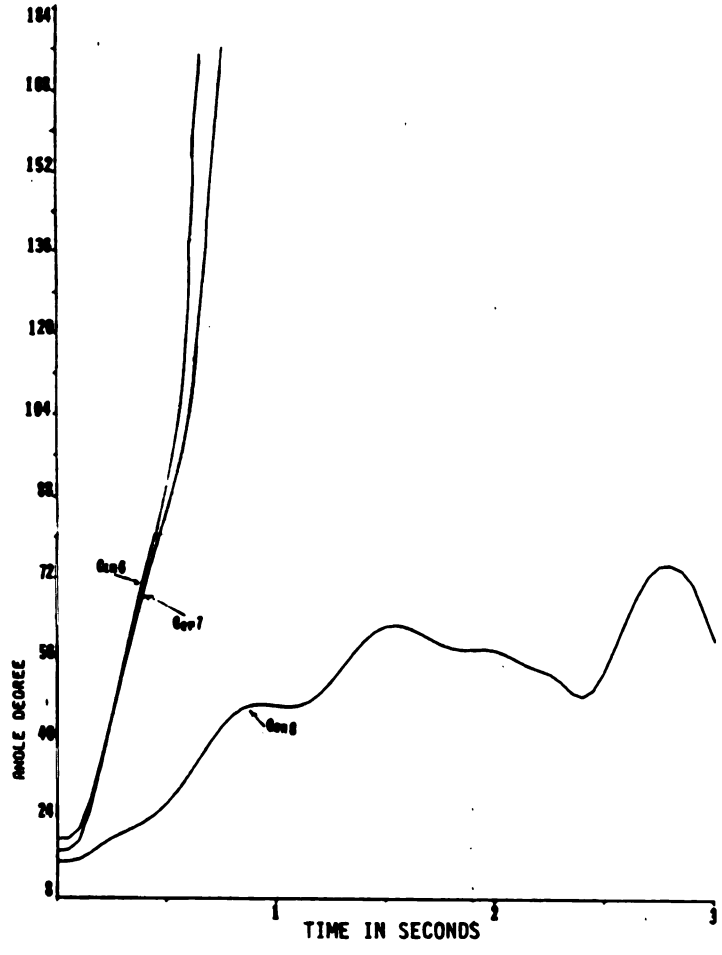

Fig. (10.b) Variations of potential, kinetic and total energy for unstable case when fault is on line 21-22. (Constant current load model)

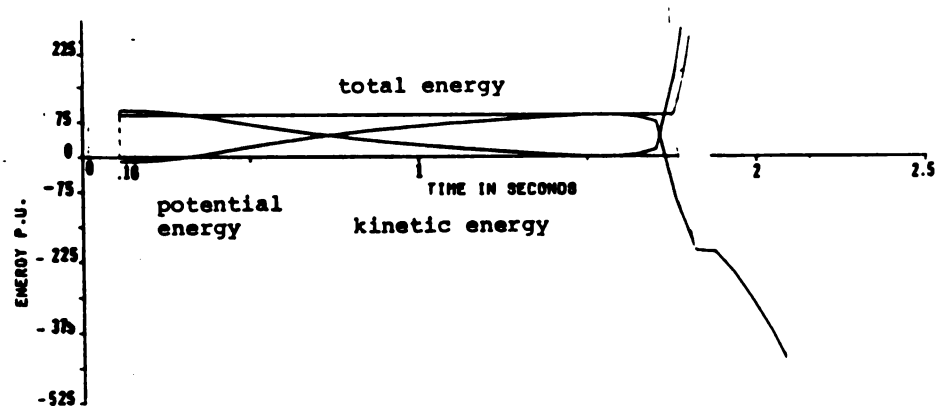

Fig. (10.c) Variations of loads real power energy, and energy stored in transmission lines and energy due to generator angle displacement for unstable case when fault is on line 21-22. (Constant current load model)

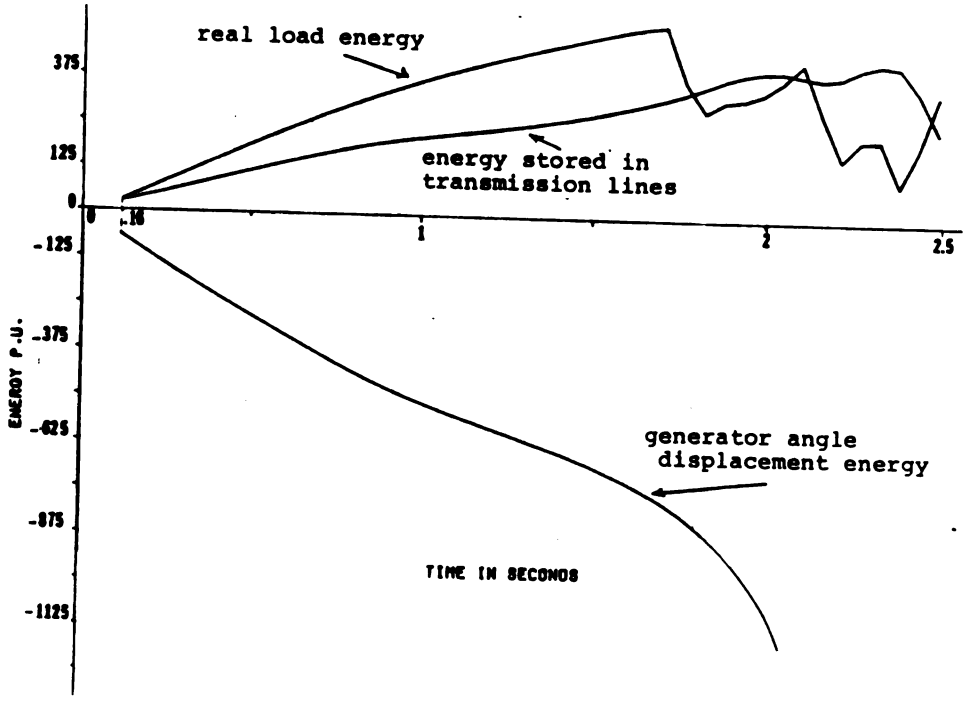

Fig. (10.d) Variations of loads reactive power energy for the unstable case when fault is on line 21-22. (Constant current load model)

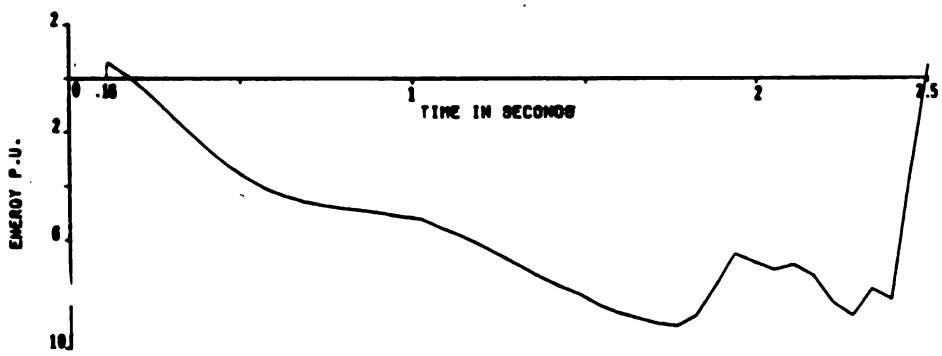

Fig. (11.a) Variation of angle of generators 6, 7 and 8 for the stable case when fault occurs on line 21-22. The fault is cleared at 0.13 seconds and line 21-22 is removed. (Constant impedance load model)

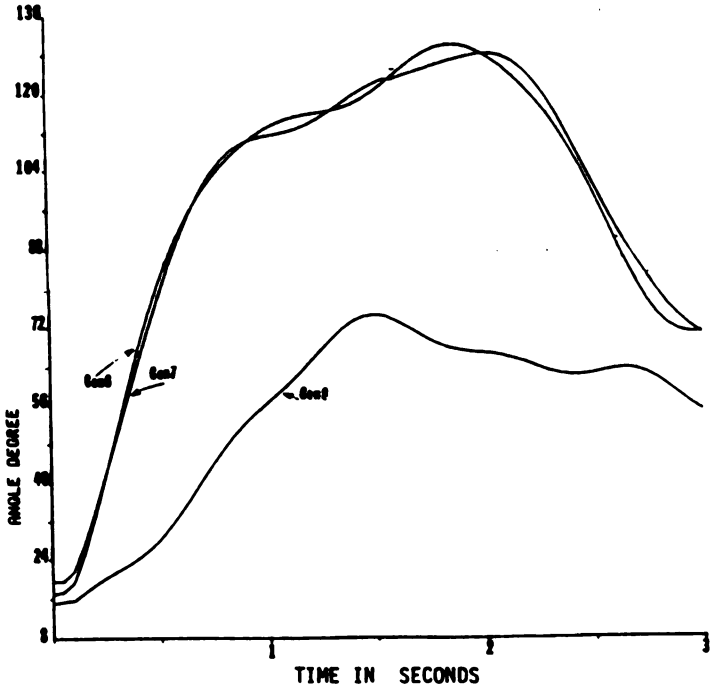

Fig. (11.b) Variations of total, kinetic and potential energies for the stable case when the fault is on line 21-22. (Constant impedance load model)

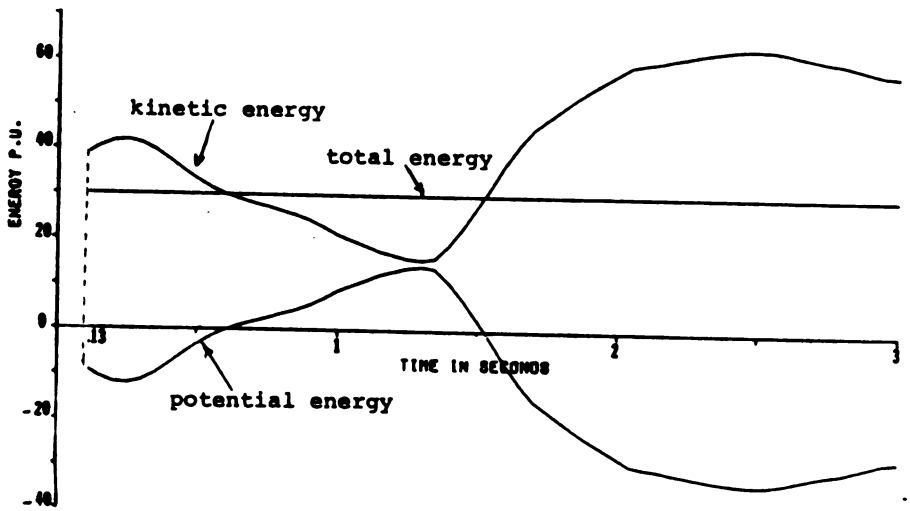

Fig. (11.c) Changes of energy stored in transmission line and energy due to generator angle displacement, and energy stored in real power loads for the stable case when the fault is on line 21-22. (Constant impedance load model)

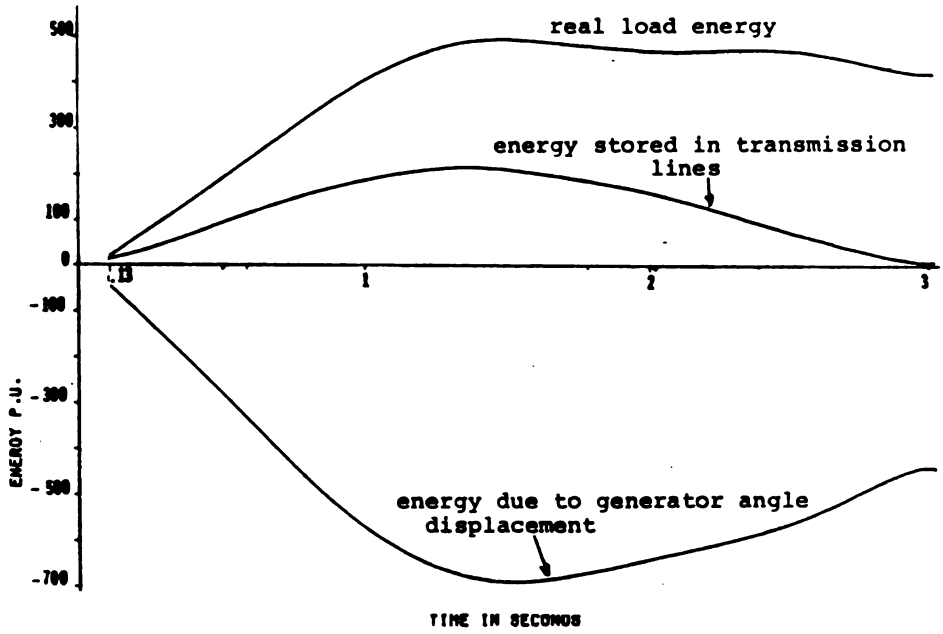

Fig. (11.d) Variations of reactive load power energy for the stable case where fault is on line 21-22. (Constant impedance load model)

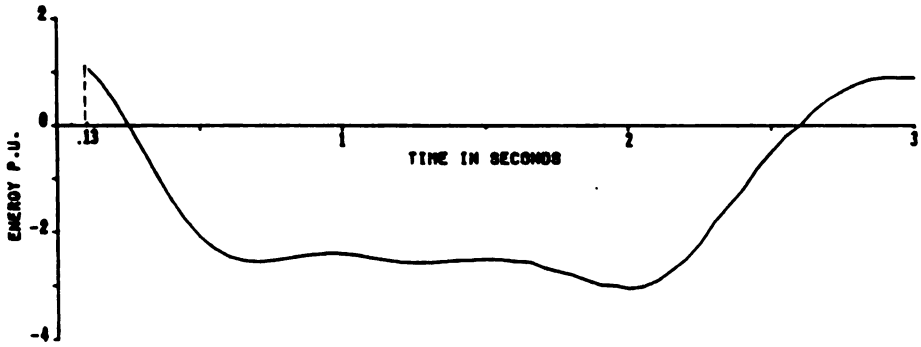

Fig. (12.a) Variation of angle of generators 6, 7 and 8 for unstable case when the fault occurs on line 21-22. The fault is cleared at 0.14 seconds and line 21-22 is removed. (Constant impedance load model)

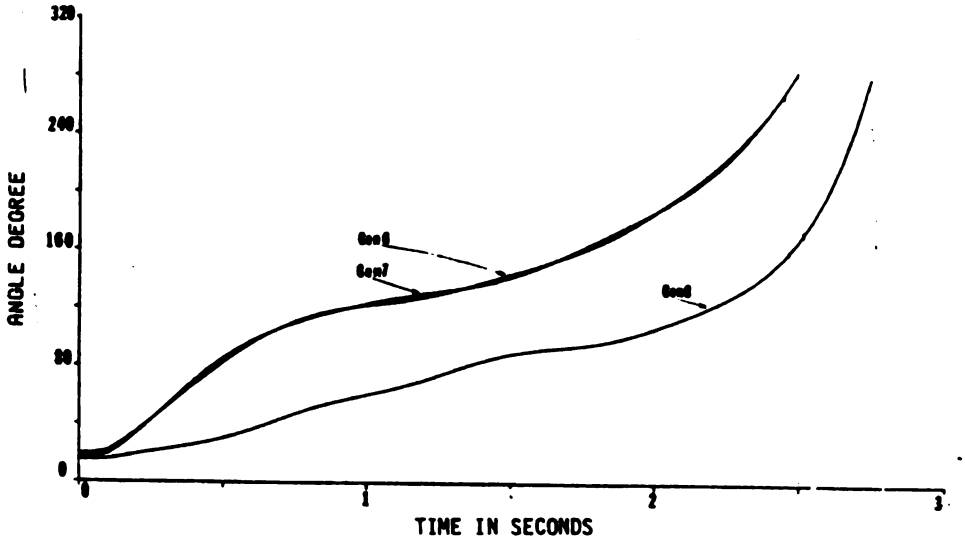

Fig. (12.b) The variation of total, potential and kinetic energy for the unstable case when the fault is on line 21-22. (Constant impedance load model)

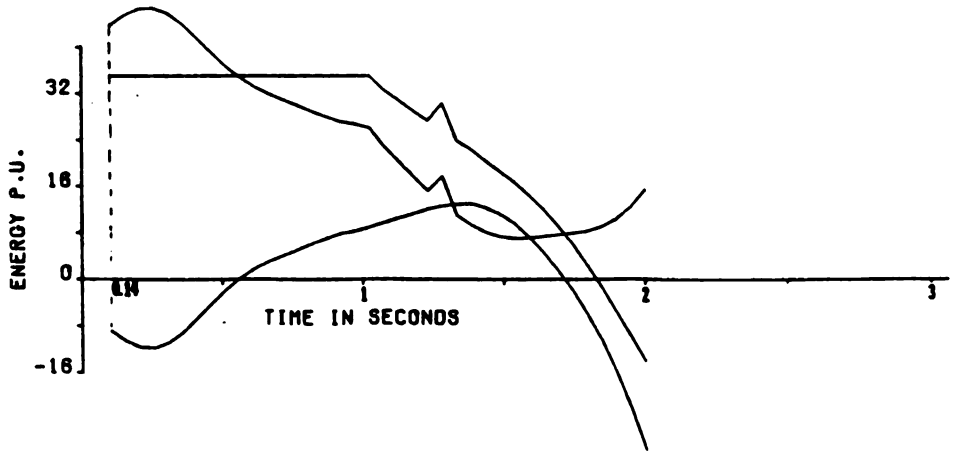

Fig. (12.c) Changes of real load energy and energy due to generator angle displacement and energy stored in transmission lines for the unstable case when the fault is on line 21-22. (Constant impedance load model)

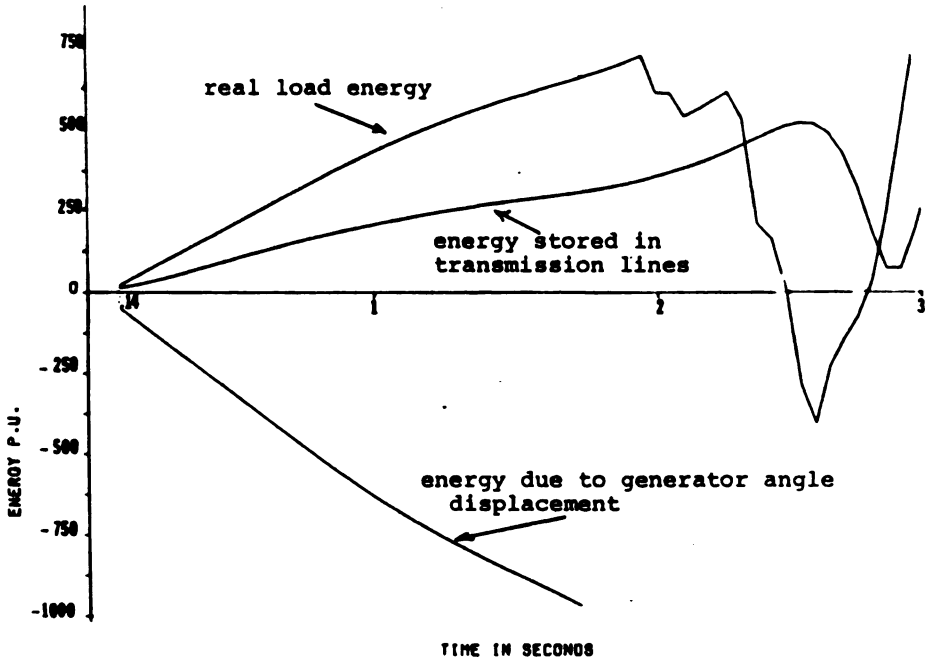

Fig. (12.d) Changes of reactive load power energy for the unstable case when the fault is on line 21-22. (Constant impedance load model)

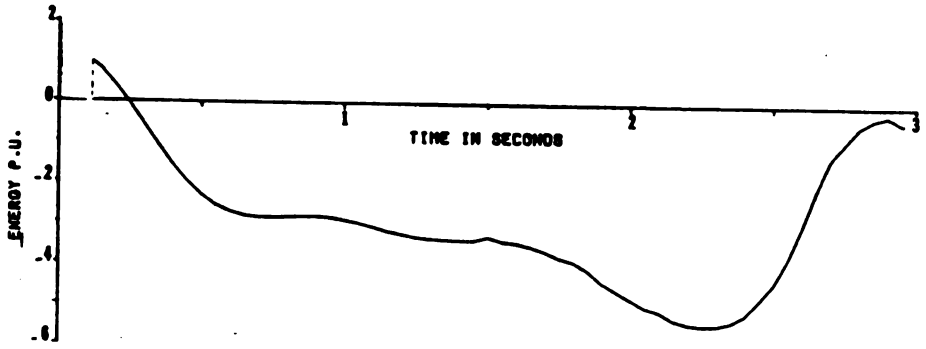

APPENDIX 3-A

Notation and system modeling:

N number of buses

N_g number of generators

P_{li} real load at load bus i

P_{mi} mechanical power input at generator i

M_i inertia constant at generator i

E_i voltage of generator bus i

V_i voltage of nongenerator bus i

B_{ij} imaginary part of admitance of line i-j

P_i real power leaving bus i, through the transmission system

Q_i reactive power leaving bus i, through the transmission system

m_i fictitious inertia for load buses where $M_i = \varepsilon m_i$

M_T $M_T = \sum_{i=1}^{N_g} M_i + \varepsilon \sum_{k=N_{g+1}}^{N} m_k$

where ε is pertubation factor

δ_o center of inertia angle $\delta_o = \frac{1}{M_T} \sum_{i=1}^{N_g} M_i \delta_i + \varepsilon \sum_{k=N_{g+1}}^{N} M_k \delta_k$

δ_i angle of generator bus i

θ_i angle of nongenerator bus i

ω_i $\omega_i = \dot{\delta}_i$

ω_o center of inertia frequency $\omega_o = \frac{1}{M_T} \sum_{i=1}^{N_g} M_i\omega_i + \varepsilon \sum_{k=N_{g+1}}^{N} M_k\omega_k$

$\tilde{\omega}_i$ $\tilde{\omega}_i = \omega_i - \omega_o$ where $\sum_{i=1}^{N} M_i\tilde{\omega}_i = 0$

D_i damping power coefficient

d_i fictitious damping power coefficient for load buses, $D_i = \varepsilon d_i$

T'_{doi} d-axis transient open circuit time constant.

x_{di}, x'_{di} d-axis synchronous and transient reactances

The symbol "′" when appearing above matrices or vectors is standing for transposed.

The symbol "s" when appearing above characters stands for stable equilibrium point.

CHAPTER 4

A LYAPUNOV ENERGY FUNCTION

A topological Lyapunov function is derived in this chapter for

1) a nonaggregated network model;

2) a constant real power load model;

3) a constant current reactive load model;

4) a single axis generator model that includes flux decay.

The Lyapunov function is derived based on assuming that a fictitious single axis machine exists at every load bus that is eliminated by allowing the inertia to approach zero and appropriate impedances to become infinite. The resultant Lyapunov function is constructed based on showing that the power system transient stability model is a Lure type model and can satisfy the Popov stability criterion, and the conditions imposed by the Moore-Anderson theorem [9] in some domain of the state space. The construction method of Willems [11] is then applied to determine the resultant Lyapunov function. The fictitious generators at load buses are then eliminated and the resultant Lyapunov function is shown to be identical to the energy function derived in the previous chapter if the real power load is constant power, the reactive power load is constant current, and the single

axis generator model is assumed to be a constant voltage behind transient reactance model.

The resultant Lyapunov function and its region of stability S provide the basis for determining necessary and sufficient conditions at some time t* that determine a region of instability. These region of instability and the region of stability derived and discussed in Chapter 5 are both based on the network conditions imposed by the Popov stability criterion and provide an accuracy in characterizing retention and loss of stability that was previously impossible.

The energy components of the Lyapunov energy function associated with different components of the transient stability model are plotted for different fault cases in Section 4.

4.1 Theoretical Background

The theoretical background required to derive the Lyapunov function is now presented.

a) Popov Criteria

For the system:

$$\dot{\underline{x}} = \underline{A}\ \underline{x} - \underline{B}\ \underline{f}(\underline{\sigma}) \qquad (4.1)$$

$$\underline{\sigma} = \underline{c}'\underline{x} \qquad (4.2)$$

where $\underline{f}(\underline{\sigma})$ is a nonlinear function of $\underline{\sigma}$ satisfying the following conditions:

i) $\underline{f}(\underline{\sigma})$ is continuous and maps R^N into R^N

ii) for some real constant matrix $\underline{H}$:

$$\underline{f}'(\underline{\sigma})\ \underline{H}\ \underline{\sigma} \geq 0 \qquad \text{for all } \underline{\sigma} \in R^N \tag{4.3}$$

and $\underline{f}(\underline{\sigma}) = \underline{0}$ for $\underline{\sigma} = \underline{0}$

iii) there exists a function $V_1 \in C^1$ mapping R^N into R such that

$V_1(\underline{\sigma}) \geq 0$ for all $\underline{\sigma} \in R^N$

and $V_1(\underline{\sigma}) = \underline{0}$ for $\sigma = 0$

and for some constant real matrix $\underline{Q}$

$$\Delta V_1(\underline{\sigma}) = \underline{Q}'\underline{f}(\underline{\sigma}) \quad \text{for all } \underline{\sigma} \in R^N \tag{4.4}$$

b) It can be verified [6] that the transfer function for the linear part of (4.1) is an NxN matrix:

$$\underline{W}(s) = \underline{C}'(s\underline{I}-\underline{A})^{-1}\underline{B}$$

$$\text{and } W(\infty) = 0 \tag{4.5}$$

The Moore-Anderson theorem that establishes sufficient conditions for a system to be asymptotically stable is now presented.

Moore-Anderson Theorem 1 [9]

If there exists real matrices $\underline{H}$ and $\underline{Q}$ such that:

$$\underline{Z}(s) = (\underline{H}+\underline{Q}s)\ \underline{W}(s) \tag{4.6}$$

is positive real, then the system defined by (4.1) and (4.2) satisfying the Popov criterion asymptotically stable in the large providing $(\underline{H} + \underline{Q}s)$does not cause any pole zero cancellation with $\underline{W}(s)$.

The conditions for $\underline{W}(s)$ to be positive real are:

1) $Z(s)$ has elements which are analytic for $Re(s)>0$ (4.6.a)

2) $Z^*(s) = Z(s^*)$ for $Re\ S>0$ (4.6.b)

3) $Z^T(s^*) + Z(s)$ is positive semidefinite for $ReS>0$ (4.6.c)

The notation (*) stands for conjugate of a complex variable.

Theorem 2 [6]

Given $\underline{H}$ and $\underline{Q}$ satisfying the condition of the Moore-Anderson theorem, then a Lyapunov energy function of the form:

$$V(x) = \frac{1}{2}\,\underline{x}'\,\underline{P}\,\underline{x} + V_1(\underline{\sigma}) \tag{4.7}$$

exists. $\underline{P}$ is obtained as a positive definite matrix satisfying the following set of nonlinear algebraic equations:

$$\underline{A}'\underline{P} + \underline{P}\,\underline{A} = -\,\underline{L}\,\underline{L}' \tag{4.8}$$

$$\underline{P}\,\underline{B} = \underline{C}\,\underline{H}' + \underline{A}\,\underline{C}\,\underline{Q}' - \underline{L}\,\underline{W}_o \tag{4.9}$$

$$\underline{W}_o'\underline{W}_o = \underline{Q}\,\underline{C}'\underline{B} + \underline{B}'\underline{C}\,\underline{Q} \tag{4.10}$$

where $\underline{L}$ and $\underline{W}_o$ are auxiliary matrices, the derivative of this Lyapunov function:

$$\dot{V}(x) = -\frac{1}{2}[\underline{x}'C - \underline{f}(\underline{\sigma})\underline{W}_o']\ [\underline{L}'\underline{x} - \underline{W}_o\underline{f}(\underline{\sigma})] - \underline{f}(\underline{\sigma})\underline{H}\underline{\sigma} \tag{4.11}$$

should be negative definite.

After recalling these theorems the next step is to test and apply the conditions embodied in these theorems to construct a Lyapunov function for a power system model that

1) retains the network and does not aggregate the network back to internal generator model;

2) utilizes a one axis synchronous machine model that incorporates flux decay for each generator in the system;

3) a fictitious one axis synchronous machine model at each load bus that is ultimately eliminated from the model after the Lyapunov function is constructed. This one axis synchronous machine model is eliminated by letting its inertia approach zero, transient reactance approach infinity and the differences between the synchronous and transient reactance approach infinity. These three assumptions eliminate the electromechanical model of the machine, and eliminate the armature reaction effects of stator current on the magnitude of the induced voltage on the stator;

4) a constant current reactive load model;

5) a constant power real power load model.

4.2 Lyapunov Energy Function Derivation

The notation used in this chapter is identical to that used in Chapter 3 except that E_i is used to represent the voltage magnitude at internal generator buses and network buses. Furthermore, since there is no need to distinguish the energy associated with generator transient reactance, x'_{di} from the energy stored in any network branch the generator internal buses will be numbered 1,2,....,Ng the general terminal buses will be numbered Ng+1,...2Ng, and the network buses will be numbered as 2Ng+1,...N. The generator transient reactance will be included as

$$B_{ii} = -B_{i+Ng}\ i = -B_{i,\ i+Ng} = -\frac{x}{x_d}$$

$$B_{i+Ng,\ i+Ng} = -\sum_{j=Ng+1}^{N_{g+N}} B_{i+Ng,j} - \frac{1}{x_d}$$

$$B_{ij} = 0 \quad i \neq j;\ ij \neq j + Ng,\ j \text{ and } i,\ Ng+i$$

$$i,j = 1,2,\ldots,Ng$$

Since the internal generator admittance of the fictitious generators is zero and ultimately will disappear, the transient admittance of these machines is omitted and the internal generator bus of the fictitious generator at load bus i is assumed to be the load bus i itself. These assumptions allow derivation of the Lyapunov function.

4.2.1 System Modeling

a) Generators -

The flux linkage is considered in generator modeling hence the generator i is governed by the following equation [6]

$$M_i\ddot{\delta}_i + D_i\dot{\delta}_i = \sum_{j=1}^{N} B_{ij}(E_i^s E_j^s \text{ Sin } \delta_{ij}^s - E_i E_j \text{ Sin } \delta_{ij}) \quad (4.12)$$

$$\dot{E}_i = -\alpha_i(E_i - E_i^s) - \beta_i \sum_{\substack{j=1 \\ j\neq i}}^{N} B_{ij}(E_j^s \text{ Cos } \delta_{ij}^s - E_j \text{Cos}\,\delta_{ij}) \quad (4.13)$$

where $i=1,\ldots,Ng$

$$\alpha_i = [1-(x_{di}-x'_{di})B_{ii}]/T'_{doi} \text{ and } \beta_i = (x_{di}-x'_{di})/T'_{doi} \quad (4.14)$$

b) Load Buses -

Loads are modeled by fictitious generators connected to the load buses hence:

$$\varepsilon m_i \ddot{\delta}_i + \varepsilon d_i \dot{\delta}_i = \sum_{i=1}^{N} B_{ij}(E_i^s E_j^s \text{ Sin } \delta_{ij}^s - E_i E_j \text{ Sin } \delta_{ij}) \quad (4.15)$$

and

$$\dot{E}_i = -\alpha_i(E_i - E_i^s) - \beta_i \sum_{\substack{j=1 \\ j\neq i}}^{N} B_{ij}(E_j^s \text{ Cos } \delta_{ij}^s - E_j \text{ Cos } \delta_{ij})$$

$$\text{for } i = N_{g+1}, \ldots, N \quad (4.16)$$

where

$$\alpha_i = (1 - \frac{(x_{di} - x'_{di})}{\varepsilon} B_{ii})/T'_{doi}$$

$$= (1 - (x_{di} - x_{di}) B_{ii})/T'_{doi} \quad (4.17a)$$

$$\beta_i = \frac{(x_{di} - x'_{di})}{\varepsilon}/T'_{doi} = (x_{di} - x'_{di})/T'_{doi} \quad (4.17b)$$

It is also assumed that the real power delivered to each load bus is constant and

$$Pl_i = \sum_{i=1}^{N} B_{ij} E_i E_j \text{ Sin } \delta_{ij} = \text{Constant} \quad (4.18)$$

and that the mechanical input power to each generator is constant and given by:

$$Pm_i = \sum_{j=1}^{N} E_i^s E_j^s B_{ij} \text{ Sin } \delta_{ij}^s \qquad \text{for } i = N_{g+1}, \ldots . N \quad (4.19)$$

All the equations presented in sections a and b are true for the post fault network.

4.2.2 Satisfaction of Moore-Anderson Theorem Conditions

Having defined the power system model we must

1) express it in Lure form (4.1)(4.2);

2) show that Popov statutory criterion is satisfied

3) establish that $\underline{Z}(s)$ is positive real.

In order to show that it satisfies the conditions in the Moore-Anderson theorem, having shown that the above conditions can be satisfied, then Theorem 2 can be applied to actually construct the Lyapunov function in the next subsection.

The first task in derivation of the Lyapunov function is to express (4.12), (4.13), (4.15) and (4.16) has Lure form given in (4.1) and (4.2). The following definitions are necessary:

$$\underline{x} = (\underline{\delta}_r' \quad \underline{\omega}' \underline{\Delta E}') \tag{4.20}$$

where

$$\delta_r = \delta_{1(i+1)} - \delta^s_{1(i+1)} \qquad \text{for } i=1,2,\ldots,N-1$$

$$\omega_i = \dot{\delta}_i \qquad \text{for } i=1,2,\ldots,N$$

$$\Delta E = E_i - E_i^o \qquad \text{for } i=1,2,\ldots,N$$

and also:

$$\underline{f}(\sigma) = \left[\underline{f}_1'(\sigma) \quad \underline{f}_2'(\sigma)\right] \tag{4.21}$$

where $\underline{f}_1(\underline{\sigma})$ is an m-vector defined by:

$$f_1(\sigma) = B_{ij}(E_iE_j \text{ Sin } (\sigma_k+\delta^s_{ij})-E^s_iE^s_j \text{ Sin } \delta^s_{ij}) \qquad (4.22)$$

for i=1,2,....,N-1 and j=i+1,....N

and k=1,2,....m where $m = \frac{N(N-1)}{2}$

and $f_2(\sigma)$ is a N-vector defined by:

$$f_{2i}(\sigma) = \sum_{j=1}^{N} B_{ij}(E^s_j \text{ Cos } \delta^s_{ij} - E_i \text{ Cos } \delta_{ij})$$

for i=1,2,....,N (4.23)

The members of vector σ used in function $f_1(\sigma)$ are defined as:

$$\sigma_k = \delta_{ij}-\delta^s_{ij} \qquad \text{for } k=1,2,....,m \qquad (4.24)$$

The members of vector σ used in function $f_{2i}(\sigma)$ are:

$$\sigma_k = E_i-E^s_i \qquad \text{for } k=m+1,....,M+N \qquad (4.25)$$

Considering the above definitions, the state equation matrices are:

$$\underline{A} = \begin{bmatrix} 0 & \underline{K}'_{N(N-1)} & 0 \\ 0 & -\underline{M}^{-1}\underline{D}_{NN} & 0 \\ 0 & 0 & -\underline{\alpha}_{NN} \end{bmatrix}, \quad \underline{B} = \begin{bmatrix} 0 & 0 \\ \underline{M}^{-1}\underline{T}_{NN} & 0 \\ 0 & \underline{\beta}_{NN} \end{bmatrix}$$

and

$$\underline{c} = \begin{bmatrix} \underline{G}_{(N-1)m} & 0 \\ 0 & 0 \\ 0 & \underline{I}_{NN} \end{bmatrix} \qquad (4.26)$$

where:

$$\underline{M}_{NN} = \text{diag}\ (M_i) \tag{4.27.a}$$

$$\underline{D}_{NN} = \text{diag}\ (D_i) \tag{4.27.b}$$

$$\underline{\alpha}_{NN} = \text{diag}\ (\alpha_i) \tag{4.27.c}$$

$$\underline{\beta}_{NN} = \text{diag}\ (\beta_i) \tag{4.27.d}$$

and

$$\underline{K}_{N(N-1)} = \begin{bmatrix} \underline{1}_{1(N-1)} \\ -\underline{I}_{(N-1)(N-1)} \end{bmatrix} \tag{4.28.a}$$

$$\underline{G}_{(N-1)m} = \begin{bmatrix} \underline{I}_{(N-1)(N-1)} & -T_{(N-1)(m-N+1)} \end{bmatrix} \tag{4.28.b}$$

The matrix $\underline{T}_{Nm}$ is of the following form:

$$\underline{T}_{Nm} = \begin{bmatrix} \underline{T}_1 & \underline{T}_2 & \underline{T}_3, \ldots, & \underline{T}_{Nm} \end{bmatrix} \tag{4.29}$$

$\underline{T}_i$ is an Nx($\underline{N}$-1) matrix of the form:

$$\underline{T}_i = \begin{bmatrix} \underline{0}_{(i-1)(N-i)} \\ \cdots\cdots\cdots\cdots\cdots\cdots \\ 1 \quad 1 \cdots\cdots\cdots\cdots\cdots 1 \\ -1 \quad 0 \cdots\cdots\cdots\cdots\cdots 0 \\ 0 \quad -1 \cdots\cdots\cdots\cdots\cdots 0 \\ \vdots \\ 0 \quad 0 \cdots\cdots\cdots\cdots\cdots -1 \end{bmatrix} \tag{4.30}$$

and:

$$\underline{T}_{Nm} = \left[\begin{array}{cc} 1_{1(N-1)} & 0_{1(m-N+1)} \\ \hline -I_{(N-1)(N-1)} & \underline{K}_{(N-1)(m-N+1)} \end{array}\right] \tag{4.31}$$

and:

$$\underline{T}_{Nm} = \underline{K}_{N(N-1)} \quad \underline{G}_{(N-1)m} \tag{4.32}$$

The system equations are now in the form of equations (4.1) and (4.2) and hence the conditions (i) and (ii) and (iii) of Popov criteria could be checked at this point. Let:

$$\underline{H} = \left[\begin{array}{cc} \frac{1}{q}\,\underline{I}_{mm} & \underline{0} \\ \underline{0} & \underline{0}_{NN} \end{array}\right] \tag{4.33}$$

With this choice of H the inequality of (4.3) is in the following simpler form:

$$f_1(\sigma_k)\ \sigma_k \geq 0 \text{ for all } k=1,2,\ldots,m \tag{4.44}$$

defines the region of stability S.

The above inequality is satisfied for the range of:

$$\sigma_{min}{}^k \leq \sigma_k \leq (0 \text{ or } \sigma_{s_k}) \text{ and } (0 \text{ or } \sigma_s) \leq \sigma_k \leq \sigma_{max}{}^k$$

where

$$\sigma_{min}{}^k = -\pi - (\delta^s_{ij} + \delta^o_{ij}) \quad , \ \sigma_{s_k} = \delta^o_{ij} - \delta^s_{ij}$$

and

$$\sigma_{max}{}^k = \pi - \delta^o_{ij} + \delta^s_{ij} \quad \text{and} \quad \delta^o_{ij} = \text{Sin}^{-1}\,(E^s_i E^s_j \text{ Sin } \delta^s_{ij} / E_i E_j)$$

which will be discussed further in Chapter 5 when the region of stability is more thoroughly discussed.

Considering the transfer function for the linear part of the system:

$$\underline{W}(s) = \underline{C}'(\underline{sI}-\underline{A})\ \underline{B} = \begin{bmatrix} \underline{T}'(s(s\underline{I}+\underline{M}^{-1}\underline{D})^{-1} & \underline{M}^{-1}\underline{T} & 0 \\ 0 & & S(SI+\alpha)^{-1}\ \beta \end{bmatrix}$$

$$= \begin{bmatrix} \underline{W}_1(s) & 0 \\ 0 & \underline{W}_2(s) \end{bmatrix} \qquad (4.34)$$

The matrices $\underline{H}$ and $\underline{Q}$ should be found satisfying the conditions Moore-Anderson theorem including the constraint (4.3) of the Popov criterion. A possible choice of $\underline{H}$ could have been the zero matrix but this would have caused $\underline{H}+\underline{Q}s$ to have a pole zero cancellation with $\underline{W}(s)$ which has a pole at s=0, this justifies the choice of $\underline{H}$ as in (4.33). The next step is the choice of $V_1(\sigma)$ in (iii) of the Popov criteria, and consequently matrix $\underline{Q}$.

$V_1(\sigma)$ is chosen as:

$$V_1(\sigma) = \sum_{k=1}^{m} \int_0^{\sigma_k} f_1(\sigma)d\sigma = \frac{1}{2}\sum_{i=1}^{N}\sum_{j=1}^{N} B_{ij}(E_iE_j(\text{Cos}\ \delta_{ij}^{s}-\text{Cos}\ \delta_{ij})$$

$$- (\delta_{ij}-\delta_{ij}^{s})E_i^{s}E_j^{s}\ \text{Sin}\ \delta_{ij}^{s}) - \frac{1}{2}\sum_{i=1}^{N}\sum_{\substack{j=1 \\ j\neq 1}}^{N}(E_i-E_i^{s})(E_j-E_j^{s})B_{ij}\ \text{Cos}\ \delta_{ij}^{s})$$

(4.35)

It is obvious that $V_1(\sigma)$ is positive just for a range of $\underline{\sigma}$ around $\underline{\sigma=0}$. This condition is very practical in the stable case because the angle separation of the lines remains almost the same and in the stable case there is no voltage collapse or large increase.

After the choice of $V_1(\sigma)$ matric $\underline{Q}$ could be chosen to satisfy (4.4), that is:

$$V_1(\underline{\sigma}) = \underline{Q}'\underline{f}(\underline{\sigma}) \qquad \text{for all } \underline{\sigma}\epsilon R^N \qquad (4.4)$$

The components of $\underline{\Delta}V_1(\sigma)$ are:

$$\frac{dV_i}{d\sigma_k} = B_{ij}\,(E_iE_j \text{ Sin } (\sigma_k+\delta^s_{ij})-E^s_iE^s_j \text{ Sin } \delta^s_{ij}) \qquad (4.36)$$

$$\text{for } k=1,2,\ldots,m$$

and

$$\frac{dV_i}{d\sigma_k} = -\sum_{\substack{j=1\\ j\neq i}}^{N} B_{ij}(E_j-E^s_j) \text{ Cos } \delta^s_{ij}+B_{ij}E_j(\text{Cos}\delta^s_{ij}-\text{Cos}\delta_{ij}) =$$

$$\sum_{\substack{j=1\\ j\neq i}}^{N} B_{ij}(E^s_j \text{ Cos } \delta^s_{ij}-E_j \text{ Cos } \delta_{ij}) \qquad \text{for } k=m+1,\ldots,m+N \qquad (4.37)$$

It could be concluded that [6]:

$$V_{\underline{1}}(\underline{\sigma}) = \underline{I}_{(m+N)(m+N)}\underline{f}(\underline{\sigma}) \qquad (4.38)$$

and the value of $\underline{Q}$ by comparing (4.4) and (4.38) is:

$$\underline{Q} = \underline{I}_{(m+N)(m+N)} \qquad (4.39)$$

Having found the matrices $\underline{H}$ and $\underline{Q}$ for the Moore-Anderson theorem, the next step is verifying the positive realness of matrix Z(s), defined in (4.6) as:

$$\underline{Z}(s) = (\underline{H}+\underline{Q}s)\underline{W}(s) \qquad (4.6)$$

Substituting for $\underline{H}$ and $\underline{Q}$ and $\underline{W}(s)$ in (4.6):

$$\underline{Z}(s) = \begin{bmatrix} ((\frac{1}{q} + s)\ \underline{T}'[s\underline{I}\ \underline{M}^{-1}\underline{D}]^{-1}\ \underline{M}^{-1}\underline{T}\ ) & 0 \\ 0 & s[s\underline{I}+\underline{\alpha}]^{-1}\ \underline{\beta} \end{bmatrix}$$

$$= \begin{bmatrix} \underline{Z}_1(s) & 0 \\ 0 & \underline{Z}_2(s) \end{bmatrix} \qquad (4.40)$$

Since $\underline{Z}(s)$ is block diagonal with diagonal blocks $\underline{Z}_1(s)$ and $\underline{Z}_2(s)$, each one of them can be looked at separately.

It is obvious that conditions (4.6.a) and (4.6.b) hold for $\underline{Z}_1$ and $\underline{Z}_2$. Condition (4.6.c) holds under the condition $q > m_i/d_i$ and $\beta_i > o$ for $i=1,2,\ldots,N$.[6]

4.3 Construction of the Lyapunov Function

It could be shown that it is possible to find matrices H and Q to satisfy the Moore-Anderson theorem condition such that a Lyapunov function of the form:

$$V(X) = \frac{1}{2}\ \underline{X}'\ \underline{P}\ \underline{X} + V_1(\underline{\sigma}) \qquad (4.7)$$

can be constructed, where $\underline{P}$ is a positive definite symetric matrix satisfying 4.8 and 4.9 and 4.10 and has the form:

$$\underline{P} = \begin{bmatrix} \underline{P}_1 & 0 \\ 0 & \underline{P}_2 \end{bmatrix} \qquad (4.41.a)$$

L and W_o in 4.8 and 4.9 and 4.10 are auxiliary matrices.

Considering the fact that Z(s) is positive real and recalling Lemmas 4-A-3 and 4-A-4 and results of 4-A-1 from appendix 4-A, Z(s) + Z(-s) can be factorized as:

$$Z(s)+Z'(-s) = Y'(-s)Y(s) \qquad (4.41.b)$$

where Y(s) has the minimum realization (A,B,L) i.e.

$$Y(s)-Y(\infty) = L'(SI-A)^{-1}B \qquad (4.41.c)$$

and

$$W_o = Y(\infty) \qquad (4.41.d)$$

The matrix $\underline{W}_1(s)$ in (4.34) can also be written as:

$$W_1(s) = \underline{C}_1'(S\underline{I}-\underline{A}_1)^{-1}\underline{B}_1 \qquad (4.42)$$

where:

$$\underline{A}_1 = \begin{bmatrix} 0 & K' \\ 0 & -\underline{M}^{-1}\underline{D} \end{bmatrix}, \quad \underline{B}_1 = \begin{bmatrix} 0 \\ \underline{M}^{-1}\underline{T} \end{bmatrix} \text{ and } \underline{C}_1 = \begin{bmatrix} \underline{G} \\ 0 \end{bmatrix} \qquad (4.43)$$

It is trivial that $\underline{C}_1'\underline{B}_1=0$ and $\underline{B}'_1\underline{C}_1=0$ and so from (4.8) and (4.9) and (4.10) the following matrix equations hold for $\underline{P}_1$:

$$\underline{A}'_1\underline{P}_1 + \underline{P}_1\underline{A}_1 = -\underline{L}_1\underline{L}'_1 \leq 0 \qquad (4.44)$$

$$\underline{P}_1\underline{B}_1 = \underline{C}_1\underline{H}'_1 + \underline{A}'_1\underline{C}_1\underline{Q}'_1 \qquad (4.45)$$

Expanding (4.44):

$$\begin{bmatrix} \underline{P}_{11} & \underline{P}_{12} \\ \underline{P}_{21} & \underline{P}_{22} \end{bmatrix} \begin{bmatrix} 0 & \underline{K}' \\ 0 & -\underline{M}^{-1}\underline{D} \end{bmatrix} + \begin{bmatrix} 0 & 0 \\ \underline{K} & -\underline{M}^{-1}\underline{D} \end{bmatrix} \begin{bmatrix} \underline{P}_{11} & \underline{P}_{12} \\ \underline{P}_{21} & \underline{P}_{22} \end{bmatrix} =$$

$$\begin{bmatrix} 0 & \underline{P}_{11}\underline{K}'-\underline{P}_{12}\underline{M}^{-1}\underline{D} \\ \underline{K}\underline{P}_{11}-\underline{M}^{-1}\underline{D}\underline{P}_{21} & \underline{P}_{21}\underline{K}'+\underline{K}\underline{P}_{12}-\underline{P}_{22}\underline{M}^{-1}\underline{D}-\underline{M}^{-1}\underline{D}\underline{P}_{22} \end{bmatrix} = -\begin{bmatrix} \underline{L}_{11} \\ \underline{L}_{12} \end{bmatrix} [\underline{L}'_{11}\ \underline{L}'_{12}]$$

$$= -\begin{bmatrix} \underline{L}_{11}\underline{L}'_{11} & \underline{L}_{11}\underline{L}'_{12} \\ \underline{L}_{12}\underline{L}'_{11} & \underline{L}_{12}\underline{L}'_{12} \end{bmatrix} \qquad (4.46)$$

Considering (4.46), the following equations are found to hold:

$$\underline{L}_{11}\underline{L}'_{11} = 0 \qquad \Rightarrow \qquad \underline{L}_{11} = 0 \tag{4.47}$$

and:

$$\underline{P}_{11}\,\underline{K}' - \underline{P}_{12}\underline{M}^{-1}\underline{D} = \underline{L}_{11}\underline{L}'_{12} = 0$$

$$\underline{P}_{12}\,\underline{K}' + \underline{K}\,\underline{P}_{12} - \underline{P}_{22}\underline{M}^{-1}\underline{D} - \underline{M}^{-1}\underline{D}\,\underline{P}_{22} = -\underline{L}_{12}\underline{L}'_{12} \tag{4.48}$$

Evaluating the component matrices in equation (4.45)

$$\underline{P}_1\underline{B}_1 = \begin{bmatrix} \underline{P}_{11} & \underline{P}_{12} \\ \underline{P}_{12} & \underline{P}_{22} \end{bmatrix} \begin{bmatrix} 0 \\ \underline{M}^{-1}\underline{T} \end{bmatrix} = \begin{bmatrix} \underline{P}_{12} & \underline{M}^{-1}\,\underline{T} \\ \underline{P}_{22} & \underline{M}^{-1}\,\underline{T} \end{bmatrix} \tag{4.49}$$

$$\underline{C}_1\underline{H}' \quad \begin{bmatrix} \underline{G}(N-1)m \\ 0 \end{bmatrix} \quad \begin{bmatrix} 1/q\ \underline{I}_{mm} & 0 \\ 0 & 0 \end{bmatrix} = \begin{bmatrix} 1/q\,\underline{G} \\ 0 \end{bmatrix} \tag{4.50}$$

and using the property of $\underline{K}\,\underline{G} = \underline{T}$

$$\underline{A}'_1\underline{C}_1\underline{Q}'_1 = \begin{bmatrix} 0 & 0 \\ \underline{K} & -\underline{M}^{-1}\underline{D} \end{bmatrix} \begin{bmatrix} \underline{G} \\ 0 \end{bmatrix} \begin{bmatrix} I & 0 \\ 0 & \underline{I} \end{bmatrix} = \begin{bmatrix} 0 \\ \underline{K}\,\underline{G} \end{bmatrix} = \begin{bmatrix} 0 \\ \underline{T} \end{bmatrix} \tag{4.51}$$

hence the equation (4.45) becomes:

$$\begin{bmatrix} \underline{P}_{12}\underline{M}^{-1}\,\underline{T} \\ \underline{P}_{22}\underline{M}^{-1}\,\underline{T} \end{bmatrix} = \begin{bmatrix} \underline{G}/q \\ \underline{T} \end{bmatrix} \tag{4.52}$$

and so:

$$\underline{P}_{12}\underline{M}^{-1}\,\underline{T} = \frac{1}{q} \cdot \underline{G} \tag{4.53}$$

$$\underline{P}_{22}\underline{M}^{-1}\,\underline{T} = \underline{T} \tag{4.54}$$

While P_{22} is NxN and symetric and T is Nxm (4.54) can be expressed as:

$$(\underline{P}_{22}\,\underline{M}^{-1} - \underline{I}_{NxN})\,\underline{T} = \underline{0}_{Nxm} \tag{4.55}$$

The solution $\underline{P}_{22}$ is obtained by multiplying (4.55) by $\underline{M}$ to obtain

$$\underline{Y}\ \underline{T}_{Nxm} = \underline{0}_{Nxm} \tag{4.56}$$

and then solving it for $\underline{Y}$ =

$$\underline{Y} = \underline{M}\ [\underline{P}_{22}\underline{M}^{-1} - \underline{I}_{NxN}] \tag{4.57}$$

Y is an unknown symmetric matrix (NxN). P_{22} is then obtained knowing the solution for $\underline{Y}$. The procedure for determining $\underline{Y}$ is now discussed.

Considering the structure of matrix $\underline{T}$, each column contains only two nonzero elements, 1 and -1. This shows that all elements on the same row of Y are equal, and since Y is symmetric it follows that all elements of Y are equal. Hence a necessary and sufficient condition for a symmetric matrix Y to be a solution of (4.56) is that it has the form $Y=\mu U$, where μ is a scalar constant and U is an NxN matrix with all its elements equal to 1.

Now $\underline{M}\ \underline{P}_{22}\underline{M}^{-1} - \underline{M}$, is symmetric so from the above discussion

$$\underline{Y} = \underline{M}\ \underline{P}_{22}\underline{M}^{-1} - \underline{M} = \mu U \tag{4.58}$$

and:

$$\underline{M}\ \underline{P}_{22}\underline{M}^{-1} = \underline{M} + \mu\underline{U} \tag{4.59}$$

$$\underline{M}\ \underline{P}_{22} = \mu\underline{M}^{-1}\underline{U} + \underline{I} \tag{4.60}$$

$$\underline{P}_{22} = \underline{M} = \mu\underline{M}^{-1}\underline{U}\ \underline{M} \tag{4.61}$$

Since $\underline{P}_{12}$ is not symmetric consider (4.48):

$$\underline{P}_{11}\underline{K}' - \underline{P}_{12}\underline{M}^{-1}\underline{D} = \underline{0} \tag{4.62}$$

and

$$\underline{K}\ \underline{P}_{11}\ \underline{K}' - \underline{K}\ \underline{P}_{12}\ \underline{M}^{-1}\underline{D} = \underline{0} \tag{4.63}$$

Since $\underline{K}\ \underline{P}_{11}\ \underline{K}'$ is symmetric, then $\underline{K}\ \underline{P}_{12}\ \underline{M}^{-1}\underline{D}$ is symmetric from (4.63). From (4.53), it is apparent that

$$\underline{K}\ \underline{P}_{12}\underline{M}^{-1}\underline{T} = \underline{K} \cdot \frac{1}{q} \cdot \underline{G} = \frac{1}{q} \cdot \underline{T} \tag{4.64}$$

hence:

$$(\underline{K}\ \underline{P}_{12}\underline{M}^{-1}\underline{D} - \frac{1}{q} \cdot \underline{D})\ \underline{D}^{-1}\ \underline{T} = \underline{0}_{Nxm} \tag{4.65}$$

Matrix $\underline{K}\ \underline{P}_{12}\underline{M}^{-1}\underline{D}-\frac{1}{q}\underline{D}$is symmetric since $\underline{K}\ \underline{P}_{12}\underline{M}^{-1}\underline{D}$ is symmetric. Multiplying both sides by $\underline{D}^{-1}$:

$$\underline{D}^{-1}(\underline{K}\ \underline{P}_{12}\underline{M}^{-1}\underline{D} - \frac{1}{q}.\underline{D})\underline{D}^{-1}\underline{T} = \underline{Y}'\underline{T} = \underline{0}_{Nxm} \tag{4.66}$$

and following the same argument as before

$$\underline{Y}' = \underline{D}^{-1}(\underline{K}\ \underline{P}_{12}\underline{M}^{-1}\underline{D} - \frac{1}{q}D)D^{-1} = \rho\underline{U} \tag{4.67}$$

and thus:

$$\underline{K}\ \underline{P}_{12} = \underline{M} \cdot \frac{1}{q} + \underline{D}\ \underline{U}\ \underline{M} \tag{4.68}$$

The solution for $\underline{P}_{11}$ could therefore be concluded as:

$$\underline{K}\ \underline{P}_{11}\underline{K}' = \underline{K}\ \underline{P}_{12}\underline{M}^{-1}\underline{D} = \frac{1}{q} \cdot \underline{D} + \rho\underline{D}\ \underline{U}\ \underline{D} \tag{4.69}$$

In the above equations μ and ρ are nonnegative scalars and $\underline{U}$ is an NxN matrix with all elements equal to 1 and satisfying the following inequality:

$$2(D-M/q) + (\mu-\rho)\ (D\ U\ M + M\ U\ D) \geq 0 \tag{4.70}$$

The inequality (4.70) is originally obtained from an assures satisfaction of the following inequality:

$$\underline{P}_1\underline{A}_1 + \underline{A}'\underline{P}_1 \leq 0 \tag{4.71}$$

Considering the right hand side of (4.46) and recalling that $L_{11} = 0$, (4.71) would reduce to:

$$-L_{12}L'_{12} \leq 0 \tag{4.72}$$

Now by comparing the left hand side of (4.72) and right hand side of (4.46) it could be concluded that the following inequality should hold:

$$\underline{P}_{21}\ \underline{K}' + \underline{K}\ \underline{P}_{12} - \underline{P}_{22}\underline{M}^{-1}\underline{D} - \underline{M}^{-1}\underline{D}\ \underline{P}_{22} \leq 0 \tag{4.73}$$

Since the element $\underline{P}_{21}K'$ has not been defined yet at this point it is necessary to find the solution for $\underline{P}_{21}\underline{K}'$.

From (4.46) recall this equation:

$$\underline{K}\ \underline{P}_{11} = \underline{M}^{-1}\underline{D}\ \underline{P}_{21} = 0 \tag{4.74}$$

multiplying (4.74) from the right by K' and taking the second term to the right hand side:

$$\underline{K}\ \underline{P}_{11}\underline{K}' = \underline{M}^{-1}\underline{D}\ \underline{P}_{21}\underline{K}' \tag{4.75}$$

Substituting the result of (4.69) in (4.75):

$$\frac{1}{q} \cdot \underline{D} + \rho\underline{D}\ \underline{U}\ \underline{D} = \underline{M}^{-1}\underline{D}\ \underline{P}_{21}\ \underline{K}' \tag{4.76}$$

multiplying (4.76) from left by $\underline{D}^{-1}\underline{M}$:

$$\underline{M}.\frac{1}{q} + \underline{M}\ \underline{U}\ \underline{D} = \underline{P}_{21}\ \underline{K}' \tag{4.77}$$

now substituting (4.77) and (4.68) and (4.54) in (4.73):

$$2(\underline{D}-\underline{M}/q) + (\mu-\rho)\ (\underline{D}\ \underline{U}\ \underline{M} + \underline{M}\ \underline{U}\ \underline{D}) \geq 0 \tag{4.70}$$

The following discussion gives the condition for (4.70) to hold when it is equal to zero.

Let $\mu^* = \mu-\rho$, and consider:

$$2(\underline{D}-\frac{\underline{M}}{q} + \mu^*\ (\underline{D}\ \underline{U}\ \underline{M} + \underline{M}\ \underline{U}\ \underline{D}) = 0 \tag{4.78}$$

then

$$\frac{1}{2}\mu^*\ (\underline{D}-\frac{\underline{M}}{q})^{-1}(\underline{D}\ \underline{U}\ \underline{M} + \underline{M}\ \underline{U}\ \underline{D}) = -\underline{I}_{NxN} \tag{4.79}$$

Since μ^* is a scalar and the maximum rank of $\underline{D}\ \underline{U}\ \underline{M} + \underline{M}\ \underline{U}\ \underline{D}$ is 2, consider all the first and second order equations in terms of μ^*. The matrix $\frac{1}{2}\ [\underline{D} - \frac{\underline{M}}{q}]^{-1}[\ \underline{D}\ \underline{U}\ \underline{M} + \underline{M}\ \underline{U}\ \underline{D}]$ has the form:

$$\frac{1}{2}(D-\frac{M}{q})^{-1}(DUM+MUD)=\begin{bmatrix} \frac{2D_iM_i}{2(D_i-\frac{M_i}{q})} & \frac{D_2M_1+M_2D_1}{2(D_1-M_1/q)} & \cdots\cdots & \frac{M_nD_1+D_nM_1}{2(D_1-M_1/q)} \\ \frac{M_1D_2+D_1M_2}{2(D_2-M_2/q)} & \frac{2D_2M_2}{2(D_2-\frac{M_2}{q})} & \cdots\cdots & \frac{M_nD_2+M_2D_n}{2(D_2-\frac{M_2}{q})} \\ \vdots & & & \vdots \\ \frac{D_1M_N+M_1D_N}{2(D_N-\frac{M_N}{q})} & \cdots\cdots\cdots\cdots\cdots & & \frac{2M_ND_N}{2(D_N-\frac{M_N}{q})} \end{bmatrix} \tag{4.80}$$

Since the rank of equation (4.80) is 2 there are only two sets of equations in terms of μ^* that should be considered in (4.79). The first set are obtained by setting each diagonal element of the r.h.s. matrix in (4.80) to 1. These equations are

$$\frac{D_1M_1\mu^*}{(D_1-M_i/q} + 1 = 0 \tag{4.81}$$

$$\frac{D_NM_N\mu^*}{D_N-M_N/q} + 1 = 0$$

The other set are the second order equations that are the determinant of block diagonal 2x2 matrices in the r.h.s. matrix of (4.80). These N-1 equations are of the form:

$$\mu^{*2}\,\frac{(4D_1D_2M_1M_2-2M_1M_2D_1D_2-D2^2M_1^2-M_2^2D_1^2)}{4(D_1-\frac{M_1}{q})(D_2-\frac{M_2}{q})}-1=\frac{(D_1M_2-D_2M_1)^2\mu^{*2}}{4(D_1-\frac{M_1}{q})(D_2-\frac{M_2}{q})}-1=0$$

$$\frac{-(D_2M_3-D_3M_2)^2\mu^{*2}}{4(D_2-\frac{M_2}{q})(D_3-\frac{M_3}{q})}-1=0 \qquad (4.82)$$

$$\vdots$$

(N-1) terms

Adding these equations the following quadralic equation in i* is obtained

$$-\mu_*^2\sum_{i=1}^{N-1}\sum_{j=i+1}^{N}\frac{(D_iM_j-D_jM_i)^2}{4(D_i-\frac{M_i}{q})(D_j-M_j/q)}-(N-1)+\mu^*\sum_{i=1}^{N}\frac{D_iM_i}{D_i-\frac{M_i}{q}}+N=0 \qquad (4.83)$$

$$\therefore\ \mu^{*2}\sum_{i=1}^{N-1}\sum_{j=i+1}^{N}\frac{(D_iM_j-D_jM_i)^2}{4(D_i-\frac{M_i}{q})(D_j-\frac{M_j}{q})}-\mu^*\sum_{i=1}^{N}\frac{D_iM_i}{D_i-\frac{M_i}{q}}-1\leq 0 \qquad (4.84)$$

If μ^* lies between two roots of the solution of the quadratic equation, the above inequality holds.

When the damping torques are uniform μ^* reduces to μ_o where:

$$\mu_o=-1/\sum_{i=1}^{N}M_iD_i/(D_i-M_i/q) \qquad (4.85)$$

Having found $\underline{P}_1$, the following is a description of determining $\underline{P}_2$ of matrix $\underline{P}$.

Recalling the transfer function $W_2(s)$ from (4.34)

$$\underline{W}_2(s) = \underline{C}'_2(s\underline{I}-\underline{A}_2)^{-1}\underline{B}_2 \tag{4.86}$$

where:

$$\underline{A}_2 = -\underline{\alpha}_{NN}, \quad \underline{B}_2 = \underline{\beta}_{NN}, \quad \underline{C}_2 = \underline{I}_{NN} \tag{4.86.a}$$

Since $\underline{Z}_2(s)$ is positive real, using Lemma 4-A-3, $Z_2(s) + Z'_2(-s)$ can be factorized as

$$Z_2(s) + Z'_2(-s) = \underline{Y}'_2(-s)\underline{Y}_2(s) =$$

$$s(s\underline{I}+\alpha)^{-1}\,\underline{\beta} + s(s\underline{I}-\underline{\alpha})^{-1}\,\underline{\beta} = \text{diag}\,(\frac{s\sqrt{2}\beta_i}{s+\alpha_i}).\ \text{diag}\,(\frac{s\sqrt{2}\beta_i}{s-\alpha_i}$$

and so:

$$Y_2(s) = \text{diag}\,(\frac{s\sqrt{2}\beta_i}{s+\alpha_i}) \tag{4.87}$$

Considering Lemma 4-A-4[14], $Y_2(s)$ has the minimal realization as following:

$$\underline{Y}_2(s)-\underline{Y}_2(\infty) = \underline{L}_2(SI-A_2)^{-1}B_2 \tag{4.88}$$

solving (4.88) for $\underline{L}_2$:

$$L_2 = -\text{diag}\,(\sqrt{2}\,\alpha_i/\beta_i) \tag{4.89}$$

But L_2 and P_2 are related as:

$$\underline{P}_2\underline{A}_2 + \underline{A}'_2\underline{P}_2 = -\underline{L}_2\underline{L}'_2 \tag{4.90}$$

By solving (4.90) with (4.86.a) and (4.89), P_2 is determined as:

$$P_2 = \alpha\beta^{-1} \tag{4.91}$$

The Lyapunov energy function can now be found by substituting $\underline{P}_1$ and $\underline{P}_2$ into (4.7):

$$V(x)=\frac{1}{2}[\underline{\delta}'_r,\underline{\omega}',\Delta E']' \begin{bmatrix} \underline{P}_{11} & \underline{P}_{12} & 0 \\ \underline{P}_{21} & \underline{P}_{22} & 0 \\ 0 & 0 & \underline{P}_2 \end{bmatrix} \begin{bmatrix} \underline{\delta}_r \\ \underline{\omega} \\ \underline{\Delta E} \end{bmatrix} + V_1(\underline{\sigma}) =$$

$$\frac{1}{2}\,\delta'\,(\underline{D}/_q + \frac{1}{2}\,\underline{D}\,\underline{U}\,\underline{D})\underline{\delta} + \delta)'\,(\underline{M}/_q + P\,\underline{D}\,\underline{U}\,\underline{M})\underline{\omega}$$

$$+ \frac{1}{2}\,\underline{\omega}'(\underline{M} + \mu\underline{M}\,\underline{U}\,\underline{M})\underline{\omega} + \frac{1}{2}\underline{\Delta E}'\underline{\alpha}\,\underline{\beta}^{-1}\,\underline{\Delta E} + V_1(\sigma) \qquad (4.92)$$

The term $1/_q$ was introduced initially to avoid pole and zero cancellation in $(\underline{H}+\underline{Q}s)\underline{W}(s)$. Now that the energy function is obtained, setting $q \to \infty$ will cause all the terms that are factors of $1/_q$ to vanish. Substituting for $V_1(\sigma)$, from (4.35) and using the results of Appendix 4.B in (4.92) will result:

$$VE = \frac{1}{4\sum_{i=1}^{N} M_i} \sum_{i=1}^{N}\sum_{j=1}^{N} M_iM_j\,(\omega_i-\omega_j)^2 + \frac{1}{2}\,(\mu^*-\mu_o)\Big(\sum_{i=1}^{N} M_i\omega_i\Big)^2$$

$$+ \frac{1}{2}\,\rho\left[\sum_{i=1}^{N}(D_i(\delta_i-\delta_i^s) + M_i\omega_i)\right]^2 + \frac{1}{2}\sum_{i=1}^{N}(E_i-E_i^s)^2/(x_{di}-x'_{di})$$

$$+ \frac{1}{2}\sum_{i=1}^{N}\sum_{j=1}^{N} B_{ij}\Big[E_iE_j\,(\cos\delta_{ij}^s - \cos\delta_{ij}) - \frac{1}{2}\,(\delta_{ij}-\delta_{ij}^s)\,E_i^sE_j^s\sin\delta_{ij}^s$$

$$- \frac{1}{2}\,(E_i-E_i^s)(E_j-E_j^s)\cos\delta_{ij}^s\Big] \qquad (4.93)$$

where $\mu_o = -\frac{1}{\sum M_i}$

If damping torques are uniform, μ^* equals μ_o and the second term in (4.93) vanishes. ρ could be chosen zero to simplify the form of energy function. Also if damping torques are uniform or zero and with; $\omega_o = \Sigma M_i \omega_i / \sum M_i$ the energy function is:

$$VE = \frac{1}{2}\sum_{i=1}^{N} M_i(\omega_i - \omega_o)^2 + \frac{1}{2}\sum_{i=1}^{N}\sum_{j=1}^{N} B_{ij}((E_iE_j(\cos\delta^s_{ij} - \cos\delta_{ij})$$

$$- (\delta_{ij} - \delta^s_{ij})\, E^s_iE^s_jB_{ij} \sin\delta^s_{ij} - (E_i - E^s_i)(E_j - E^s_j)\cos\delta^s_{ij})$$

$$+ \frac{1}{2}\sum_{i=1}^{N} (E_i - E^s_i)^2 / (x_{di} - x'_{di}) \qquad (4.94)$$

The only task left in this derivation is to show that $\frac{dVE}{dt}$ for VE defined in (4.94) is negative.

Considering equations (4.12) and (4.13) and (4.15) and (4.16):

$$\frac{dVE}{dt} = \sum_{i=1}^{N}\sum_{j=1}^{N}{}' B_{ij}(E^s_iE^s_j \sin\delta^s_{ij} - E_iE_j \sin\delta_{ij})\,(\omega_i - \omega_j)$$

$$- \sum_{i=1}^{N}\sum_{j=1}^{N} B_{ij}(E^s_iE^s_j \sin\delta^s_{ij} - E_iE_j \sin\delta_{ij})(\omega_i - \omega_j)$$

$$+ \sum_{i=1}^{N}\left(\frac{dE_i}{dt}\right)\sum_{j=1}^{N} B_{ij}(E^s_j\cos\delta^s_{ij} - E_j\cos\delta_{ij})$$

$$- \sum_{i-1}^{N} T'_{doi}\left(dE_i/dt\right)^2 / (x_{di} - x'_{di}) \qquad (4.95)$$

Equation (4.95) has been proven to be true in Appendix 4.C. Hence:

$$\frac{dVE}{dt} = -\sum_{i=1}^{N} T'_{doi}(dE_i/dt)^2 / (x_{di}-x'_{di}) \qquad (4.96)$$

Since the right hand side of (4.96) is always negative, VE is derived Lyapunov function for the specific power system.

Now that the Lyapunov energy function is derived, it is time to drop the ficticious generators connected to the load buses. This could be done by setting $\varepsilon \rightarrow 0$. The differential equations become algebraic equations

$$\sum_{j=1}^{N} E_i^s E_j^s B_{ij} \text{ Sin } \delta_{ij}^s - E_i E_j B_{ij} \text{ Sin } \delta_{ij} = 0 \qquad (4.97)$$

$$\sum_{j=1}^{N} B_{ij}(E_j^s \text{ Cos } \delta_{ij}^s - E_j \text{ Cos } \delta_{ij}) = 0 \qquad (4.98)$$

and

$$E_i = E_i^s$$

where E_i^s can be a function of time. Since

$$P_{mi} = \sum_{j=1}^{N} E_i^s E_j^s B_{ij} \text{ Sin } \delta_{ij}^s \qquad i=1,....N_g \qquad (4.99)$$

$$-P_{li} = \sum_{j=1}^{N} E_i^s E_j^s B_{ij} \text{ Sin } \delta_{ij}^s \qquad i=N_{g+1},....,N \qquad (4.100)$$

$$I_{di} = \sum_{j=1}^{N} B_{ij} E_j \text{ Cos } \delta_{ij} \qquad (4.101)$$

These algebraic equations specify a constant power real power load power from (4.97) and (4.100) and a constant current reactive load model since from (4.98) and (4.101)

$$Id_i^s = Id_i$$

Since the transient reactance of the fictitious generators was omitted from the model entirely, these terms do not appear in the energy function, letting $\varepsilon \longrightarrow 0$ the inertias are

$$M_i = 0 \qquad \text{for } i=N_g+1;\ N_g+2,\ldots,N$$

and the susceptances

$$-\left(\frac{1}{x_{di}-x'_{di}}\right) = 0 \qquad \text{for } i=N_g+1,\ N_g+2,\ldots,N$$

The Lyapunov function becomes

$$VE = \frac{1}{2}\sum_{i=1}^{N_g} M_i(\omega_i-\omega_o)^2 + \frac{1}{2}\sum_{i=1}^{N}\sum_{j=1}^{N} B_{ij}\Big[(E_iE_j(\text{Cos }\delta^s_{ij}-\text{Cos }\delta_{ij})$$

$$-(\delta_{ij}-\delta^s_{ij})E^s_iE^s_j \quad \text{Sin }\delta^s_{ij}) - (E_i-E^s_i)(E_j-E^s_j)\text{Cos }\delta^s_{ij})\Big]$$

$$+\frac{1}{2}\sum_{i=1}^{N_g}\frac{(E_i-E^s_i)^2}{x_d-x'_d} \qquad (4.102)$$

The energy function matches the energy function developed in (3.35) if the flux linkage term (last term is in 4.96) and the real power load term is assumed constant in (3.35). This energy function can be written as

$$VE = \sum_{i=1}^{8} W_i$$

where:

$$W_i = \frac{1}{2} \sum_{i=1}^{N_g} M_i(\omega_i-\omega_o)^2 \qquad (4.103)$$

$$W_2 = \sum_{i=1}^{N_g}\left[(E_i^2+V_i^2-2E_iV_i \text{ Cos } (\delta_i-\theta_i))-(E_i^{s^2} + V_i^{s^2}-2E_i^sV_i^s \text{ Cos } (\delta_i^s-\theta_i^s))\right]$$

$$\cdot \frac{1}{2x'_{di}} \qquad (4.104)$$

$$W_3 = -\frac{1}{2} \sum_{i=N_g+1}^{N} \sum_{j=N_g+1}^{N} B_{ij}(V_iV_j \text{ Cos } (\theta_i-\theta_j)-V_i^sV_j^s \text{ Cos } (\theta_i^s-\theta_j^s)) \qquad (4.105)$$

$$W_4 = -\sum_{i=1}^{N_g} (\delta_i-\delta_i^s)\, P_{mi}^s = -\sum_{i=1}^{N_g} (\delta_i-\delta_i^s)\, \frac{E_i^sV_i^s}{x'_{di}} \text{ Sin } (\delta_i^s-\delta_i^s) \qquad (4.106)$$

$$W_5 = -\sum_{i=N_g+1}^{N} (\theta_i-\theta_i^s)\, Pl_i^s = -\sum_{i=1}^{N} (\theta_i-\theta_i^s)\, ((\sum_{i=1}^{N} V_i^sV_j^sB_{ij} \text{ Sin } (\theta_i^s-\theta_j^s))$$

$$+ \frac{E_i^sV_i^s}{x'_{di}} \text{ Sin } (\theta_i^s-\delta_i^s)) \qquad (4.107)$$

$$W_6 = +\sum_{i=1}^{N_g} -((E_i^{s^2}+V_i^{s^2}-2E_i^sV_i^s \text{ Cos } (\delta_i^s-\theta_i^s))$$

$$+ E_iE_i^s + V_iV_i^s - (E_iV_i^s+V_iE_i^s) \text{ Cos } (\delta_i^s-\theta_i^s))\, \frac{1}{x'_{di}} \qquad (4.108)$$

$$W_7 = + \sum_{i=N_g+1}^{N} \sum_{j=N_g+1}^{N} V_i^sV_j^s\, B_{ij} \text{ Cos } (\theta_i^s-\theta_j^s)\, (\frac{V_i}{V_i^s} - 1) \qquad (4.109)$$

$$W_8 = \frac{1}{2} \sum_{i=1}^{N_g} \frac{(E_i-E_i^s)^2}{x_{di}-x'_{di}} \qquad (4.110)$$

The terms W_i can be associated with the following

1) W_1 represents the kinetic energy and W_2 represents the magnetic energy stored in the transient reactances of generators.

2) W_3 represents the magnetic energy stored in transmission lines and transformers.

3) W_4 represents the position energy due to angle displacement of generators.

4) W_5 represents the position energy stored in the real power of the loads.

5) W_6 is the energy due to the reactive power produced by the generator and the energy stored in the transient reactance.

6) W_7 is the magnetic energy stored in the reactive loads.

7) W_8 is the form of kinetic energy and is due to consideration of flux linkages.

The terms W_2, W_3, W_4, W_5 and W_6 and W_7 are all the different components of the potential energy of the generator.

The procedure followed in the development of this Lyapunov energy function could be utilized to produce a topological Lyapunov function for the case where

1) the synchronous generator model is more complex and includes amortisseur effects;

2) excitation system models are included;

3) power system stabilizer models are included;

4) governor turbine energy system models are included

as long as a constant current reactive and constant power real power load models are assumed. The development of Lyapunov functions for the case where general real and reactive load models with constant impedance, constant

current, and constant power components would require the development of a different construction procedure than were used in this Chapter.

4.4 Simulation Results

The Lyapunov energy function derived as (4.97) is tested on the 39-bus, 10 generator system of New England. The schematic of this network is given in Figure 4. The tests have been performed on two fault cases. The fault cases considered is a fault on line 28-29 and a fault on line 14-23 where in each case the line is removed to clear the fault.

i) Fault on Line 28-29 -

The fault occurs on line 28-29 at t=0 and the critical clearing time has been determined by iterative simulation runs to be .21 seconds. Figures (13.a) and (14.a) show the variations of angles of generators which are close to faulted line. As can be observed in (14.a) generator 9 is the first generator that loses synchronism and thus would be called the critical generator for this fault.

Figures (13.b) and (14.b) show the total and potential and kinetic energies for both stable and unstable cases. In both cases the kinetic energy at the time that fault is cleared is very large and the potential energy is very small. The kinetic energy gradually decreases and the potential energy increases, but in the unstable case when the generators lose synchronism the kinetic energy has a

sharp jump and continues increasing due to loss of synchronism. The total energy in both the stable and unstable cases is nonconstant because of the damping caused by generator voltage variation.

Figures (13.c) and (14.c) give the three different components of potential energy. It shows that in the stable case energy due to generator angle displacement decreases until a minimum is reached and then it starts increasing again, but in the unstable case it is always decreasing. The fact that generator angles continue increasing with respect to the stable equilibrium point justifies this behavior. The energies due to real load power and transmission grid in the stable case have a maximum and then decrease. This is caused because the load bus angles and voltages oscillate around stable equilibrium point. In the unstable case, the continuous increase in angles cause these energies to increase for a time and later drop when the loss of synchronism occurs (when bus angle differences across particular branches exceed 360°). The flux linkage and reactive load energies are shown in Figures (13.c) and (14.c) for both stable and unstable cases. These energies are relatively small compared to other forms of energies.

ii) Fault on Line 14-23 -

The results of this test are the same as case (i). The angles of generators and different components of energy for stable and unstable case are shown in Figures (15) and (16).

Fig. (13.a) Variation of generator angles for the stable case where the fault occurs on line 28-29, the fault is cleared at 0.2 seconds and line 28-29 is removed.

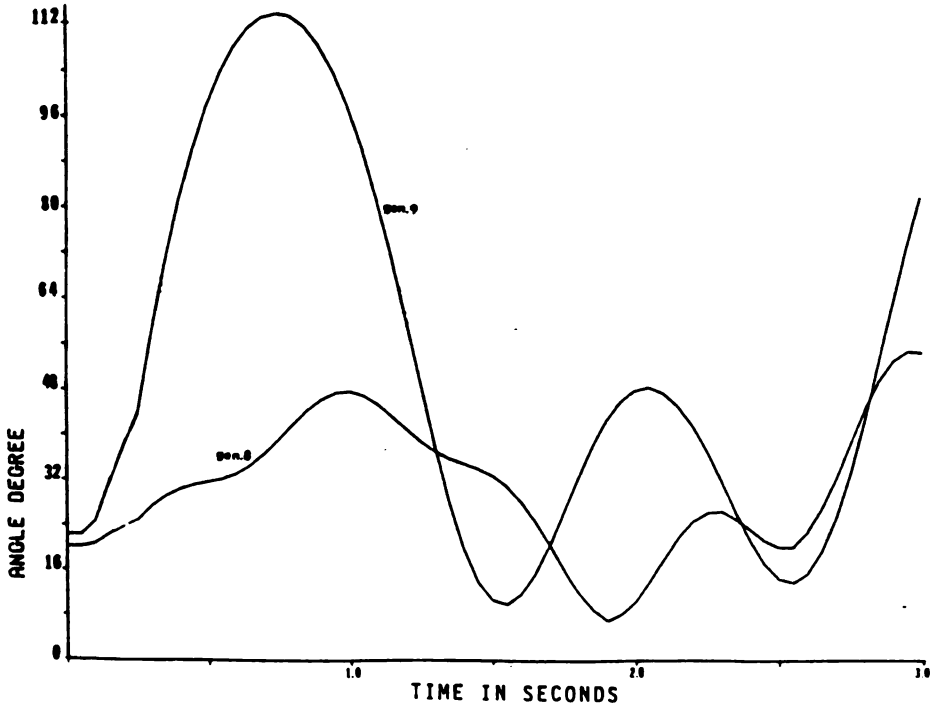

Fig. (13.b) Variation of potential, kinetic and total energies for the stable case where the fault occurs on line 28-29, the fault is cleared at 0.2 seconds and line 28-29 is removed.

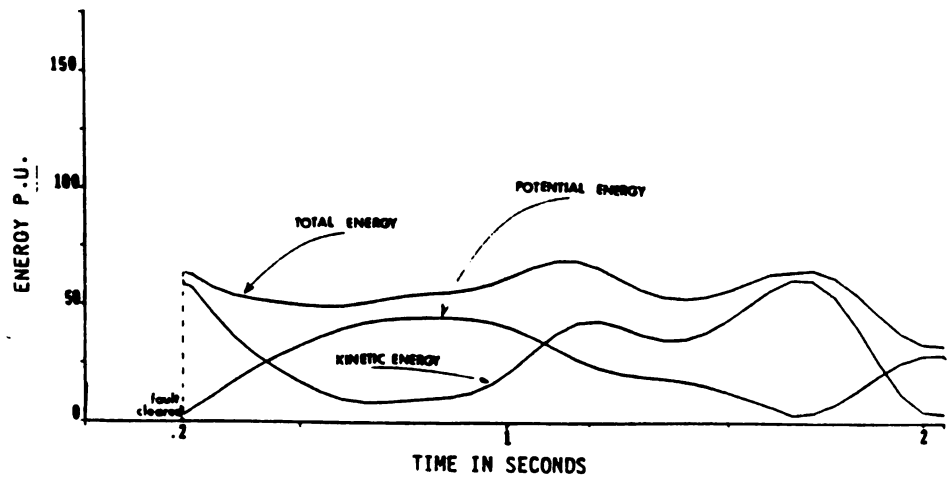

Fig. (13.c) Comparison of different components of potential energy for the stable case when fault occurs on line 28-29, the fault is cleared at 0.2 seconds and line 28-29 is removed.

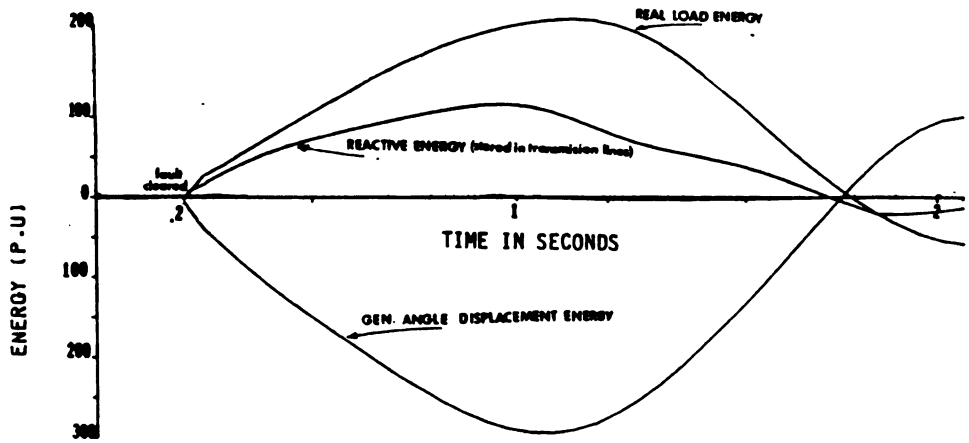

Fig. (13.d) Variation of flux linkage and reactive load energies for the stable case when the fault occurs on line 28-29, the fault is cleared at 0.2 seconds and line 28-29 is removed.

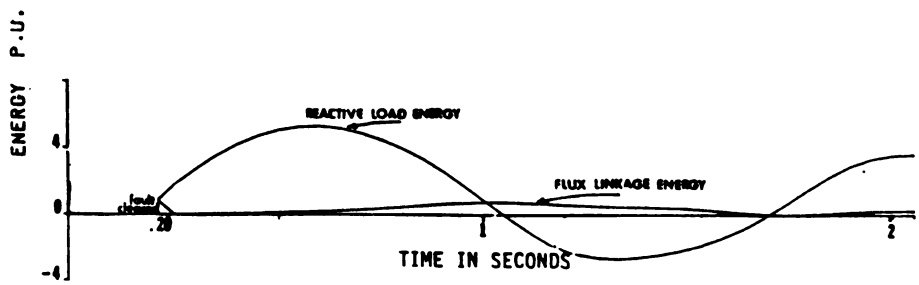

Fig. (14.a) Variations of generators angles for unstable case when the fault occurs on line 28-29, the fault is cleared at 0.21 seconds and line 28-29 is removed.

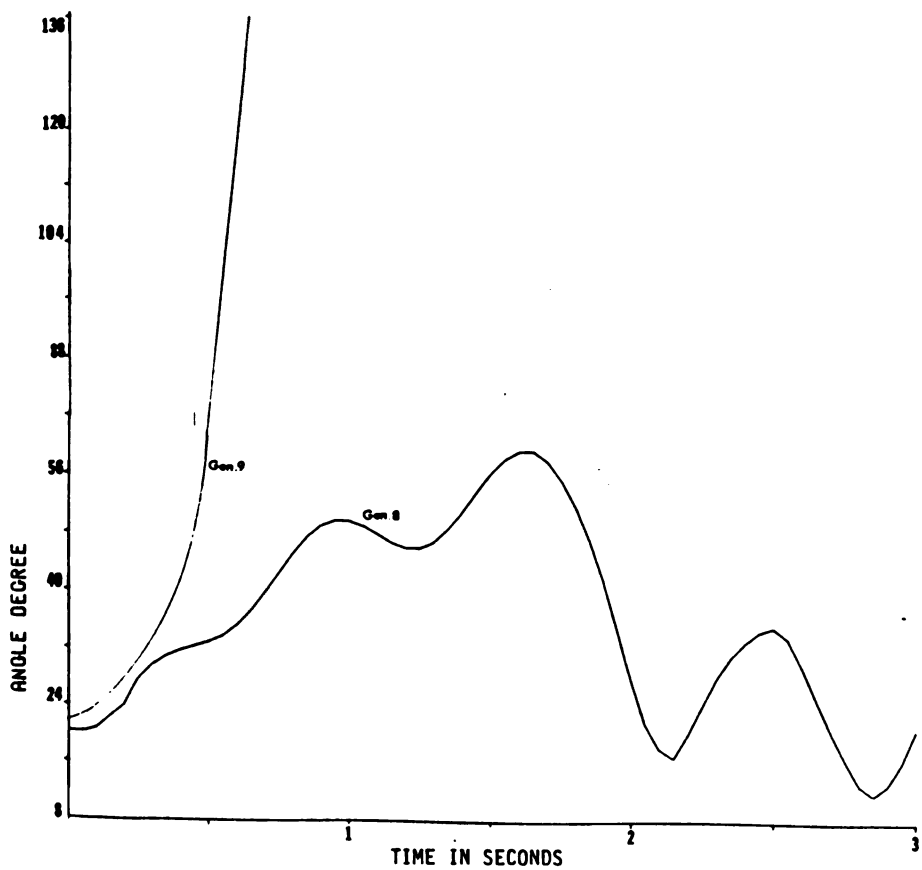

Fig. (14.b) Variation of potential, kinetic and total energy for the unstable case when fault occurs on line 28-29, the fault is cleared at 0.21 seconds and line 28-29 is removed.

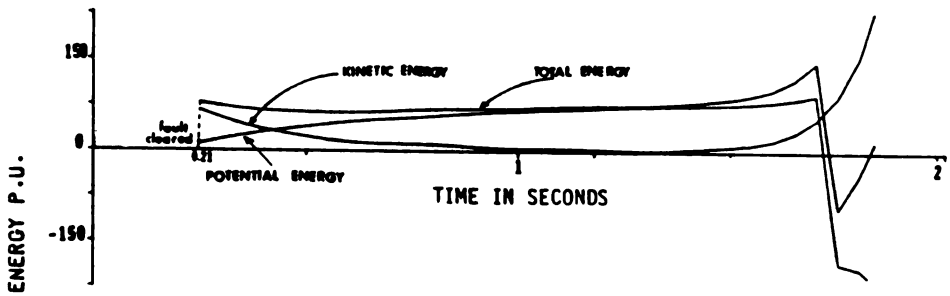

Fig. (14.c) Comparison of different components of potential energy for the unstable case when fault occurs on line 28-29, the fault is cleared at 0.21 seconds and line 28-29 is removed.

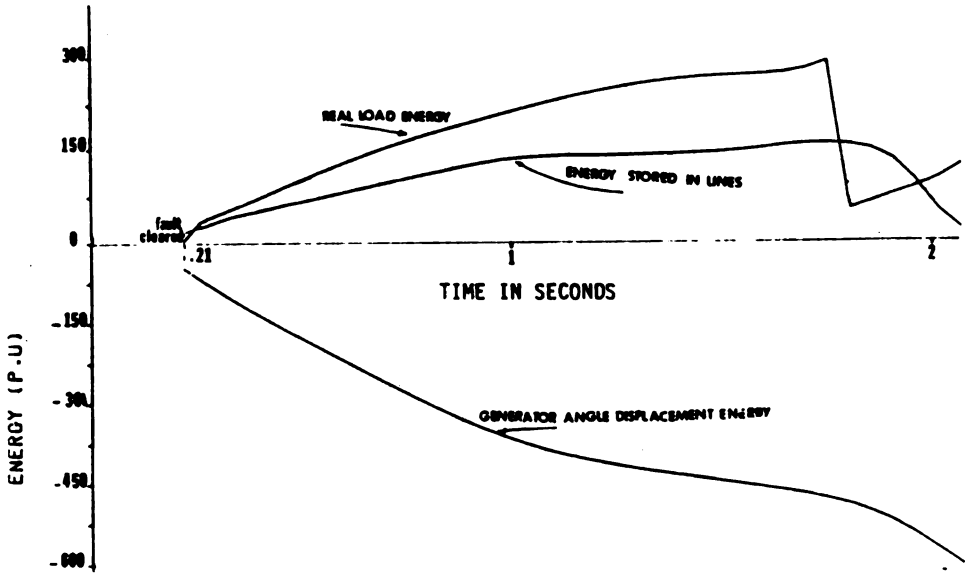

Fig. (14.d) Variation of flux linkage and reactive load energies for the unstable case when the fault occurs on line 28-29, the fault is cleared at 0.21 seconds and line 28-29 is removed.

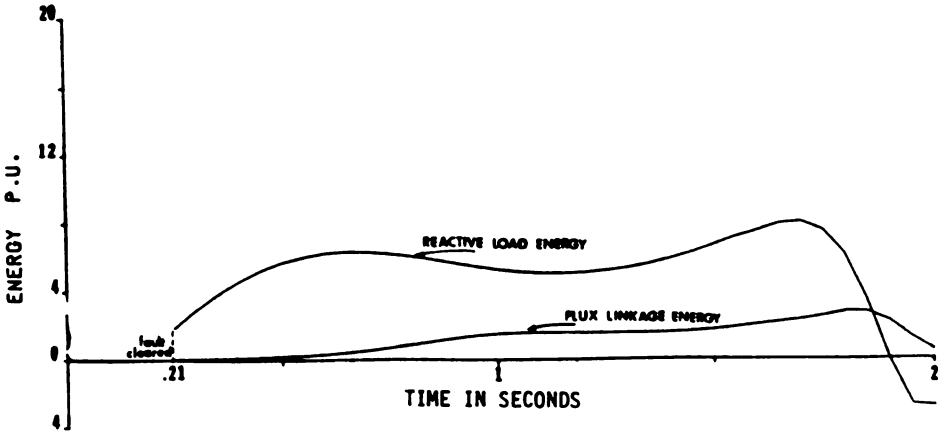

Fig. (15.a) Variation of generator angles for stable case when the fault occurs on line 14-33, the fault is cleared at 0.23 seconds and line 14-33 is removed.

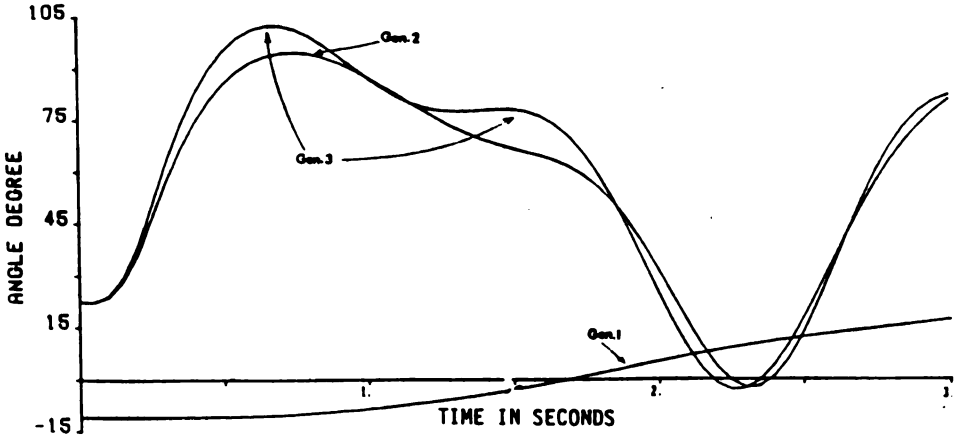

Fig. (15.b) Variation of potential, kinetic and total energies for the stable case when the fault occurs on line 14-33, the fault is cleared at 0.23 seconds and line 14-33 is removed.

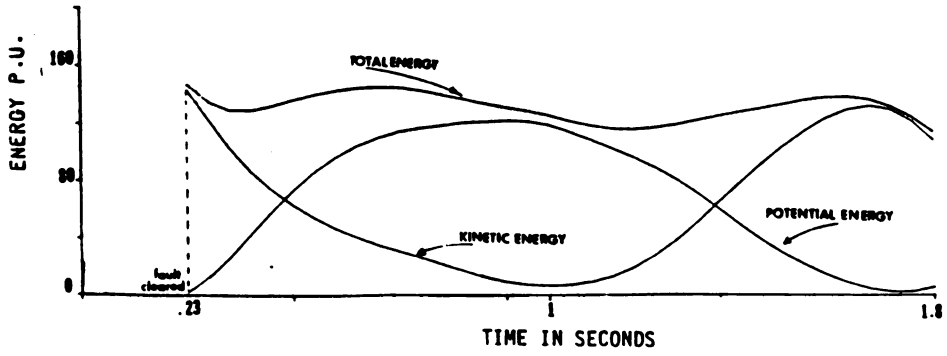

Fig. (15.c) Comparison of different components of potential energy for the stable case when fault occurs on line 14-33, the fault is cleared at 0.23 seconds and line 14-33 is removed.

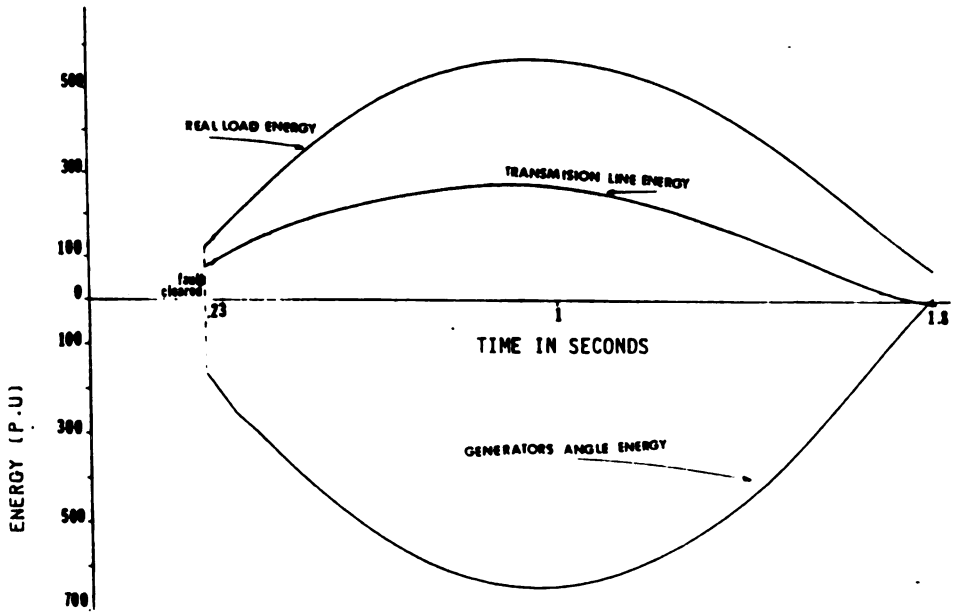

Fig. (15.d) Variation of flux linkage and reactive load energies for the stable case when the fault occurs on line 14-33, the fault is cleared at 0.23 seconds and line 14-33 is removed.

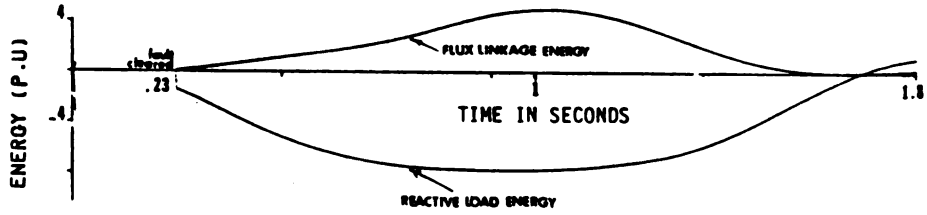

Fig. (16.a) Variation of generators angles for the unstable case when the fault occurs on line 28-29, the fault is cleared at .24 seconds and line 14-33 is removed.

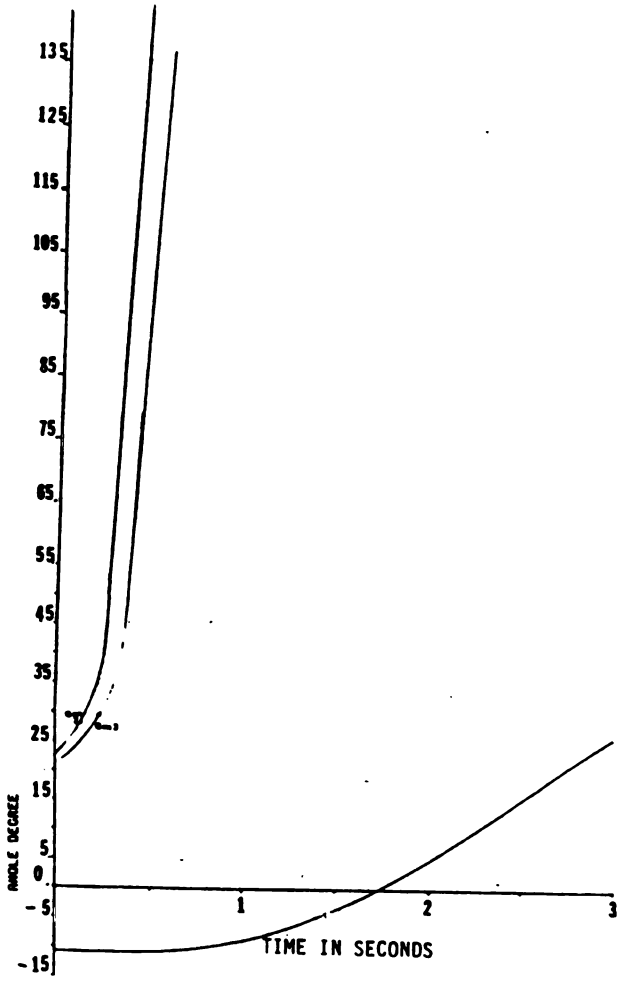

Fig. (16.b) Variaton of potential, kinetic and total energies for the unstable case when the fault occurs on Line 14-33, the fault is cleared at 0.24 seconds and line 14-33 is removed.

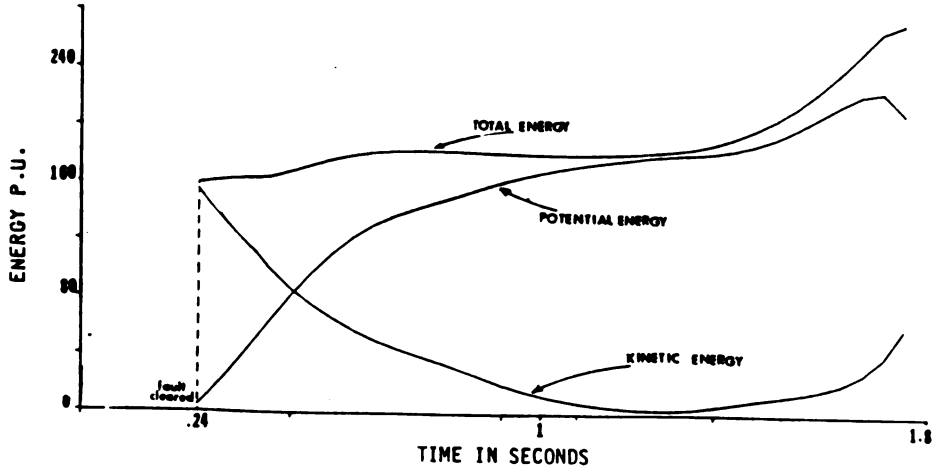

Fig. (16.c) Comparison of different components of potential energy for the unstable case when the fault occurs on line 14-33, the fault is cleared at 0.24 seconds and line 14-33 is removed.

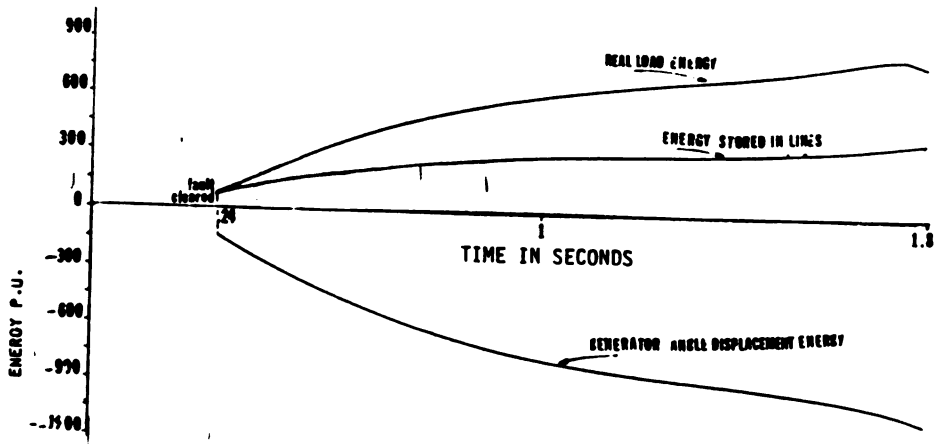

Fig. (16.d) Variation of flux linkage and reactive load energies for unstable case when the fault occurs on line 14-33, the fault is cleared at 0.24 seconds and line 14-33 is removed.

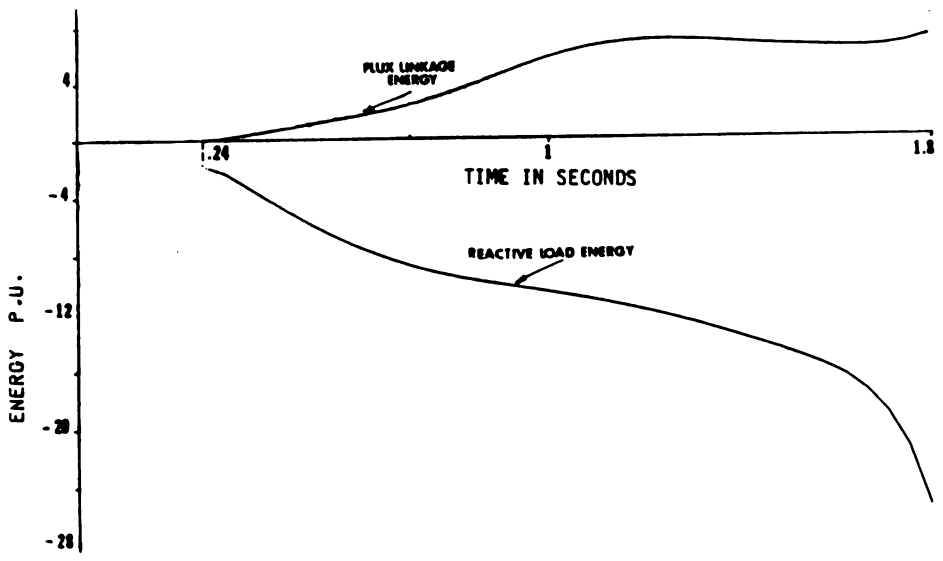

APPENDIX 4.A

4.A.1) Minimum realization of matrix Z(s) in (4-6) - expanding Z(s) with respect to A,B, and C:

$$Z(s) = (H+Q_S)W(s) =$$

$$Nc'(sI-A)^{-1}B+Qc'((sI-A)+A)(sI-A)^{-1}B$$

$$= Q'B+(N'+Q'A)(sI-A)^{-1}B$$

if $Z\to\infty$ $Z(\infty) = QcB$ so:

$$Z(s)-Z(\infty) = (Nc+QcA)(sI-A)^{-1}B$$

thus the minimum realization of $Z(s)-Z(\infty)$ is:

$$(A,B,CN'+ A'cQ')$$

Lemma 4.A.2 [14]

Let Z(s) be a matrix of rational transfer functions such that $Z(\infty)$ is finite and Z(s) has poles which lie in ReS<0, or are simple on ReS=0. Let (A,B,C) be a minimal realization of $Z(s)-Z(\infty)$. Then Z(s) is positive real if and only if there exists a symetric positive definite matrix P and matrices W_o and L such that:

$$PA + A'P = -LL'$$

$$PB = C-LW_o$$

$$W_o'W_o = Z(\infty) + Z'(\infty)$$

Lemma 4.A.3 [14]

Let the nxn matrix Z(s) be positive real and suppose that $Z(s) + Z'(-s)$ has rank r almost everywhere, then there exists an rxn matrix Y(s) such that

$$Z(s) + Z'(-s) = Y'(-s)\ Y(s)$$

Lemma 4.A.4 [14]

Let Z(s) have a minimal realization (A,B,C) and Z and Y be related as in Lemma 4.A.4. Then there exists a matrix $\hat{L}$ such that (A,B,L) is a minimum realization for Y.

APPENDIX 4.B

In this Appendix an expansion for each term in (4.92) is presented:

4.B.1 Term $\omega' P_{22} \omega$

The solution obtained for P_{22} in Chapter 4 is:

$$P_{22} = M + \mu MUM \qquad \text{(B-1-1)}$$

Substituting for M and U

$$P_{22} = \begin{bmatrix} M_i+\mu M_1^2 & \mu M_1 M_2 & \cdots\cdots & \mu M_1 M_N \\ \mu M_1 M_2 & \cdots\cdots & \cdots\cdots & M M_2 M_N \\ \vdots & & & \\ \mu M_1 M_N & \cdots\cdots & \cdots\cdots & M_N+\mu M_N^2 \end{bmatrix} \qquad \text{(B-1-2)}$$

Substituting for P_{22} in $\omega' P_{22} \omega$ the following form will be obtained:

$$\begin{aligned} \omega' P_{22} \omega = \mu\,(&M_1^2\omega_1^2 + M_1M_2\omega_1\omega_2 + M_1M_3\omega_1\omega_3 + M_1M_2\omega_1\omega_2 \\ &+ M_2^2\omega_2^2 + M_2M_3\omega_2\omega_3 + M_1M_3\omega_1\omega_3 + M_2M_3\omega_2\omega_3 + M_3^2\omega_3^2 + \\ &+ \cdots\cdots\cdots + M_N^2\omega_N^2) + (M_1\omega_1^2 + M_2\omega_2^2 + \cdots\cdots + M_N\omega_N^2) \end{aligned} \qquad \text{(B-1-3)}$$

But $\mu = \mu^* + \rho$, substituting this value for μ in (B-1-3) and rearranging it.

$$\omega' P_{22} \omega = (\mu^* + \rho)(M_1^2\omega_1^2 + M_2^2\omega_2^2 + \cdots + M_N^2\omega_N^2 + 2M_1M_2\omega_1\omega_2$$

$$+ 2M_1M_3\omega_1\omega_3 + \cdots + 2M_{N-1}M_N(\omega_{N-1}\omega_N) + (M_1\omega_1^2 + M_2\omega_2^2 + \cdots + M_N\omega_N^2)$$

$$= \mu^*(M_1^2\omega_1^2 + M_2^2\omega_2^2 + \cdots + M_N^2\omega_N^2 + 2M_1M_2\omega_1\omega_2 + 2M_1M_3\omega_1\omega_3 + \cdots$$

$$+ 2M_{N-1}M_N\omega_N) + \rho(M_1^2\omega_1^2 + \cdots + 2M_{N-1}M_N\omega_N)$$

$$+ (M_1\omega_1^2 + M_2\omega_2^2 + \cdots + M_N\omega_N^2) \qquad \text{(B-1-4)}$$

Now considering the last term in (B-1-4) and calling it F:

$$F = M_1\omega_1^2 + M_2\omega_2^2 + \cdots + M_N\omega_N^2 \qquad \text{(B-1-5)}$$

Multiplying and dividing the r.h.s. of (B-1-5) by $\dfrac{\sum_{i=1}^{N} M_i}{\sum_{i=1}^{N} M_i}$:

$$F = \frac{(M_1^2\omega_1^2 + M_1M_2\omega_1^2 + \cdots + M_1M_N\omega_1^2)}{(M_1 + M_2 + \cdots + M_N)} + \frac{(M_1M_2\omega_2^2 + M_2^2\omega_2^2 + \cdots M_2M_N\omega_N^2)}{(M_1 + M_2 + \cdots + M_N)}$$

$$+ \cdots + \frac{(M_NM_1\omega_N^2 + \cdots + M_N^2\omega_N^2)}{(M_1 + M_2 + \cdots + M_N)} \qquad \text{(B-1-6)}$$

Rearranging (B-1-6) and considering the fact that $\mu_o = -\dfrac{1}{\sum_{i=1}^{N} M_i}$

$$F = -\mu_o(M_1^2\omega_1^2 + M_2^2\omega_2^2 + \cdots + M_N^2\omega_N^2) - (M_1M_2\omega_1^2 + M_1M_2\omega_2^2 + M_1M_3\omega_1^2$$

$$+ M_1M_3\omega_3^2 + M_1M_2\omega_1^2 + M_1M_2\omega_2^2 + \cdots + M_{N-1}M_N\omega_N^2)\mu_o \qquad \text{(B-1-7)}$$

Now adding and subtracting $\mu_o \sum_{i=1}^{N} \sum_{\substack{j=1 \\ j\neq i}}^{N} M_i M_j \omega_i \omega_j$ to the r.h.s. of (B-1-7) will result:

$$F = -\mu_o \left(\sum_{i=1}^{N} M_i \omega_i\right)^2 - \frac{\mu_o}{2} \sum_{i=1}^{N} \sum_{j=1}^{N} M_i M_j (\omega_i - \omega_j)^2 \qquad \text{(B-1-8)}$$

Substituting (B-1-8) in (B-1-4):

$$\frac{1}{2}\omega P_{22}\omega = \frac{1}{2}\mu^* \left(\sum_{i=1}^{N} M_i \omega_i\right)^2 - \frac{1}{2}\mu_o \left(\sum_{i=1}^{N} M_i \omega_i\right)^2 - \frac{\mu_o}{4} \sum_{i=1}^{N} \sum_{j=1}^{N} M_i M_j (\omega_i - \omega_j)^2 + F_1$$

$$= \frac{1}{4 \sum_{i=1}^{N} M_i} \sum_{i=1}^{N} \sum_{j=1}^{N} M_i M_j (\omega_i - \omega_j)^2 + \frac{1}{2}(\mu^* - \mu_o) \left(\sum_{i=1}^{N} M_i \omega_i\right)^2 + F_1 \qquad \text{(B-1-9)}$$

where $F_1 = \rho (M_1^2 \omega_1^2 + \cdots + 2M_{N-1} M_N \omega_N)$ (B-1-10)

now let $\bar{\omega} = \dfrac{\sum_{i=1}^{N} M_i \omega_i}{\sum_{i=1}^{N} M_i}$

and consider

$$\frac{\mu_o}{4} \sum_{i=1}^{N} \sum_{j=1}^{N} M_i M_j (\omega_i - \omega_j)^2 = \frac{\mu_o}{4}(2M_1 M_2 \omega_1^2 + 2M_1 M_2 \omega_2^2 + \cdots\cdots$$

$$+ 2M_{N-1} M_N \omega_N^2 - 4M_1 M_2 \omega_1 \omega_2 - 4M_1 M_3 \omega_1 \omega_3 - \cdots\cdots - 4M_{N-1} M_N \omega_{N-1} \omega_N)$$

$$= \frac{1}{4} \left(2M_1 \omega_1^2 + 2M_2 \omega_2^2 + \cdots\cdots + 2M_N \omega_N^2 + \frac{2\bar{\omega}^2}{\sum_{i=1}^{N} M_i} - 4\bar{\omega}\left(\sum_{i=1}^{N} M_i \omega_i\right)\right)$$

$$= \frac{1}{2} \sum_{i=1}^{N} M_i (\omega_i - \bar{\omega})^2 \qquad \text{(B-1-11)}$$

4-B-2) Term $\delta'_r P_{11} \delta_r$

The solution obtained for P_{11} in Chapter 4 is:

$$K\ P_{11}\ K' = D\ U\ D \qquad \text{(B-2-1)}$$

The matrix K is:

$$K = \begin{bmatrix} 1_{1(N-1)} \\ -I_{(N-1)(N-1)} \end{bmatrix} \qquad \text{(B-2-2)}$$

The left inverse of matrix K is:

$$K_L^{-1} = \begin{bmatrix} 0_{(N-1)1} & -I_{(N-1)(N-1)} \end{bmatrix} \qquad \text{(B-2-3)}$$

the right inverse of matrix K is:

$$K_R^{-1} = \begin{bmatrix} 0_{1(N-1)} \\ -I_{(N-1)(N-1)} \end{bmatrix} \qquad \text{(B-2-4)}$$

multiplying the right hand side of (B-2-1) from the left by K_L^{-1} and from the right by K_R^{-1}, the first row and column of matrix D U D will vanish and P_{11} will be obtained as:

$$P_{11} = \rho \begin{bmatrix} D_2^2 & D_2D_3 & \cdots\cdots & D_2D_N \\ \vdots & & & \vdots \\ D_2D_N & \cdots\cdots & \cdots\cdots & D_N^2 \end{bmatrix} \qquad \text{(B-2-5)}$$

Now multiplying the both sides of P_{11} by δ'_r and δ_r:

$$\delta'_r\ P_{11}\delta_r = \rho (D_2^2(\delta_{12}-\delta_{12}^s)^2 + D_3^2(\delta_{13}-\delta_{13}^s)^2 + \cdots\cdots + D_N^2(\delta_{1N}-\delta_{1N}^s)^2$$

$$+ 2D_2D_3(\delta_{13}-\delta_{13}^s)(\delta_{12}-\delta_{12}^s) + \cdots\cdots + 2D_{N-1}D_N(\delta_{1(N-1)}-\delta_{1(N-1)})\cdot(\delta_{1N}-\delta_{1N}^s)$$

(B-2-6)

Each term of the r.h.s. of (B-2-6) could be written as:

$$D_2^2(\delta_{12}-\delta_{12}^s)^2=D_2^2(\delta_2-\delta_2^s)^2+D_2(\delta_1-\delta_1^s)^2-2(\delta_1-\delta_1^s)(\delta_2-\delta_2^s)D_2^2$$

But since δ_1 is the reference angle $\delta_1-\delta_1^s$ could be assumed to be zero and so by adding some zero terms to (B-2-6) the form of $\delta'_r P_{11}\delta_r$ would be

$$\delta'_r P_{22}\delta_r = (D_1^2(\delta_1-\delta_1^s)^2+D_2^2(\delta_2-\delta_2^s)^2+\cdots\cdots+D_N^s(\delta_N-\delta_N^s)^2$$

$$+2D_1D_2(\delta_1-\delta_1^s)(\delta_2-\delta_2^s)+\cdots\cdots+2D_{(N-1)}D_N(\delta_N-\delta_N^s)(\delta_{N-1}-\delta_{N-1}^s) \qquad \text{(B-2-8)}$$

Now combining the F_1 from (B-1-10) and (B-2-8) and term $\delta'_r P_{12}\omega$ the third term of energy function will be:

$$\frac{1}{2}\rho\left(\sum_{i=1}^{N}(D_i(\delta_i-\delta_i^s)+M_i\omega_i)\right)^2$$

The other terms of energy function of (4.93) could easily be related to corresponding terms in (4.92).

APPENDIX 4.C

In this appendix it is proved that the derivative of total energy in (4.94) is negative definite.

If the first term is called V_k for kinetic energy:

$$\frac{\partial V_k}{\partial \omega_i} = \frac{1}{2\sum_{i=1}^{N} M_i} \sum_{j=1}^{N} M_i M_j (\omega_i - \omega_j) \tag{C-1}$$

$$\frac{d\omega_i}{dt} = \frac{1}{M_i} \sum_{j=1}^{N} B_{ij} (E_i^s E_j^s \text{ Sin } \delta_{ij}^s - E_i E_j \text{ Sin } \delta_{ij}) \tag{C-2}$$

$$\frac{\partial V_k}{\partial \omega_i} \cdot \frac{d\omega_i}{dt} = \frac{1}{2\sum_{i=1}^{N} M_i} \sum_{j=1}^{N} M_j B_{ij} (E_i^s E_j^s \text{ Sin } \delta_{ij}^s - E_j E_i \text{ Sin } \delta_{ij}) (\omega_i - \omega_j) \tag{C-3}$$

thus

$$\sum_{i=1}^{N} \frac{\partial V_k}{\partial \omega_i} \cdot \frac{d\omega_i}{dt} = \frac{dV_k}{dt} = \frac{1}{2} \sum_{i=1}^{N} \sum_{j=1}^{N} B_{ij} (E_i^s E_j^s \text{ Sin } \delta_{ij}^s - \text{Sin} \delta_{ij}) (\omega_i - \omega_j) \tag{C-4}$$

Now considering the potential energy terms in (4.94) and calling them V_p:

$$\frac{\partial V_p}{\partial \delta_{ij}} = \frac{-1}{2} \sum_{j=1}^{N} B_{ij} (-E_i E_j \text{ Sin } \delta_{ij} + E_i^s E_j^s \text{ Sin } \delta_{ij}^s) \tag{C-5}$$

$$\frac{d\delta_{ij}}{dt} = \omega_i - \omega_j \tag{C-6}$$

So

$$\frac{dV_p}{\partial \delta_{ij}} \cdot \frac{d\delta_{ij}}{dt} = -\frac{1}{2} \sum_{j=1}^{N} B_{ij}(E_i^s E_j^s \text{ Sin } \delta_{ij}^s - E_i E_j \text{ Sin } \delta_{ij})(\omega_i - \omega_j)$$

and

$$\sum_{i=1}^{N} \frac{dV_p}{d\delta_{ij}} \cdot \frac{d\delta_{ij}}{dt} = -\frac{1}{2} \sum_{i=1}^{N} \sum_{j=1}^{N} B_{ij}(E_i^s E_j^s \text{ Sin } \delta_{ij}^s - E_i E_j \text{ Sin } \delta_{ij})(\omega_i - \omega_j) \quad \text{(C-7)}$$

$$\frac{\partial V_p}{\partial E_i} = \sum_{j=1}^{N} B_{ij}(E_i^s \text{ Cos } \delta_{ij}^s - E_i \text{ Cos } \delta_{ij}) \quad \text{(C-8)}$$

Equation (C-8) is obtained from second and fourth term in (4.94) thus:

$$\sum_{i=1}^{N} \frac{dE_i}{dt} \cdot \frac{\partial V_p}{\partial E_i} = \sum_{j=1}^{N} \frac{dE_i}{dt} \sum_{j=1}^{N} B_{ij}(E_i^s \text{ Cos } \delta_{ij}^s - E_i \text{ Cos } \delta_{ij}) \quad \text{(C-9)}$$

Now differentiating the last term in (4.94) with respect to time and calling the last term V_F:

$$\frac{dV_F}{dt} = \sum_{i=1}^{N} \frac{dE_i}{dt} \cdot \frac{(E_i - E_i^s)}{(x_{di} - x'_{di})} \quad \text{(C-10)}$$

Substituting for $(E_i - E_i^s)$ from (4.13)

$$\frac{dV_F}{dt} = -\sum_{i=1}^{N} T'_{doi} \left(\frac{dE_i}{dt}\right)^2 / (x_d - x'_{di}) - \sum_{i=1}^{N} \frac{dE_i}{dt} \sum_{j=1}^{N} B_{ij}(E_i^s \text{ Cos } \delta_{ij}^s - E_i \text{ Cos } \delta_{ij}) \quad \text{(C-11)}$$

Summing equations (C-4) and (C-7) and (C-9) and (C-11) will give equation (4.95).

CHAPTER 5

STABILITY CRITERIA BASED ON REGION OF STABILITY AND INSTABILITY

5.1 Introduction

The research presented in the previous two chapters has for the first time provided the theoretical foundation required to develop and theoretically justify stability criteria for determining retention or loss of stability given a particular fault, fault clearing time, and line switching action required to clear the fault. Several stability criteria and associated methods have been proposed [18, 17, 7, 2] but could never truly be justified theoretically because Lyapunov and energy integral based energy functions were never developed that

1) described the energy associated with both the real and reactive current flows in every branch, load bus and generator in the system;

2) determined the theoretical conditions imbedded in the Popov stability criterion that permit characterizing the region of stability and the region of instability for a power system.

With this theoretical basis a discussion of the region of stability based on the Popov stability criterion will be given in Section 5.2. A definition of the loss of transient stability will also be given. Theorems stating necessary and sufficient conditions for the loss of transient

stability are established in Section 5.3. The conditions stated in these theorems describe an estimate of the region of instability. Although a precise boundary between the region of stability and the region of instability is not established and is a subject for future research, a relationship is established between the region of stability and the region of instability that allows a more precise characterization of exactly what conditions are required for retention and loss of stability.

In section 5.4, a cutset integral criterion is established based on the theoretical description of the region of stability and the region of instability. A brief discussion of how this theoretical description of the region of stability for this transient stability model could be repeated for the classical transient stability model to theoretically justify the PEBS method based on the individual machine energy function is given. A theoretical justification of the PEBS method based on the cutset energy function developed from the topological energy function of Bergen and Hill [7] is also given. This discussion indicates that the methods of characterizing the region of stability and instability either directly in terms of constraints on the state variables or indirectly using the integral criterion in this research relate to stability criteria developed previously based on simpler transient stability models.

5.2 Regions of Stability and Instability for Transient Stability Models.

A loss of stability for the transient stability model (4.12) can be observed by noting that the angles for one set of internal generator and transmission network buses will continue to increase with respect to the other buses (both internal generator and network buses). The angle differences across the cutset of branches that connect these two mutually exclusive bus subsets will continue to increase and ultimately exceed 360° indicating a loss of transient stability has occurred. Although one could associate a pole slippage and a loss of synchronism with an increase in angles across all branches belonging to some cutset, one might not always experience the continued increase in angles beyond 360° normally associated with a loss of stability. For the purpose of the theoretical developments in this chapter a loss of transient stability will be defined as a continuing increase in angles differences across branches in a cutset that ultimately lead at some point in time t** to

$$\delta_{ij}(t^{**}) > 360 + \delta^{s}_{ij}$$

for all branch pairs ij belonging to some cutset. The cutset for which the angles exceed 360° is called the critical outset and the bus pairs belonging to this cutset is denoted $ij \varepsilon J$. It is assumed that this "loss of synchronism", that is called a loss of transient stability, occurs on only one cutset for a particular fault. This assumption may or may not be true and in no way effects the theory to be presented.

A more precise definition of loss of transient stability will be given after defining what is meant by the critical group and stationary group of buses. The critical group and stationary group are characterized by

1) maximum bus angle differences of less than Δ^{o} for all bus pairs ij in the stationary group;

2) maximum bus angle differences of less than Δ^{o} for all bus pairs in the critical group;

3) minimum bus angle differences for any bus "i" in the stationary group and any bus "j" in the critical group must exceed $360°+\delta^{o}_{ij}(t)$ where

$$\min\{ \delta_{ij}(t) - \delta^{o}_{ij}(t) \} \geq 360°$$

$$\delta^{o}_{ij}(t) = \mathrm{Sin}^{-1} \left[\frac{E^{s}_{i} E^{s}_{j} \mathrm{Sin}\, \delta^{s}_{ij}}{E_i(t) E_j(t)} \right]$$

A model relating the inertial center of the critical group $\delta_c(t)$ and stationary group $\delta_{sa}(t)$ is now derived in preparation for proving the theorems that are to be stated. The voltage for each generator or load bus is represented by E_i and the angle by δ_i. There is a fictitious generator connected to each of the load buses with inertia constant

$$M_i = \varepsilon m_i \qquad i=N_g+1,\ldots,N$$

and N_g generator buses with generator inertias M_i for $i=1,2,\ldots,N_g$. The N buses are reordered and then divided into two different groups. A group of L buses is called the critical group and N-L remaining (generator and load) buses are called the stationary group.

Group 1 $i=1,\ldots,L$ critical group

Group 2 $i=L+1,\ldots,N$ stationary group

The following center of angles are defined for groups 1 and 2.

$$\delta_c = \sum_{k=1}^{L} M_k\delta_k \Big/ \sum_{k=1}^{L} M_k \tag{5.1}$$

$$\delta_{sa} = \sum_{k=L+1}^{N} M_k\delta_k \Big/ \sum_{k=L+1}^{N} M_k \tag{5.2}$$

and the following center of inertias are defined as

$$M_c = \sum_{i=1}^{L} M_k \tag{5.3}$$

$$M_{sa} = \sum_{k=L+1}^{N} M_k \tag{5.4}$$

Since load buses have fictitious generators, a differential equation can represent the variation in the bus angle at every bus in the system.

$$\ddot{M_i\delta_i} = P_{mi} - \sum_{j=1}^{N} E_iE_jB_{ij} \text{ Sin } (\delta_i-\delta_j) \tag{5.5}$$

where $i=1,2,\ldots,N$

Considering (5.1) and (5.2):

$$\ddot{M_{sa}\delta_{sa}} = \sum_{i=L+1}^{N} M_i \left[\frac{\sum_{i=L+1}^{N} \ddot{M_i\delta_i}}{\sum_{i=L+1}^{N} M_i} \right] = \sum_{i=L+1}^{N} \ddot{M_i\delta_i} \tag{5.6}$$

Substituting (5.5) in (5.6), one obtains:

$$M_{sa}\ddot{\delta}_{sa} = \sum_{i=L+1}^{N} P_{mi} - \sum_{i=L+1}^{N}\sum_{j=1}^{N} E_i E_j B_{ij} \operatorname{Sin} \delta_{ij}$$

$$+ \sum_{i=L+1}^{N}\sum_{j=1}^{L} E_i^s E_j^s B_{ij} \operatorname{Sin} \delta_{ij}^s$$

$$+ \sum_{i=L+1}^{N}\sum_{j=L+1}^{N} E_i^s E_j^s B_{ij} \operatorname{Sin} \delta_{ij}^s$$

$$- \sum_{i=L+1}^{N}\sum_{j=1}^{L} E_i E_j B_{ij} \operatorname{Sin} \delta_{ij}$$

$$- \sum_{i=L+1}^{N}\sum_{j=L+1}^{N} E_i E_j B_{ij} \operatorname{Sin} \delta_{ij} \qquad (5.7)$$

The terms that are $\sum_{i=L+1}^{N}\sum_{j=L+1}^{N} \cdot$ are zero because they are the sum of real power in different directions.

Hence the equation (5.12) can be written as:

$$M_{sa}\ddot{\delta}_{sa} = \sum_{i=L+1}^{N}\sum_{j=1}^{L} E_i^s E_j^s B_{ij} \operatorname{Sin} \delta_{ij}^s$$

$$- \sum_{i=L+1}^{N}\sum_{j=1}^{L} E_i E_j B_{ij} \operatorname{Sin} \delta_{ij} \qquad (5.8)$$

Using the same procedure used to develop (5.8), it can be shown that:

$$M_c\ddot{\delta}_c = \sum_{i=1}^{L}\sum_{j=L+1}^{N} E_i^s E_j^s B_{ij} \operatorname{Sin} \delta_{ij}^s$$

$$- \sum_{i=1}^{L}\sum_{j=L+1}^{N} E_i E_j B_{ij} \operatorname{Sin} \delta_{ij} \qquad (5.9)$$

A formal definition of loss of stability for a topological transient stability model is now given so that

1) a discussion of the region of stability can be given, and;

2) the theorems stating necessary and sufficient conditions for loss of stability can be stated and proved.

DEF Given angles $\delta_i(t)$ for buses in the critical group and angles $\delta_j(t)$ for the stationary group, the system described by (4.14, 4.15) is called unstable if for $t>t^*$

$$\dot{\delta}_c(t) - \dot{\delta}_{sa}(t) \geq 0$$

until at some time t^{**}

$$\delta_i(t^{**}) - \delta_j(t^{**}) \geq 360 + \delta^o_{ij}(t^{**}) \quad \text{for all } ij \in J$$

where

$$\delta^o_{ij}(t^{**}) = \text{Sin}^{-1}\, E^s_i E^s_j \text{ Sin } \delta^s_{ij}/E_i(t^{**})E_j(t^{**})$$

This definition of instability for a power system is based on the Popov criterion condition (ii) that states

$$\sigma_{ij}\, f_{ij}(\sigma_{ij}) = [E_i(t)E_j(t)B_{ij} \text{ Sin } \delta^s_{ij}(t) - [E^s_i E^s_j B_{ij} \text{ Sin } \delta^s_{ij}]\, [\delta_{ij}(t) - \delta^s_{ij}] \geq 0$$

Although this condition is assumed to hold for all $\sigma_{ij} = \delta_{ij}(t) - \delta^s_{ij}$, it only holds for ranges

$$-\pi - \delta^o_{ij}(t) \leq \delta_{ij}(t) \leq \delta^s_{ij} \qquad (5.10)$$
$$\delta^o_{ij}(t) \leq \delta_{ij}(t) \leq \pi - \delta^o_{ij}(t)$$

if either $E_i(t)E_j(t) \leq E_i^s E_j^s$ and $\delta_{ij}^s \geq 0$ or $E_i(t)E_j(t) > E_i^s E_j^s$ and $\delta_{ij}^s < 0$

$$-\pi - \delta_{ij}^o(t) \leq \delta_{ij}(t) \leq \delta_{ij}^o(t)$$
$$\delta_{ij}^s \leq \delta_{ij}(t) \leq \pi - \delta_{ij}^o(t) \tag{5.11}$$

if $E_i(t)E_j(t) > E_i^s E_j^s$ and $\delta_{ij}^s > 0$ or $E_i(t)E_j(t) < E_i^s E_j^s$ and $\delta_{ij}^s \leq 0$

and

$$-\pi - \delta_{ij}^o \leq \delta_{ij}(t) \leq \pi - \delta_{ij}^o \tag{5.12}$$

if $E_i(t)E_j(t) = E_i^s E_j^s$ and $\delta_{ij}(t) = \delta_{ij}^o$ where $\delta_{ij}^s = \delta_i^s - \delta_j^s$

δ_{ij}^s the angle difference at buses i and j at the post fault stable equilibrium point

E_i^s voltage at bus i as the post fault stable equilibrium point

Thus the system is not asymptotically stable in the large but is only stable if the state $\underline{x}^T(t) = (\underline{\delta}^T(t)\underline{\omega}^T(t)\underline{E}^T(t))$ satisfies $\theta(t)=\underline{C}_1\underline{x}(t)\ \varepsilon S(t)$ where

$$\underline{\theta} = (\delta_{12}\ \delta_{13} \quad \delta_{1N}\delta_{21}\delta_{23}\cdots\delta_{2N},\cdots,\delta_{N-1N})$$

and S(t) is the angle subspace given by constraints (5.10-5.12) for all $t \geq t_c^*$.

A more formal definition of the region of stability is

$$\theta(t^*) = \underline{C}\ \underline{x}\ (t^*)\ \varepsilon\ S(t^*) \tag{5.13}$$
$$\underline{\omega}(t^*) = 0 \tag{5.14}$$
$$\underline{E}(t^*) = \underline{E}^s \tag{5.15}$$

for some times $t^* \geq t_c$ where $\underline{E}^s$ is the voltage magnitude at the post fault equilibrium point. This is a very conservative but mathematically precise manner of specifying the region of stability because it constrains every element of the state and places these constraints at a specific time.

The formal definition of the loss of transient stability is consistent with the formal definition of the region of stability because

1) the criterion that a loss of stability has occurred requires that the angle exceed $360+\delta^o_{ij}(t)$ for all $ij \in J$ at some time t^{**} where the boundary of the region of stability is $\delta_{ij}(t) \leq 180° - \delta_{ij}(t)$ at t^* for all pairs $ij \in J$;
2) both are based on the Popov stability criterion.

5.3 A Necessary and Sufficient Condition for Loss of Transient Stability

The theorems will now be stated and proved to establish necessary and sufficient conditions for loss of stability in the power system. The conditions stated in the theorems can be applied at any time $t \geq t_c^+$ and if satisfied indicate the system trajectory for that fault, clearing time, and line switching action will be unstable or if the system is unstable indicate that these conditions had to hold at some $t^* \geq t_c^+$.

Theorem 3

Given that

1) the maximum bus angle difference Δ between bus pairs in the stationary and bus pairs in the critical group is $\Delta = 90°$;

2) the angle differences across branches in the critical cutset are all positive in the post fault equilibrium state

$$\delta_{ij}(t) \geq \delta_i^s \geq 0 \qquad \text{all } ij \in J$$

3) $|E_i(t) - E_i^s| < \varepsilon$ (5.16)

then a sufficient condition for loss of transient stability is

$$[E_i(t)E_j(t)B_{ij} \text{ Sin } \delta_{ij}(t) - E_i^s E_j^s B_{ij} \text{ Sin } \delta_{ij}^s][\delta_{ij}(t) - \delta_{ij}^s] < 0 \tag{5.17}$$

and

$$\dot{\delta}_c(t) - \dot{\delta}_{sa}(t) \geq \varepsilon_2 > 0 \qquad \begin{matrix} i=1,2,\ldots,L \\ j=L+1,L+2,\ldots,N \end{matrix} \tag{5.18}$$

for some instant $t^* \geq t_c$ where δ_{ij}^s and E_j^s are the bus angle differences and voltage magnitude of the post fault stable equilibrium point.

Proof

The differential equation describing the relative motion of the equivalent machines representing the critical and stationary group of buses is

$$\ddot{\delta}_c(t) - \ddot{\delta}_{sa}(t) = -\left(\frac{1}{M_c} + \frac{1}{M_{sa}}\right) \sum_{i=1}^{L} \sum_{j=L+1}^{N} B_{ij}[E_i(t)E_j(t) \text{ Sin } \delta_{ij}(t) - E_i^s E_j^s \text{ Sin } \delta_{ij}^s] \tag{5.19}$$

Angle differences satisfy

$$\delta_{ij}(t) - \delta_{ij}^s \geq 0 \qquad \begin{matrix} i=1,2,\ldots,L \\ j=L+1,L+2,\ldots,N \end{matrix}$$

by the definition of the stationary and critical group. Thus, from condition (5.17) and (5.16), it is clear that

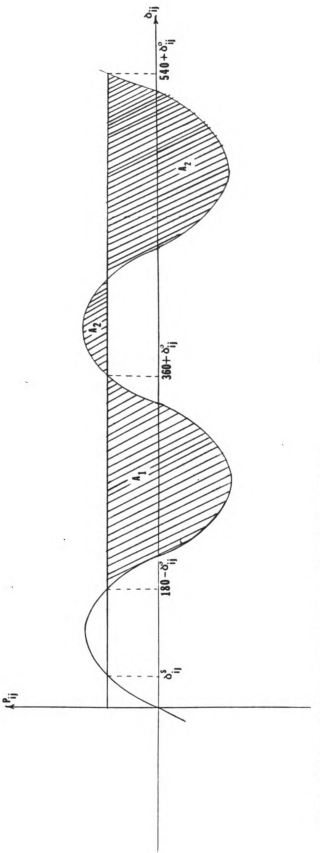

Fig. (17) Popov criterion for branch ij.

$$B_{ij}[E_i(t)E_j(t)\ \mathrm{Sin}\ \delta_{ij}(t) - E_i^s E_j^s\ \mathrm{Sin}\ \delta_{ij}^s] < 0$$

$$i=1,2,\ldots,L$$
$$j=L+1,L=2,\ldots,N$$

and $\ddot{\delta}_i(t^*) - \ddot{\delta}_j(t^*) \geq 0$.

Since $\ddot{\delta}_c(t^*) - \ddot{\delta}_{sa}(t^*) \geq 0$ and $\dot{\delta}_c(t^*) - \dot{\delta}_{sa}(t^*) \geq 0$ from 5.10 $\delta_c(t) - \delta_{sa}(t)$ will increase monotonically and exponentially until for some t_1 and some pair $ij \epsilon J$

$$\delta_{ij}(t_1) \geq 360 + \delta_{ij}^o(t_1) \qquad (5.20)$$

Although one branch $ij \epsilon J$ crosses the threshold (5.20) not all branches must necessarily cross threshold (5.20) if sufficient deceleration is experienced after time t_1. A branch causes acceleration of the critical group based on (5.19) over the range

$$180° - \delta_{ij}^o(t) \leq \delta_{ij}(t) \leq 360° + \delta_{ij}^o(t)$$

since

$$B_{ij}E_i(t)E_j(t)\ \mathrm{Sin}\ \delta_{ij}(t) < B_{ij}E_i^s E_j^s\ \mathrm{Sin}\ \delta_{ij}^s$$

and causes deceleration over

$$360° + \delta_{ij}^o(t) \leq \delta_{ij}(t) \leq 540° - \delta_{ij}^o(t)$$

since

$$B_{ij}E_i(t)E_j(t)\ \mathrm{Sin}\ \delta_{ij}(t) > B_{ij}E_i^s E_j^s\ \mathrm{Sin}\ \delta_{ij}^s$$

as can be observed from Figure 17.

This analysis is similar to that performed for the equal area criterion based on Figure 1.a in Chapter 2. Some

branches may cause deceleration on the critical group with respect to the stationary group before a time t** when all generators exceed the instability region threshold 360°+ $\delta^{o}_{ij}(t)$. The basic question is whether the acceleration energy due to each branch ij picked up as angle $\delta_{ij}(t)$ increases from $180°-\delta^{o}_{ij}(t)$ to $360+\delta^{o}_{ij}(t)$ will exceed the deceleration energy caused by excursion of angle $\delta_{ij}(t)$ beyond $360°+\delta^{o}_{ij}(t)$. If the acceleration energy exceeds the deceleration energy on all branches up to t** when all branch $ij \in J$ exceed

$$\delta_{ij}(t) \geq 360° + \delta^{o}_{ij}(t) \tag{5.21}$$

then a loss of stability will occur since all angles on all branches $ij \in J$ exceed (5.21) and $\dot{\delta}_{c}(t)-\dot{\delta}_{sa}(t)\geq 0$ for all t satisfying $t^* \leq t \leq t^{**}$.

Since the bus angle differences in the stationary group and the bus angle differences in the critical group do not exceed $\Delta=90°$ then

$$\max_{ij\in J}\{\delta_{ij}(t)\} - \min_{ij\in J}\{\delta_{ij}(t)\} \leq 2\Delta = 180°$$

Moreover, if all angles exceed $360+\delta^{o}_{ij}(t)$ where branch $i_o j_o$ satisfies

$$\min_{ij\in J}\{\delta_{ij}(t^{**}) - 360 - \delta^{o}_{ij}(t^{**})\}$$

$$= \delta_{i_o j_o}(t^{**}) - 360 - \delta^{o}_{i_o j_o}(t^{**}) = 0$$

then the maximum bus angle difference satisfies

$$\max_{ij\varepsilon J} \delta_{ij}(t^{**}) \leq \delta_{i_o j_o}(t^{**}) + 2\Delta + 360^\circ$$

$$= 540^\circ + \delta_{i_o j_o}(t^{**})$$

The energy A_{2ij} defined by

$$A_{2ij} = \int_{360^\circ + \delta^o_{ij}(t)}^{540 + \delta^o_{i_o j_o}(t^{**})} B_{ij}(E_i E_j \text{ Sin } \delta_{ij} - E^s_i E^s_j \text{ Sin } \delta_{ij})\, d\delta_{ij} \tag{5.22}$$

is always less than

$$A_{1ij} = \int_{180^\circ - \delta^o_{ij}(t)}^{360^\circ + \delta^o_{ij}(t)} B_{ij}(E_i E_j \text{ Sin } \delta_{ij} - E^s_i E^s_j \text{ Sin } \delta_{ij})\, d\delta_{ij} \tag{5.23}$$

assuming E_i is sufficently close to E^s_i $i=1,2,\ldots,N$ from observing Figure 17 because $\delta^s_{ij}>0$ $ij\varepsilon J$.

Thus, the net acceleration energy for each branch ij will exceed the deceleration energy at t** so (5.21) is satisfied. Thus, the conditions for the loss of transient stability are satisfied and the theorem is proved.

The above theorem only concerns the case where

$$\delta^s_{ij} \geq 0$$

for all $ij\varepsilon J$ on the critical cutset. Although this restriction limits the generality of the result, a cutset where some or all the angles δ^s_{ij} $ij\varepsilon J$ are negative is

less vulnerable to a loss of synchronism than if $\delta_{ij}>0$ since the area A_{3ij} defined by

$$A_{3ij} = \int_{\delta^s_{ij}}^{180^o - \delta^s_{ij}} B_{ij}(E^s_i E^s_j \text{ Sin } \delta_{ij} - E^s_i E^s_j \text{ Sin } \delta^s_{ij})\, d\delta_{ij}$$

that represents the deceleration energy from the angle across the branch at the post fault equilibrium point to the boundary of the region of stability is larger for $\delta^s_{ij}<0$ than for $\delta^s_{ij}>0$. The cutset where loss of transient stability will occur for a particular clearing time and line switching action is thus much more likely to be a cutset where $\delta^s_{ij}>0$ for all $ij \epsilon J$ than for a cutset where one or all

$$\delta^s_{ij} < 0$$

for $ij \epsilon J$. Although the case for $\delta^s_{ij}<0$ may be somewhat less important, the following theorem establishes a result for some $\delta^s_{ij}<0$.

Theorem 4

Given that

1) the maximum bus angle difference Δ for bus pairs in the stationary and bus pairs in the critical group is $\Delta = 32.48°$

2) some or all of the angle differences across branches in the critical cutset can be negative in the post fault equilibrium state

$$\delta^s_{ij} < 0 \qquad \text{for some } ij \epsilon J$$

3) $E_i = E^s_i$ (5.24)

4) The angle difference $\delta_{i_o j_o}(t^{**}) = \delta^s_{i_o j_o}$ satisfies

$$\delta^s_{ij} \geq \delta^s_{i_o j_o} = -\Delta = -32.48° \qquad (5.25)$$

then a sufficient condition for loss of transient stability is

$$[E_i(t)E_j(t)B_{ij} \text{ Sin } \delta_{ij}(t) - E^s_i E^s_j B_{ij} \text{ Sin } \delta^s_{ij}][\delta_{ij}(t) - \delta^s_{ij}] < 0 \qquad (5.17)$$

and

$$\dot{\delta}_c(t) - \dot{\delta}_{sa}(t) \geq 0 \qquad \begin{matrix} i=1,2,\ldots,L \\ j=L+1,L+1,\ldots,N \end{matrix} \qquad (5.18)$$

for some instant $t^* \geq t_c$ where δ^s_{ij} and E^s_j are the bus angle differences and voltage magnitude of the post fault stable equilibrium point.

Proof

The proof is similar to that in Theorem 3. The argument that $\ddot{\delta}_c(t) - \ddot{\delta}_{sa}(t) \geq 0$ and $\dot{\delta}_c(t) - \dot{\delta}_{sa}(t) \geq 0$ for $t^* \leq t \leq t_1$ is identical to that in Theorem 3 where t_1 is the time where for a single pair $ij \in J$

$$\delta_{ij}(t) \geq 360° + \delta^o_{ij}(t) = 360 + \delta^s_{ij}$$

since $\delta^o_{ij}(t) = \delta^s_{ij}$ because $E_i(t) = E^s_i$.

The argument that the acceleration energy A_{1ij} on each branch $ij \in J$ is less than the deceleration energy is dependent on Δ. In Theorem 3, $\Delta = 90$ but in this case $\Delta = 32.48°$. All bus pairs $ij \in J$ will satisfy (5.21) at t^{**} when the bus pair $i_o j_o \in J$ with the smallest angle difference satisfies.

$$\delta_{i_o j_o}(t^{**}) = 360 + \delta^s_{i_o j_o}$$

and the bus pair with the largest angle difference satisfies

$$\delta_{i_o j_o}(t^{**}) \leq 360 + \delta^{s}_{i_o j_o} + 2\Delta$$

Given that $\delta^{o}_{i_o j_o}(t^{**}) = -\Delta$ from (5.25)

then

$$A_{2ij} = \int_{360°+\delta^{s}_{ij}}^{360°+2\Delta-\Delta=360+\Delta} B_{ij}E^{s}_{i}E^{s}_{j}\,[\sin\delta_{ij} - \sin\delta^{s}_{ij}]\,d\delta_{ij} \qquad (5.26)$$

and

$$A_{1ij} + A_{2ij} = \int_{180-\delta^{s}_{ij}}^{360°+\Delta} B_{ij}E^{s}_{i}E^{s}_{j}\,[\sin\delta_{ij} - \sin\delta^{s}_{ij}]\,d\delta_{ij} \qquad (5.27)$$

Since one desires that $A_{1ij}+A_{2ij}<0$ for all $ij\varepsilon J$ to assume loss of transient stability. Since δ^{s}_{ij} is negative and

$$\delta^{s}_{i_o j_o} = -\Delta \leq \delta^{s}_{ij}$$

if

$$A_{1i_o j_o} + A_{2i_o j_o} = 0$$

then

$$A_{1ij} + A_{2ij} \leq 0 \text{ for all } ij\varepsilon J.$$

Evaluating $A_{1i_oj_o} + A_{2i_oj_o}$ in terms of Δ,

$$A_{1i_oj_o} + A_{2i_oj_o} = E_i^s E_j^s B_{ij} \int_{180^o + \Delta}^{360 + \Delta} (\text{Sin } \delta_{ij} - \text{Sin } (-\Delta))$$

$$= E_i^s E_j^s B_{ij} \ (-2 \text{ Cos } \Delta + \pi \text{ Sin} \Delta)$$

$A_{1i_oj_o} + A_{2i_oj_o}$ is zero for all $\Delta = \Delta_o$ where

$\tan \Delta_o = \frac{2}{\pi}$, $\Delta_o = 32.48^o$. Thus if $\min_{ij \epsilon J} = \delta^s_{i_oj_o} = -32.48^o$.

and if the bus angle differences within the stationary group and within the critical group are within $\Delta = 32.48°$ the deceleration energy on every branch is less than the acceleration energy on every branch up to a time t** when

$$\delta_{ij}(t^{**}) \geq 360 + \delta^s_{ij} \qquad ij \epsilon J$$

Thus, a loss of transient stability is experienced.

Note that since

$$\min_{ij \epsilon J} \ \delta^o_{ij} = -\Delta = -32.48°$$

and since the angle differences within the stationary group and within the critical group is Δ,

$$\max \ \delta^s_{ij} = \Delta$$

Although the minimum angle difference cross branches in the critical cutset for stable equilibrium point might be smaller than -32.48° and possibly the angle differences within the stationary and within the critical group could be larger than 32.48° and a proof of loss of transient stability still might be obtained, the present result does

not appear overly restrictive and suggests that in order to prove a loss of stability one must place a lower bound on

$$\min_{ij\epsilon J} \delta^{s}_{ij}$$

and one must place an upper bound on the bus angle differences within stationary and within the critical group. A necessary condition for loss of transient stability is now proved for the case where

$$\delta^{s}_{ij} \geq 0 \qquad \text{for all } ij\epsilon J.$$

Theorem 5

Given that

1) the maximum bus angle difference Δ for bus pairs in the stationary and bus pairs in the critical group is $\Delta = 45°$

2) that the angle differences across branches in the critical cutset are all positive in the post fault equilibrium state

$$\delta^{s}_{ij} \geq 0 \qquad \text{all } ij\epsilon J$$

3) $|E_i(t) - E^{s}_{i}| \leq \epsilon$

then a necessary condition for loss of transient stability is that there exists a time t* such that

$$[E_i(t)E_j(t)B_{ij} \text{ Sin } \delta_{ij}(t) - E^{s}_{i}E^{s}_{j}B_{ij} \text{ Sin } \delta^{s}_{ij}][\delta_{ij}(t) - \delta^{s}_{ij}] < 0 \tag{5.17}$$

and

$$\dot{\delta}_{c}(t) - \dot{\delta}_{sa}(t) \geq 0 \qquad \begin{matrix} i=1,2,\ldots,L \\ j=L+1,L+2,\ldots,N \end{matrix} \tag{5.18}$$

where δ^s_{ij} and E^s_j are the bus angle differences and voltage magnitude of the post fault stable equilibrium point.

Proof of Necessity

Given that for all t satisfying $t^* \leq t \leq t^{**}$ and all $ij \epsilon J$

$$\dot{\delta}_c(t) - \dot{\delta}_{sa}(t) \geq 0$$

and at t^{**}

$$\delta_{ij}(t^{**}) \geq 360° + \delta^o_{ij}(t^{**}) \quad \text{for all } ij \epsilon J$$

then from the definition of instability there is a t^* for which

$$\dot{\delta}_c(t^*) - \dot{\delta}_{sa}(t^*) > 0$$

and since the maximum spread of angle differences is $2\Delta = 90°$ there is a time t^* such that

$$180° - \delta^s_{ij}(t^*) \leq \delta_{ij}(t^*) \leq 360 - \delta^o_{ij}(t^*)$$

for all $ij \epsilon J$ since

1) $\delta^s_{ij}(t)$ must not vary by more than 90° over all $ij \epsilon J$ in order for the load flow conditions to converge;

2) $\delta_{ij}(t)$ must not vary by more than $2\Delta = 90°$ over all $ij \epsilon J$ by assumption.

Thus conditions (5.17) is satisfied at t^* since all the angles lie within the range where the inequality constraint holds. Since both (5.17) and (5.18) have been shown to hold at some t^*, the theorem is proved.

It should be noted that the above theorems do not offer help in identifying the critical group; stationary group; or the critical cutset $ij \epsilon J$ of branches before one simulates a particular fault. The theorem just states that if certain

constraints (5.17, 5.18) are satisfied, at some time t* during the simulation and on some cutset, then a loss of stability will occur. Note that the bus angle separation with the stationary group and critical group can be 90° for the case where the bus angles $\delta^{o}_{ij}(t)$, $ij \epsilon J$ are positive but only $\Delta = 32°$ if $\delta^{o}_{ij}(t^*)$ are negative to ensure that the acceleration experienced when

$$\delta_{ij}(t) \geq 180° - \delta^{o}_{ij}(t)$$

is not overcome before all bus pairs $ij \epsilon J$ satisfy

$$\delta_{ij}(t) \geq 360° + \delta^{o}_{ij}(t)$$

The deceleration energy can be greater than the acceleration energy only if $\delta^{o}_{ij}(t)$ is negative since when $\delta^{o}_{ij}(t)$ is positive, the acceleration energy picked up as angles pass through the band

$$180° - \delta^{o}_{ij}(t) \leq \delta_{ij}(t) \leq 360 + \delta^{o}_{ij}(t^*)$$

will always exceed the deceleration energy as angles pass through the band

$$360 + \delta^{o}_{ij}(t) \leq \delta_{ij}(t) \leq 540 - \delta^{o}_{ij}(t)$$

If $\Delta \leq 45°$, and $\delta^{s}_{ij} \geq 0$ for all $ij \epsilon J$, one can assure that if a loss of transient stability occurs, then at some time t* one has satisfied conditions (5.17, 5.18).

The constraints imposed in specifying the region of instability constrain the entire state $\underline{\delta}(t)$, $\underline{\omega}(t)$ and $\underline{E}(t)$ where the region of stability constrain only $\delta(t)$ and specify both $\underline{\omega}(t)$ and $\underline{E}(t)$. Thus the region of instability better indicates conditions that cause instability than does

the conditions that specify the region of stability. Furthermore, given that the region of stability is specified by a sufficient condition for stability there is never any way of assessing how conservative it may be but by exhaustive simulation of many fault cases on a single system and many such experiments on different systems. However, given that for $\Delta \leq 32°$, one has necessary and sufficient conditions for loss of stability for both positive and negative values on $\delta^{o}_{ij}(t)$ $ij \epsilon J$, then one can compare the region of stability and the region of instability to determine how conservative the estimate of the region of stability is. Figure 18 shows the region of stability in branch angle space and the region of instability for the case where J contains two branches. Note that the region of stability and instability touch at a point.

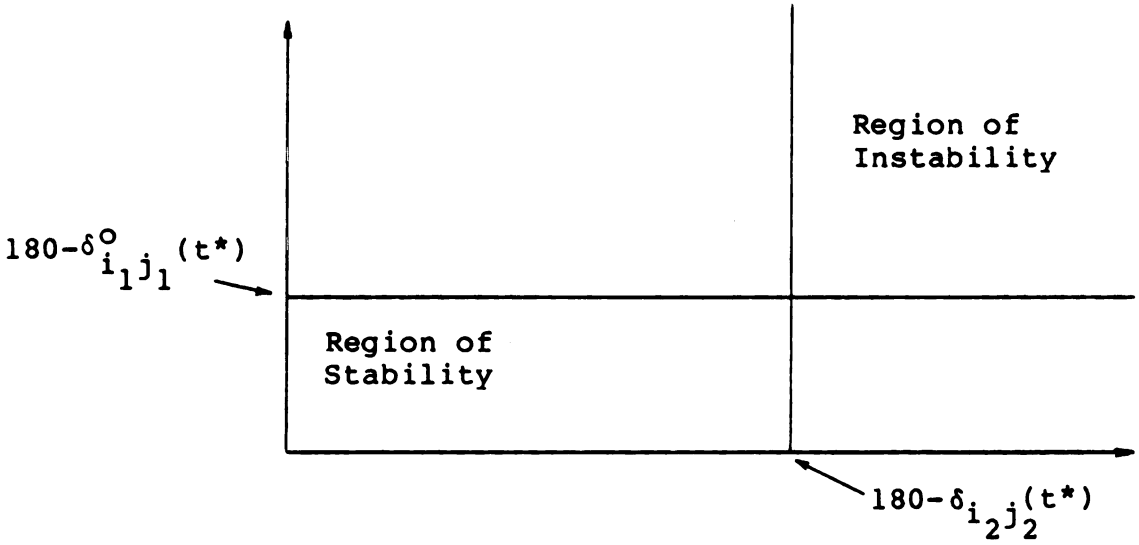

Fig. 18 Regions of stability and instability in branch angle space.

One can say that if the trajectory enters the region of instability at some t** a loss of stability will be experienced and that if one experiences a loss of stability the trajectory will enter the region of instability when $\Delta<45°$ and $\delta^{o}_{ij}(t^*)\geq 0$. One can also state that if the trajectory is within the region of stability for all time the trajectory will remain stable. Nothing can be stated about stability or loss of stability if the trajectory enters the area where one or more of the angle differences satisfy

$$\delta_{ij}(t) > 180 - \delta^{o}_{ij}(t)$$

but not all of the angle difference $ij\varepsilon J$ satisfy (5.10-5.12). Since one wishes to maintain a sufficient margin of stability and one knows if all angles exceed (5.10-5.12) at some time t* a loss of stability results. A prudent constraint for assuring retention of stability is that no branch angles $\delta_{ij}(t)$ even approach the boundary of the region of stability

$$\delta_{ij}(t) \leq 180 - \delta^{o}_{ij}(t) \qquad ij\varepsilon J$$

Thus the need to know whether the system is stable or unstable in the areas where statements about retention or loss of stability cannot be made may not be important in a practical sense.

It should be noted that the results of this chapter have

1) provided a theoretical basis for a region of instability and its relationship to the region of stability established from Popov's stability criterion;

2) provided a theoretical indication of the conservatism of the region of stability. Although the region of stability and instability do not cover the entire angle space, they touch at a single point and this suggests that the conservatism of the region of stability is modest. In a practical sense, its conservatism may be considered small compared to stability margins desired for system security with respect to the particular fault.

5.4 Stability Criteria Based on the Boundaries of the Region of Instability and Stability

A performance measure

$$V_1 = \sum_{ij\epsilon J} \int_{t_o}^{t_f} \delta_{ij}(t) f_{ij}(\delta_{ij}(t))\, dt \Big/ t_f - t_o$$

$$= \sum_{ij\epsilon J} \frac{\int_{t_o}^{t_f} (E_i(t)E_j(t)\, \mathrm{Sin}\delta_{ij}(t) - E_i^s E_j^s\, \mathrm{Sin}\, \delta_{ij}^s)(\delta_{ij}(t) - \delta_{ij}^s)dt}{t_f - t_o}$$

could be used to indicate if a loss of transient stability occurs or does not occur as well as the time t_c** when the trajectory enters the region of instability. As long as the trajectory remains in the region of stability the function being integrated is positive and the integral will increase monotonically with time. When the region of instability is entered the function being integrated becomes negative and remains negative.

The value of V_1, which integrates components of the Popov stability criterion on a cutset over the interval $t \epsilon [t_o, t_f]$, depends on the value of t_c and the system

trajectory for this clearing time. The value of V_1 for a particular value of clearing time is denoted as $V_1(t_c)$. If t_c increases for the case $t_c<t_{cc}$, the measure $V_1(t_c)$ should increase since the integrand will be larger in general over $t\varepsilon[t_o,t_f]$. If t_c exceeds the critical clearing time t_{cc}, the integrand for some portion of the interval $[t_o,t_f]$ will be negative. As t_c increases for $t_c>t_{cc}$, the portion of the interval $[t_o,t_f]$ when the integrand is negative becomes larger and thus $V_1(t_c)$ decreases. Computational results in the next chapter confirm that the maximum value of $V_1(t_c)$ should occur at the critical clearing time t_{cc}.

A second integral that represents potential energy on the cutset

$$V_2(t) = \sum_{ij\varepsilon J} \int_0^t \frac{d\sigma_{ij}}{dt}(t)\, f_{ij}(\sigma_{ij})\, dt$$

could also be used to indicate if a loss of transient stability occurs or does not occur and the time $t_o(t_c)$ when the trajectory enters the region of instability. If $E_i(t)=E_i^s$ for i=1,2,....,N, then $V_2(t)$ is the cutset energy function

$$V_2(t) = \sum_{ij\varepsilon J} B_{ij}E_i^sE_j^s \int_0^t (\text{Sin}\ \delta_{ij}(t) - \text{Sin}\ \delta_{ij}^{s2})\, d\delta_{ij}(t)$$

$$= -\sum_{ij\varepsilon J} E_i^sE_j^sB_{ij}\left[(\text{Cos}\ \delta_{ij}(t) - \text{Cos}\ \delta_{ij}^{s1}) - (\delta_{ij}(t) - \delta_{ij}^{s1})\ \text{Sin}\ \delta_{ij}^{s2}\right]$$

This cutset energy function increases monotonically with increasing δ_{ij} (t) in the region of stability. Thus if one clears the fault at $t_c \leq t_{cc}$ the measure $V_2(t)$ increases until the trajectory reaches its maximum angular excursion at $t_B(t_c)$ and $V_2(t)$ reaches its maximum value at $t_B(t_c)$. If t_c is increased but is less than t_{cc} the value of the maximum value of V(t)

$$V_2(t_B(t_c))^2 = \max_t \{V_2(t)\}$$

increases. The maximum value of $V_2(t)$ denoted V* would be reached if at some point t if

$$\delta_{ij}(t) = 180° - \delta_{ij}^s \tag{5.20}$$

for all ijεJ. Experience has shown that the trajectory very close approaches this point at $t_B(t_{cc})$ when $t_c = t_{cc}$. A criterion for stability developed in [23] was that if

$$V_2(t_B(t_c)) \leq V_2^*$$

where

$$V_2^* = \sum_{ij\ J} B_{ij} E_i^s E_j^s \left\{ \left[\text{Cos } \delta_{ij}^{s2} + \text{Cos } \delta_{ij}^{s1} \right] - \left[\pi - \delta_{ij}^{s2} - \delta_{ij}^{s1} \right] \text{ Sin } \delta_{ij}^{s2} \right\}$$

If $E_i(t) = E_i^s$ and in addition there are no load buses so that $N = N_g$, then the model reduces to the classical transient stability model. The critical cutset would correspond to the branches connecting the internal generator bus of a critical generator to the internal generator buses of other generators. In this case, the criterion for stability is

$$V_2(t_B(t_c)) \leq V_2(t_B(t^*_c))$$

where t^*_c is selected based on

$$V_2(t_B(t^*_c)) = \max_{t_c} V_2(t_B(t_c))$$

The results in [21] show that the critical clearing time can be determined with no detected error, i.e. $t^*_c=t_{cc}$. This method is called the PEBS method in [21] and $V_2(t)$ is the potential energy component of the individual machine energy function.

It is clear that the boundary of the region of stability and the region of instability touch at a point in angle space satisfying (5.28) where the performance measure $V_2=V_2^*$ and where the slope of $\frac{dV}{dt}2(t)=0$. Thus stability criteria can be established based on observing measure $V_2(t)$ as a function of time for a cutset J rather than checking the angles $\delta_{ij}(t)$ for all $ij \epsilon J$ and all t to determine loss of stability. It is also clear tht the performance criterion $V_2(t)$ is related to the cutset energy function stability criterion if $E_i(t)=E_i^s$ for all i=1,....,N and is related to the PEBS stability criterion for the individual machine energy function if $E_2(t)=E_i^s$ for i=1,2,....,N and $N=N_g$. Thus the stability criteria developed based on simpler models is justified based on the region of stability and region of instability derived in this chapter.

CHAPTER 6

VERIFICATION OF STABIILTY CRITERIA VIA SIMULATION

The objective of this chapter is to verify the accuracy and validity of the stability criteria proposed in the previous chapter.

The first stability criterion to be tested is based on the Popov stability criterion. The theoretical results of the previous chapter indicate

1) that the system will be stable if the Popov stability criterion is satisfied for all branches over the entire simulation interval

2) that the system will lose synchronism if one can find a cutset of branches for which the Popov stability criterion is violated at some time t^*.

The second stability criterion is based on measure V_1 that will continue to increase if the state is in the region of stability but will decrease sharply after the trajectory enters the region of instability. The stability criterion determines the value of the maximum value of V_1 for the interval $[t_o, t_f]$ for each clearing time for which the transient stability simulation criterion is run. The value of V_1, which integrates components of the Popov stability criterion on a cutset over the interval $t \in [t_o, t_f]$, depends on the value of t_c and the system trajectory for this clearing

time. The value of V_1 for a particular value of clearing time is denoted as $V_1(t_c)$. If t_c increases for the case $t_c<t_{cc}$, the measure $V_1(t_c)$ should increase since the integrand will be larger in general over $t\varepsilon[t_o,t_f]$. If t_c exceeds the critical clearing time, t_{cc}, the integrand for some portion of the interval $[t_o,t_f]$ will be negative. As t_c increases for $t_c>t_{cc}$, the portion of the interval $[t_o,t_f]$ when the integrand is negative becomes larger and thus $V_1(t_c)$ decreases. Computational results in this chapter confirm that the maximum value of $V_1(t_c)$ should occur at the critical clearing time t_{cc}.

Although these stability criteria were developed for a stability model that includes a topological network model, a single axis generator model, a constant power real load model, and a constant current reactive load model, the stability criteria will be tested and verified for

a) a single axis generator model, constant power load model, constant current reactive model;

b) a constant voltage behind transient reactance generator model, a constant power real load model, and a constant current reactive load model;

c) a constant voltage behind transient reactance generator model, a constant power real load model, and a constant impedance reactive load model.

The simulation of transient stability has been performed for two fault cases on the 39 bus New England system model. The two fault cases are a fault on line 26-27 and a fault on line 14-33 where in both cases the fault is cleared by removing the line.

The first stability criterion is tested by plotting

$$\sigma_{ij}(t)\ f_{ij}(\sigma_{ij}(t)) \tag{6.1}$$

as a function of time for branches that are geographically close to the fault location. It will be seen that this function will remain positive for branches far from the fault, will approach zero for branches near the fault when the clearing time is close to the critical clearing time, and will go negative for branches close to the fault when $t_c > t_{cc}$, and will reach very large negative values and oscillate for branches in the critical cutset when $t_c > t_{cc}$. Although the critical cutset is unknown before the simulation runs are performed for a particular fault to determine the critical clearing time, it is easily determined from the simulation results.

The second stability criterion

$$V(t_c) = \sum_{ij\epsilon J} B_{ij} \int_{t_o}^{t_f} [E_i(t)E_j(t)\ \mathrm{Sin}\ \delta_{ij}(t) - E_i^s E_j^s\ \mathrm{Sin}\ \delta_{ij}^s]\ [\delta_{ij}(t)-\delta_{ij}^s]\ dt \Big/ (t_f - t_o) \tag{6.2}$$

is evaluated on a transient stability simulation of a particular fault cleared at t_c and the critical cutset of branches $ij\epsilon J$ determined based on the results of the tests of the first stability criterion. The function $V(t_c)$ is plotted as a function of t_c and the value t^*_c for which

$V(t_c)$ has a maximum value should be t_{cc}. Retention of stability would be predicted to occur for $t_c < t^*_c$.

Four different fault cases have been presented in the results that follow:

Case 1) Fault on line 26-27 (flux linkage of generators considered and constant current reactive load model): Using the transient stability program the critical clearing time for this case is determined to be .37 seconds.

By considering the variations of angles of generator for the unstable case it was observed that the first generator that loses stability is generator No. 9. This conclusion could be anticipated before considering the transient stability programs results because generator No. 9 is the closest generator to the location that fault occurred.

The variations of $\sigma_{ij}(t)$ f ($\sigma_{ij}(t)$ for the stable and unstable case are plotted as functions of time for lines 28-29 and 9-29 and 26-28 and 26-25 and generator 9's transient reactance in Figure 19 for the first three seconds.

In the stable case the values of σ_{ij} f ($\sigma_{ij}(t)$) are positive and are often close to zero. This justifies the claim that σ_{ij} f_{ij} (σ_{ij}) should be greater than or equal to zero in the region of stability and should approach and remain close to zero when $t_c = t_{cc}$.

The values of $\sigma_{ij}(t) f(\sigma_{ij}(t))$ are also plotted for the unstable case when $t_c = t_{cc}^*$ in Figure 19. The values $\sigma_{ij}(t)$ f_{ij} ($\sigma_{ij}(t)$) are positive for all branches for the

first 1.2 seconds at which time the values on every branch become negative suggesting the loss of stability is imminent. The value of $\sigma_{ij}(t)$ f ($\sigma_{ij}(t)$) on the transient reactance on generator drops to a large negative number, remains constant for a short period and then begins oscillating (the values below a certain value were not plotted and when the curve returns to the range of the coordinates, the curve is again plotted.)

The large negative and positive oscillations are not observed on the plots for the other branches and thus the transient reactance of generator 9 is the critical cutset. It should be pointed out that after the first large drop in generator 9's σ_{ij} f (σ_{ij}), line 9-29 which represents a transformer has a large increase. This appears to occur because the transformer is trying to absorb the excessive energy of the generator and prevent it from loss of synchronism.

The measure of $V(t_c)$ given by (6.1) was computed for various clearing times when t_f=3.0 and the transient reactance of generator 9 is the sole branch belonging to the critical cutset. The value of $V(t_c)$ increases as t_c increases. The maximum value of $V(t_c)$ occurred at the critical clearing time determined from simulation results. The function $V(t_c)$ decreases rapidly for increase in t_c above t_{cc}. These results confirm the accuracy and validity of these stability criteria as well as the theoretical foundations upon which the stability criteria were based.

Case 2) Fault on line 14-33 (single axis generator model and constant current reactive load model): Using the transient stability program the critical clearing time for this case is determined to be .24 seconds.

In this case using the same procedure of case 1, the pair of generators 2 and 3 were determined to be the first generators that lose stability.

The variations of σ_{ij} f_{ij} (σ_{ij}) for the lines that are close to critical generators and σ_{ij} f_{ij} (σ_{ij}) for transient reactance of these generators are plotted in Figures (21.a), (21.b), (21.c), (21.d) and (21.e). With the same analogy as in case 1, the transient reactances of the group of generators 1 and 2 are identified as the critical cutset. The large negative values and the large oscillations observed on the branches in the critical cutset are not observed on the other branches. The integral measure defined in (6.1) is plotted in Figure 22 and again correctly predicts the critical clearing time. The results of this case are similar to the results of case 1 and both cases support the theory presented in Chapter 5.

The values of $\sigma_{ij}(t)$ f_{ij} (σ_{ij}) remain positive and close to zero for the critically stable case transient stability. The values of $\sigma_{ij}(t)$ f (σ_{ij}) on most of the branches go negative for a short period when the trajectory enters the region of instability followed by a period of large positive variation. The $\sigma_{ij}(t)$ f (σ_{ij}) values for the two branches in the critical cutset go negative, attain a

constant value and then start oscillating. The magnitude of the oscillation are large values.

Case 3) Fault on line 26-27 (constant current reactive load model and constant voltage behind transient reactance generator model): Using the transient stability program the critical clearing time for this case is determined to be .36 seconds. The results of this case are very similar to case 1 because the models are identical except that the single axis generator model is replaced by a constant voltage behind transient reactance generator model. The most significant difference between the cases is that generator 9 does not oscillate near the boundary of the region of stability in this case but quickly enters the region of instability. The values of σ_{ij} f_{ij} (σ_{ij}) for lines and generator 9's transient reactance are plotted in Figure 23. The integral measure is plotted in Figure (24). These results show that despite the fact that the model of the power system in this case is a little different from the model used in Chapter 5, the theory introduced in that chapter could also be used in this case.

Case 4) Fault on line 26-27 (constant impedance reactive load model and constant voltage behind transient reactance generator model): By using the transient stability simulation program the critical clearing time in this case is determined to be .31 seconds.

Despite the fact that the model used in deriving the theory in Chapter 5 is different from this case the

stability criteria based on σ_{ij} f (σ_{ij}) is successful in determining the critical clearing time and the cutset and the integral measure can accurately determine the critical clearing time.

The critical cutset, similar to previous cases, is generator No. 9's transient reactance and the value of integral measure for this cutset is positive and increasing as t_c gets close to t_{cc} and drops to negative when $t_c > t_{cc}$. The results of this case are shown in Figures 25 and 26.

Fig. (19) Comparison of $\sigma_{ij}f(\sigma_{ij})$ for stable and unstable case when the fault occurs on line 26-27. The fault has been cleared and line 26-27 has been removed. (Lyapunov energy function)

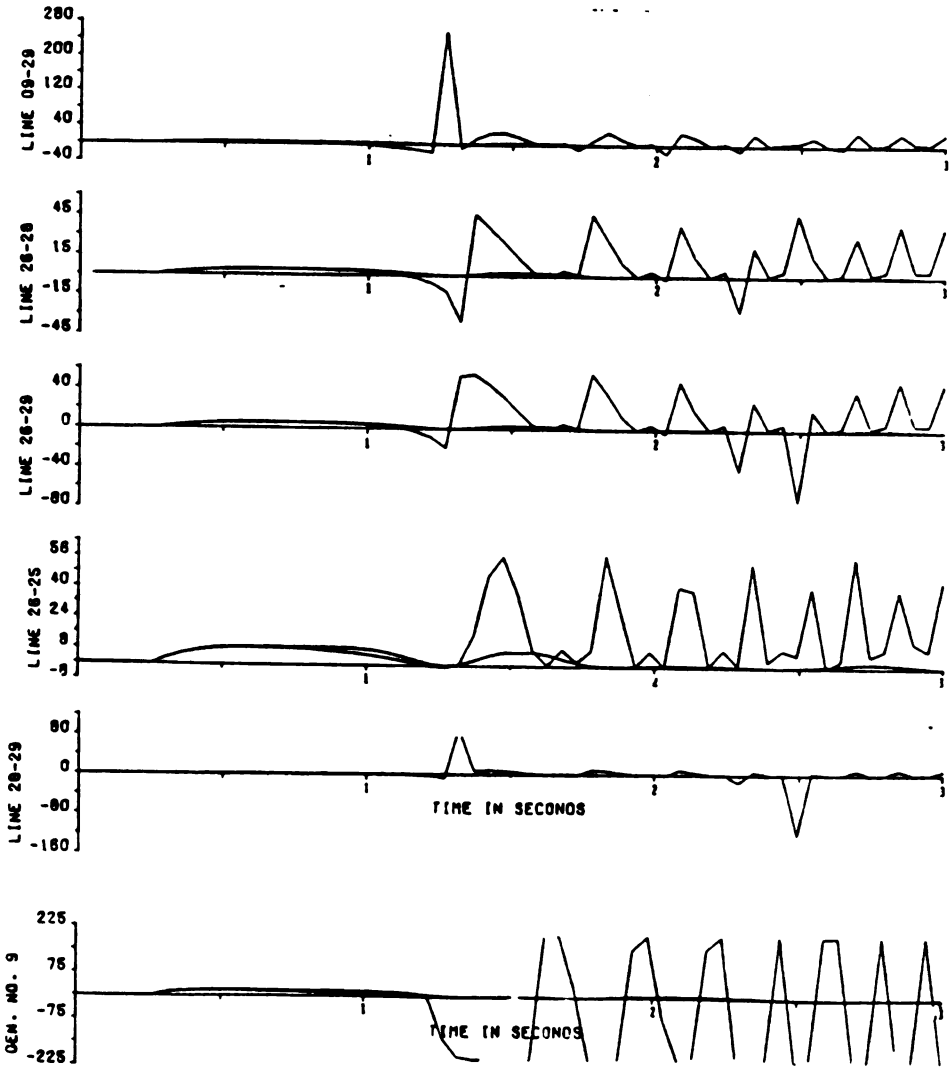

Fig. (20) Values of $V_1(t_f t_c)$ for the single axis generator model and the constant current reactive load model for the fault on line 26-27.

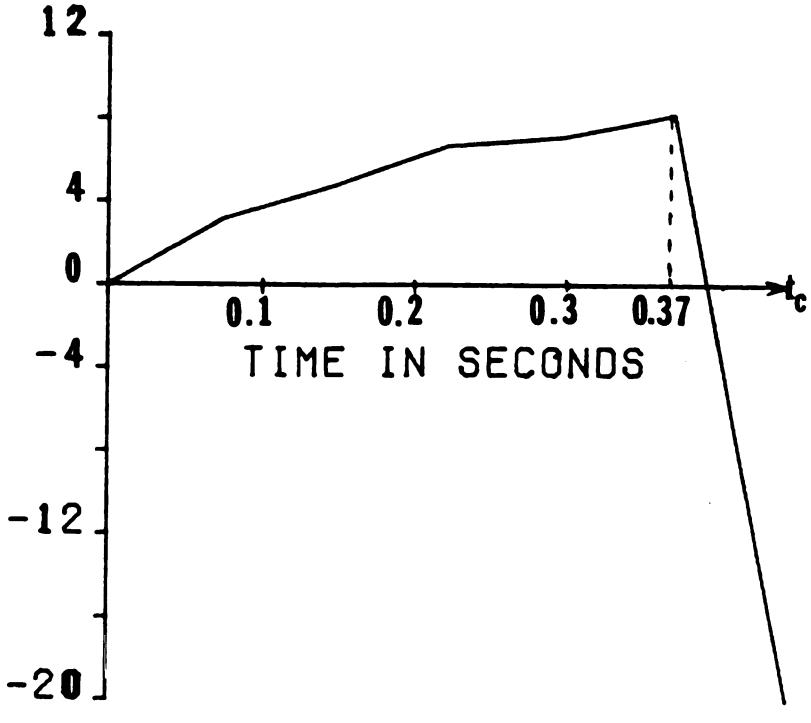

Fig. (21.a) Comparison of $\sigma_{ij}f(\sigma_{ij})$ for stable and unstable case when the fault occurs on line 14-33. The fault has been cleared and line 14-33 has been removed. (Lyapunov energy function)

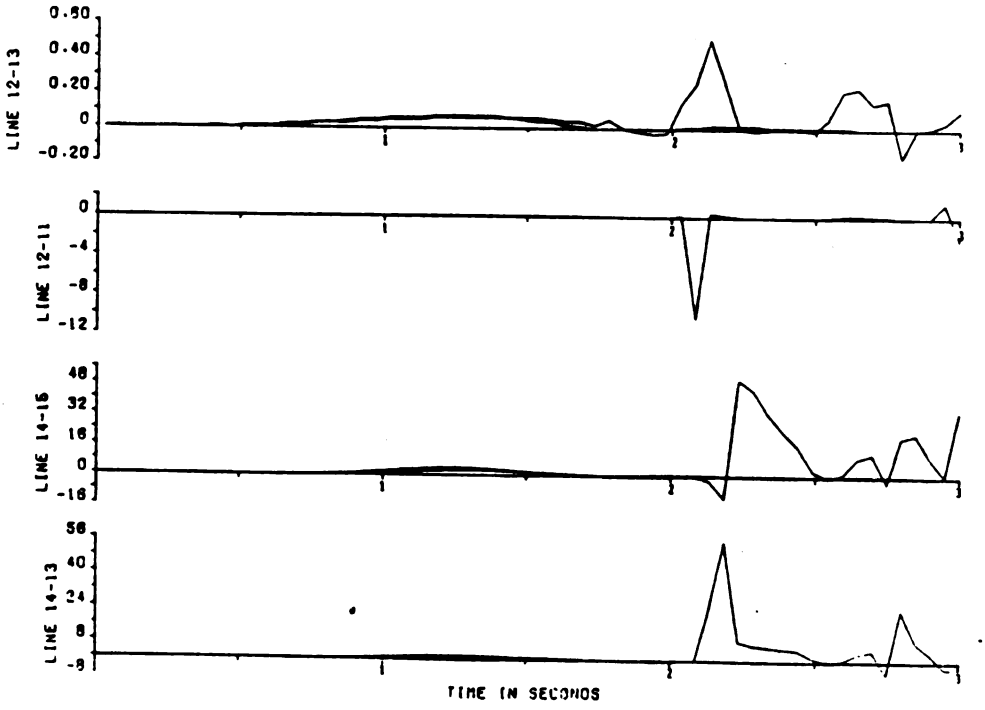

Fig. (21.b) Comparison of $\sigma_{ij} f(\sigma_{ij})$ for different lines on stable and unstable case when the fault occurs on line 14-33. The fault is cleared and line 14-33 is removed. (Lyapunov energy function)

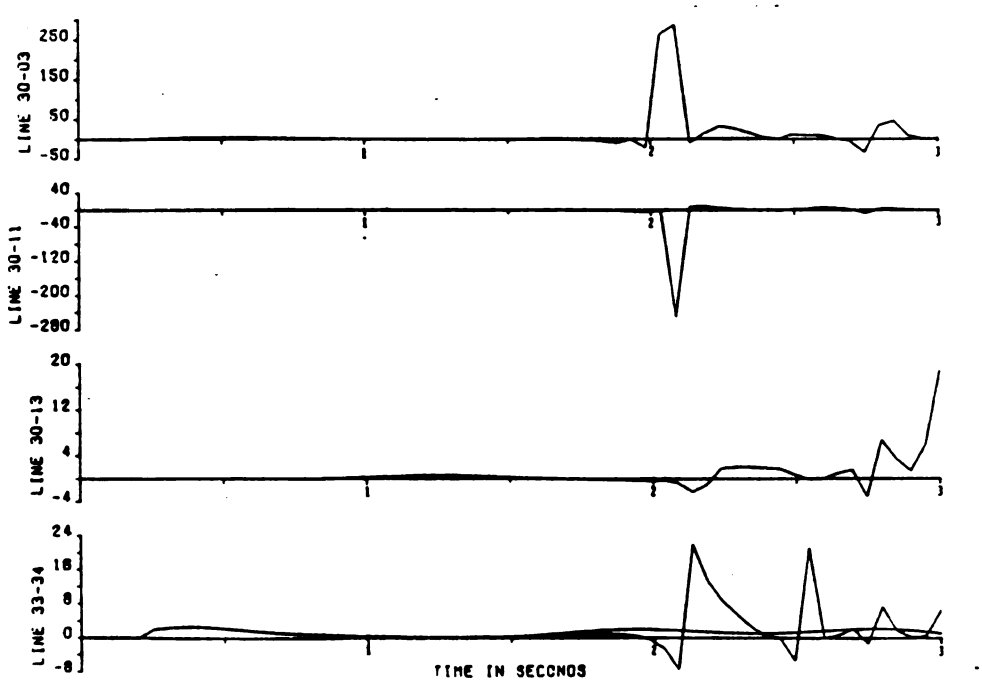

Fig. (21.c) Comparison of $\sigma_{ij} f(\sigma_{ij})$ for different lines on stable and unstable case when the fault occurs on line 14-33. The fault is cleared and line 14-33 is removed. (Lyapunov energy function)

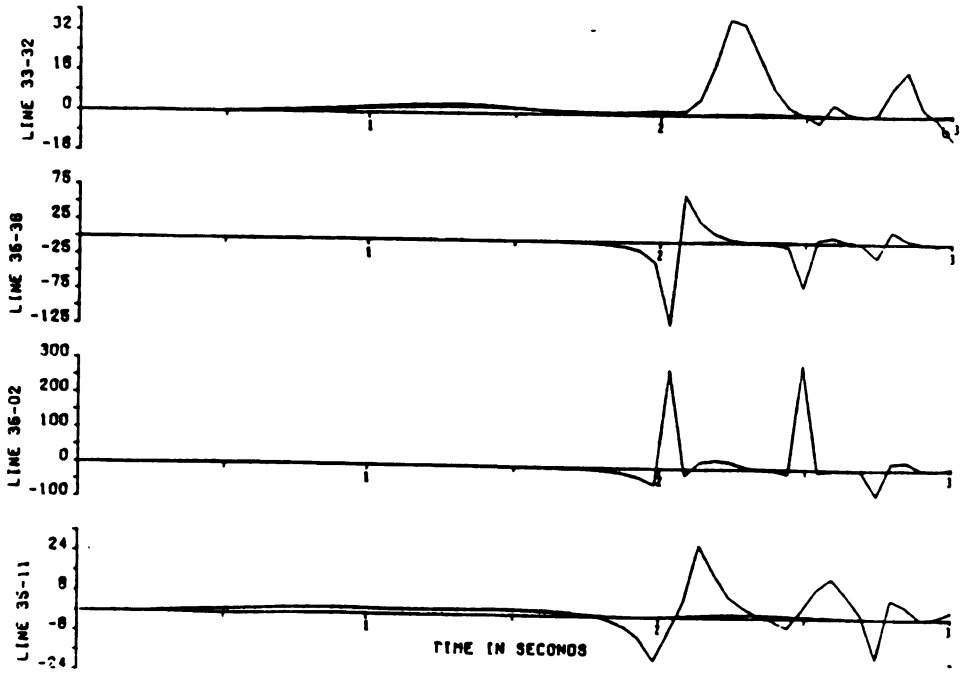

Fig. (21.d) Comparison of $\sigma_{ij} f(\sigma_{ij})$ for different lines on stable and unstable case when the fault occurs on line 14-33. 14-33 is removed after the fault is cleared. (Lyapunov energy function)

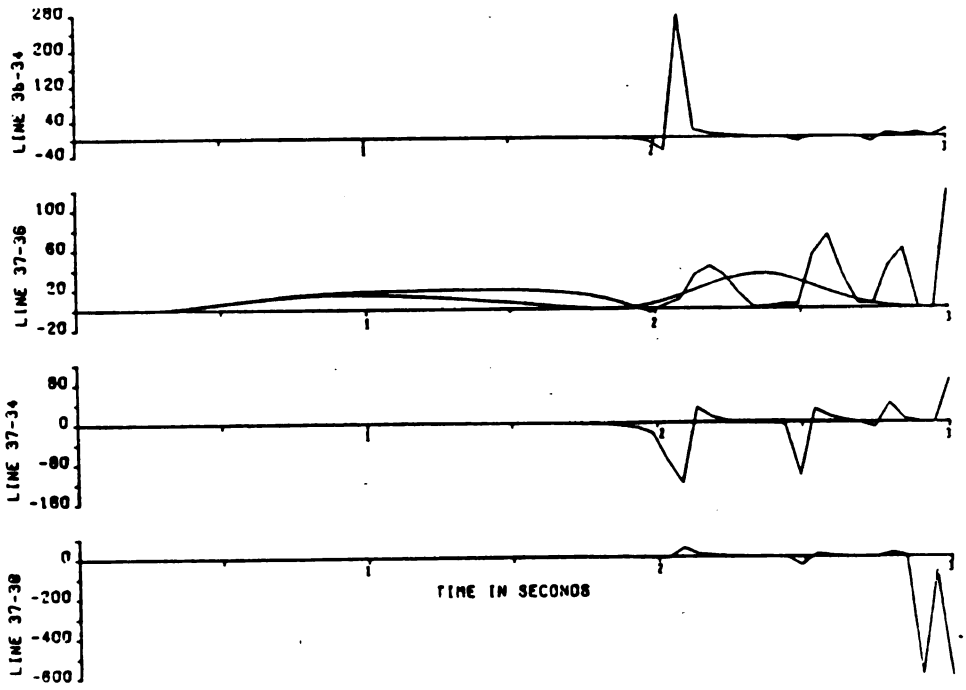

Fig. (21.e) Comparison of $\sigma_{ij}f(\sigma_{ij})$ for stable and unstable case when the fault occurs on line 14-33. The fault has been cleared and line 14-33 has been removed. (Lyapunov energy function)

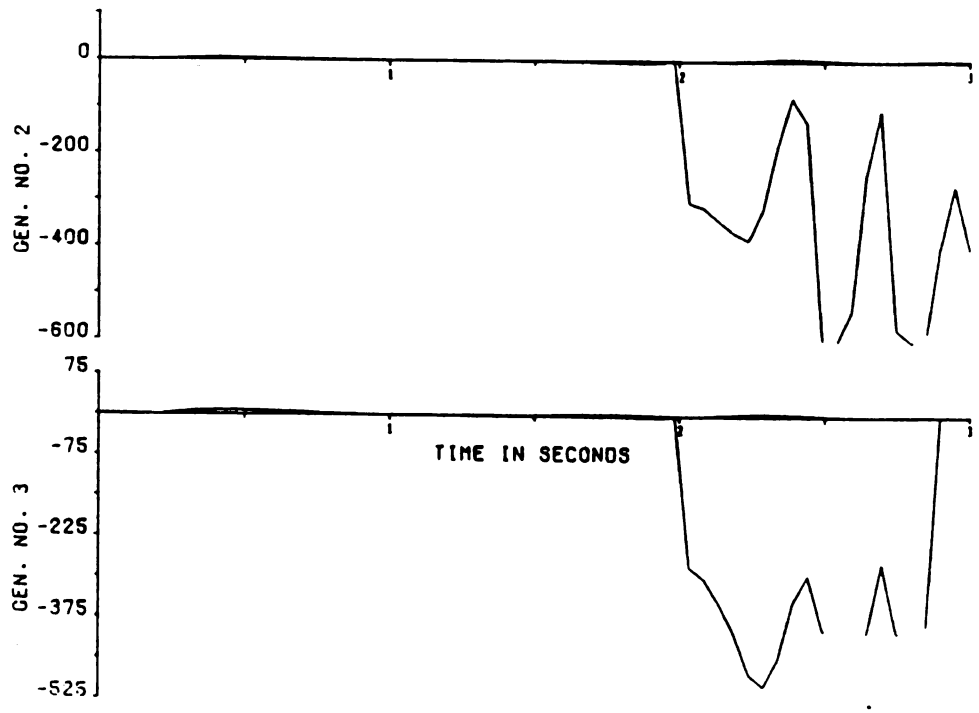

Fig. (22) Values of $V_1(t_f,t_c)$ for the single axis generator model and the constant current reactive load model for the fault on line 14-33.

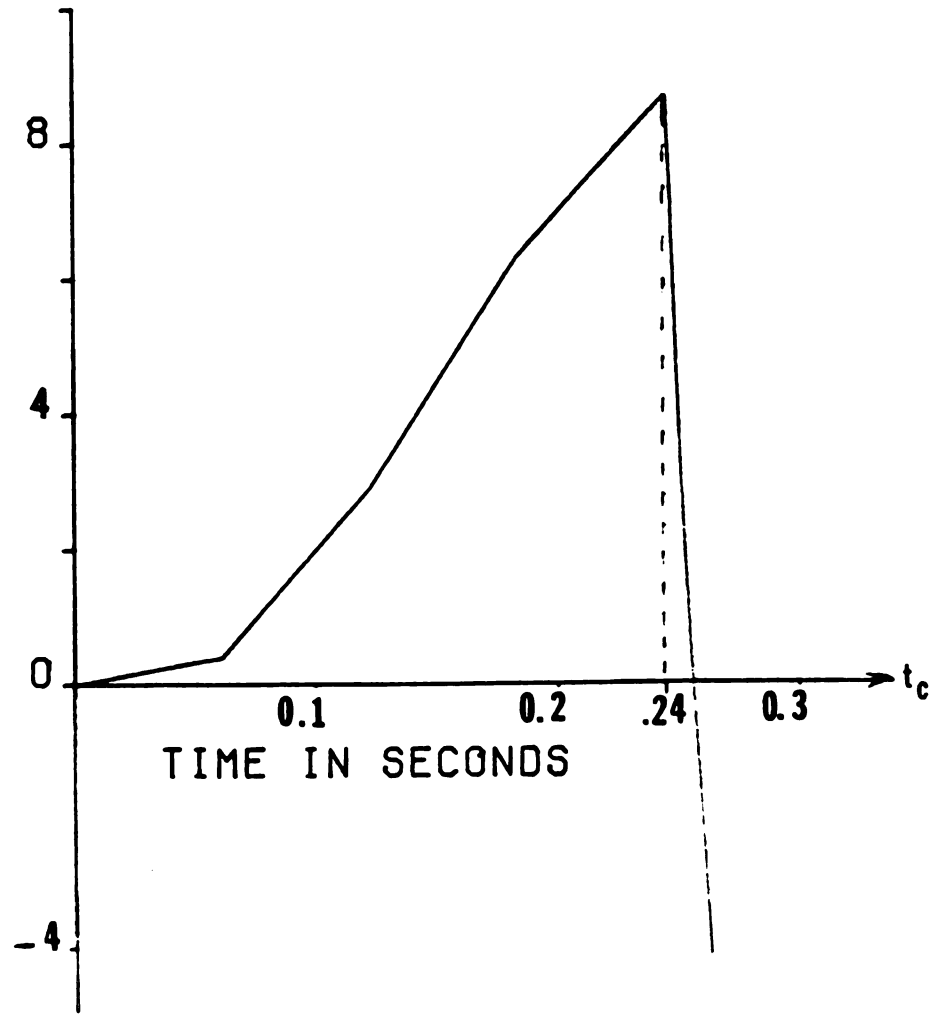

Fig. (23) Comparison of $\sigma_{ij} f(\sigma_{ij})$ for stable and unstable case where the fault occurs on line 26-27. The fault is cleared and line 26-27 is removed. (Constant current load model)

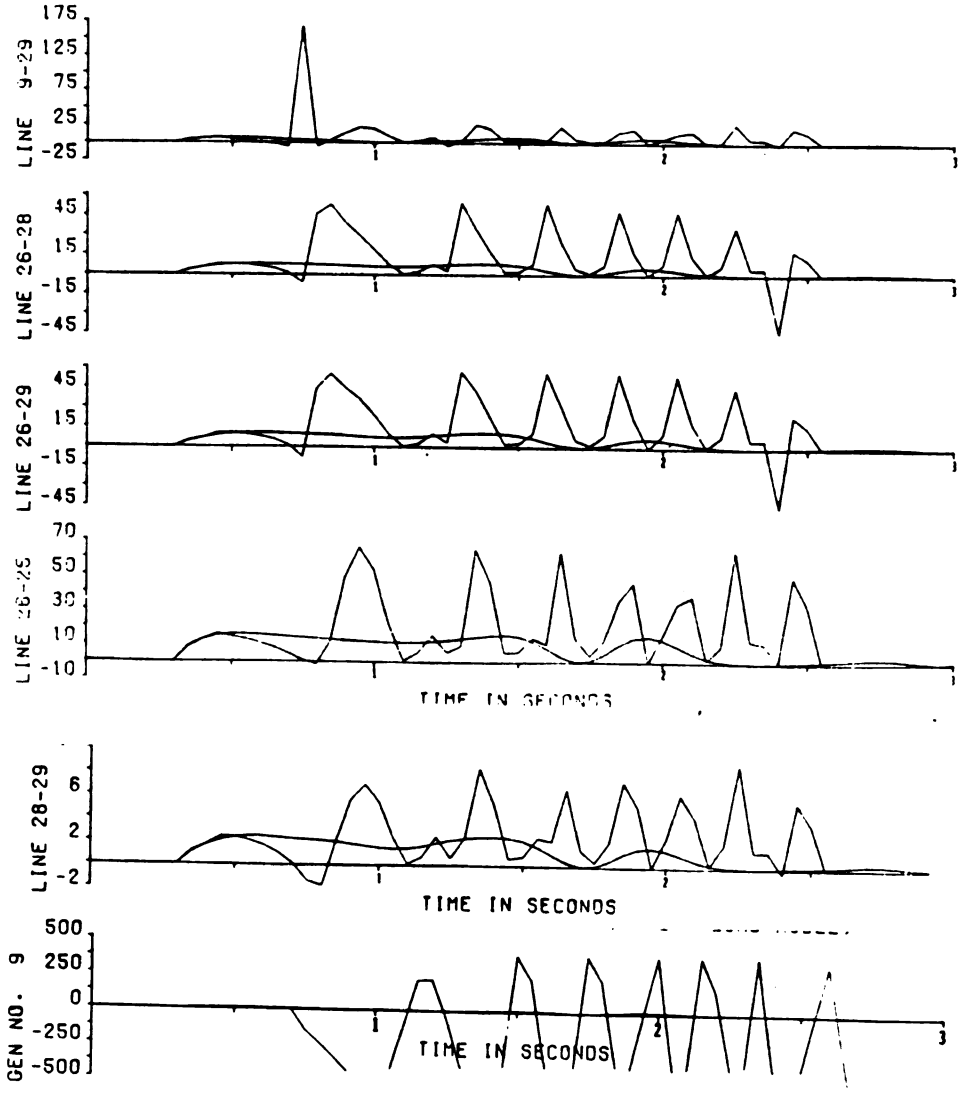

Fig. (24) Values of $V_1(t_f, t_c)$ for the constant voltage behind transient reactance generator model and the constant current reactive load model.

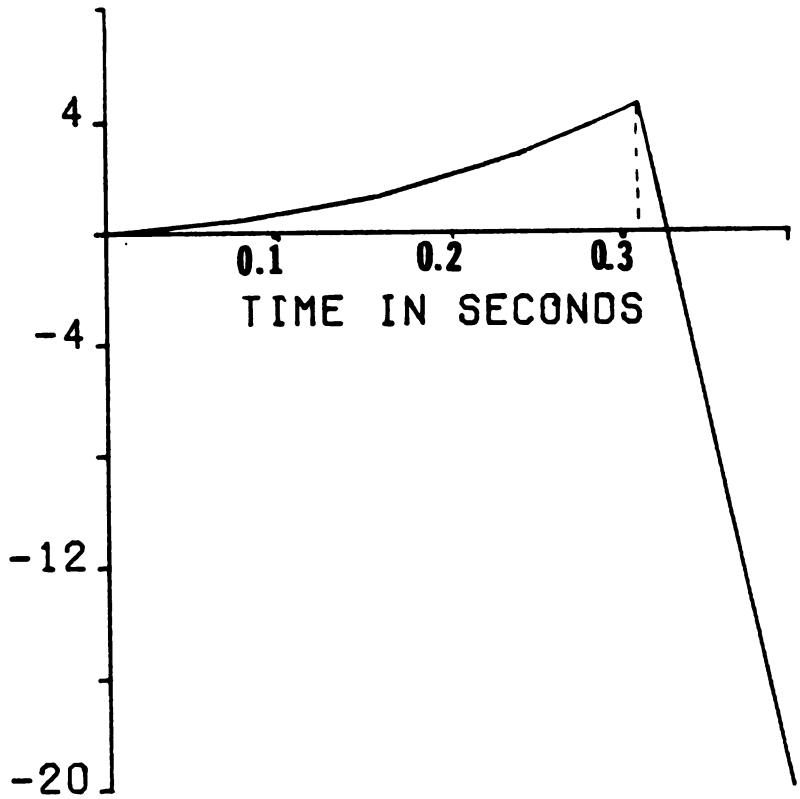

Fig. (25) Comparison of $\sigma_{ij} f(\sigma_{ij})$ for different lines on stable and unstable case when fault occurs on line 26-27. The fault is cleared and line 26-27 is removed. (Constant impedance load model)

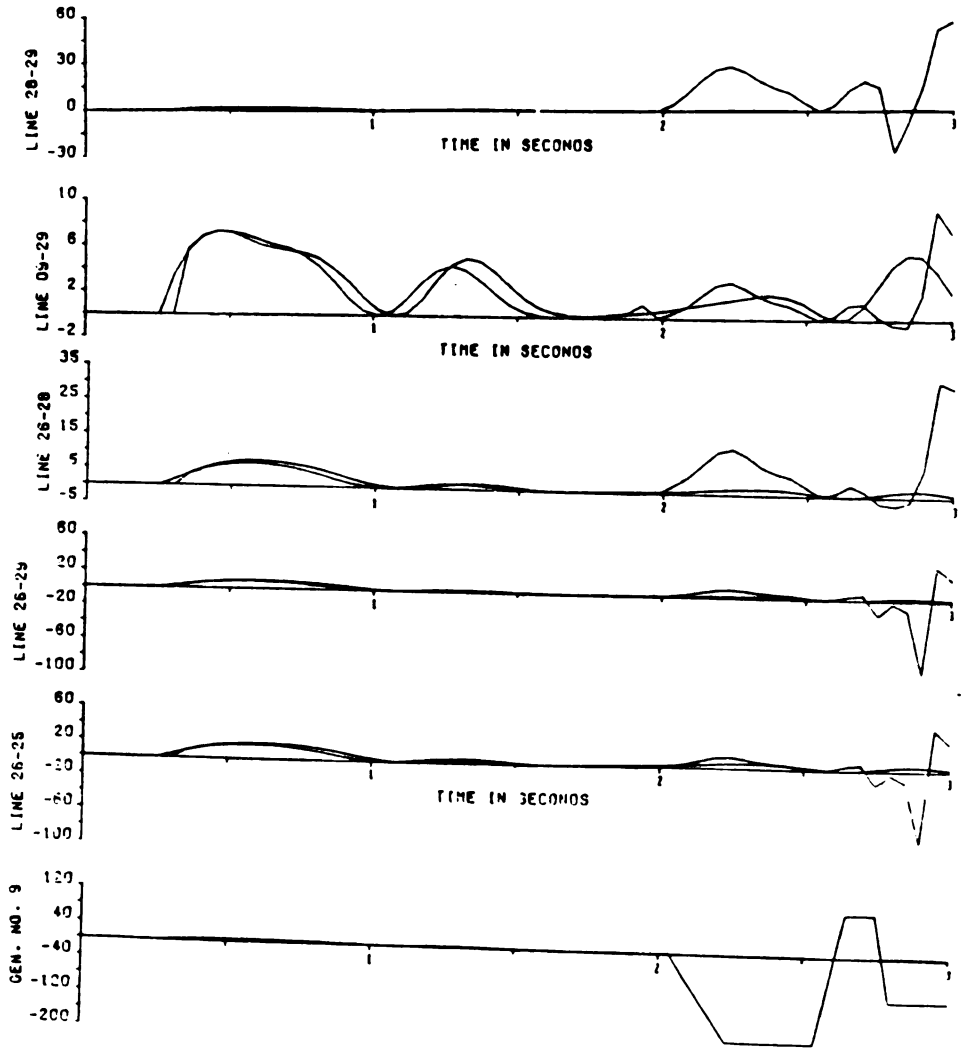

Fig. (26) Values of $V_1(t_f,t_c)$ for the constant voltage behind transient reactance and constant impedance load model.

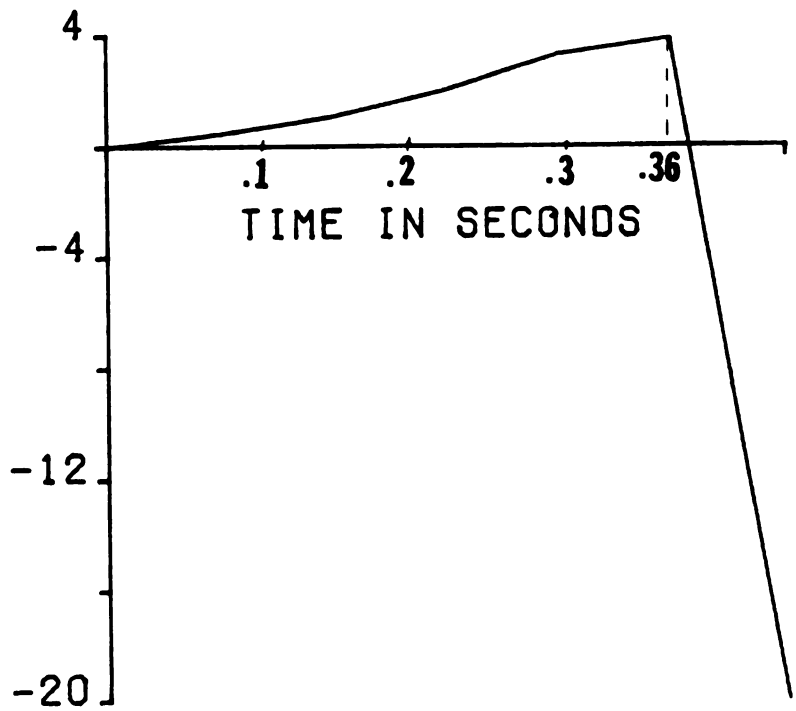

CHAPTER 7

OVERVIEW AND FUTURE RESEARCH

7.1 Overview

An overview of the research performed in this thesis and its contributions are now provided. A review of the literature on the development of Lyapunov functions and energy functions is given in Chapter 2, along with discussion of the equal area and PEBS methods for determining retention or loss of stability.

In Chapter 3, a topological energy function has been derived from the first principles that retain the network without aggregation back to generators internal buses and includes a description of real and reactive power load models as a function of voltage. This energy function has been tested on a 39 bus system and the results are presented at the end of Chapter 3. This is the first attempt at deriving a topological energy function using the energy integral method. This topological energy function also permits both a general real and reactive load model description for the first time.

In Chapter 4, a Lyapunov energy function is derived for a model that

1) retains the network and does not aggregate the network back to internal buses;

2) models the real power load as constant power and the reactive power load as constant current;

3) models the flux linkage decay in the synchronous machine as well as the electromechanical component of the machine model.

This Lyapunov function has been derived using the Popov criterion, the Moore-Anderson theorem [10] and the construction method of Willems [3]. The last section of Chapter 4 contains the computational test of this Lyapunov energy function. Although a topological Lyapunov has been derived previously, it did include flux decay effects in the generator model and completely ignores both the reactive load power energy, and the reactive energy produced by the generators. The Lyapunov energy function can be shown to be identical to the energy functions derived in Chapter 3 when the real load power model is constant power, the reactive load model is constant current and the generator model is the constant voltage behind transient reactance generator model.

In Chapter 5, a discussion of the region of stability based on the Popov stability criterion and a definition of loss of transient stability has been presented. Three different theorems stating necessary and sufficient conditions for the loss of transient stability have been established. The conditions stated in those theorems describe an estimate of the region of instability. Although a precise boundary between the region of stability and the region of instability is not established, a relationship

between the regions of stability and instability has been established. At the end of Chapter 5, a cutset integral criterion based on the theoretical description of the regions of stability and instability has been introduced and justified. The cutset energy function criterion [7] for the topological function and the PEBS method [21] for the individual machine energy function were also justified based on this theory.

A description of the region of stability and instability determined has a common boundary point which establishes for the first time the level of conservatism of the region of stability developed based on the Popov stability criterion. The necessary condition for instability provides a condition that must have occurred at some instance before a loss of stability occurs. These necessary and sufficient conditions provide testable conditions on the entire state of the system that can be clearly identified with the loss of synchronism inherent in the loss of transient stability.

Two stability criteria based on the Popov stability criterion and based on the cutset integral measure are tested in Chapter 6. The criterion that established the critical cutset and the critical clearing time based on a) the satisfaction of the Popov stability criterion for all $t \geq t_c$ or b) satisfaction of the necessary and sufficient condition for instability at some $t^* > t_c$ appears very accurate and reliable based on the four fault cases studied.

The stability criterion based on the cutset integral measure $V_1(t_c)$ is shown to be a very accurate method of determining the critical clearing time. Since the integrand will be positive and generally increase for time $t \in [t_o, t_f]$ as t_c increases for $t_c < t_{cc}$, and since the portion of the interval $[t_o, t_f]$ where the integrand is negative increases with t_c for $t_c > t_{cc}$, the value of clearing time t_c at which $V_1(t_c)$ is maximum clearly and accurately determines t_{cc}. The computational results on all four fault cases verify the accuracy and validity of this stability criterion. These results for the first time provide theoretical justification of stability criteria and establish why these criteria have no apparent error in determining retention or loss of transient stability.

7.2 Future Research

The Lyapunov energy function introduced in Chapter 4 has been derived for one axis generator model for the case that reactive loads are a first order function of voltage (constant current). An important extension would be the derivation of a Lyapunov energy function with a) a more complex generator model including both the exciter and power system stabilizer and b) a general real and reactive load model.

Another useful and important investigation would be to develop a precise boundary between the region of stability and the region of instability introduced in Chapter 5.

The sensitivity of the defined regions of instability or stability could be found for operating conditions such as:

1) Network configuration
2) Energy transfers
3) Generating dispatch
4) Unit commitment
5) Voltage profile and support
6) HVDC.

The sensitivity of the region of stability could be used to derive security constraints that assure sufficient stability margins for retention of stability for these various changes in operating conditions.

Another investigation could be the development of a fast computationally efficient program that determines whether the system trajectory remains within or crossed the boundary of the stability region. An initial task of such a fast program would be the identification of the critical cutset and the critical and stationary groups defined in Chapter 5. This fast computationally efficient method could be developed based on either a Taylor series or RMS measure methods introduced by other researchers.

LIST OF REFERENCES

1. Magnusson, P.C., "Transient energy method of calculating stability," AIEE Trans., Vol. 66, 1947, pp. 747-755.

2. Aylett, P.D., "The energy integral criterion of transient stability limits of power systems," Proceedings of IEE (London), July 1958, pp. 527-536.

3. Willems, J.L., "Optimum Lyapunov Function and stability regions for multi-machine power systems," Proceedings of IEE (London), Vol. 117, No. 3, March 1970, pp. 573-578.

4. Guduru, V., "A general Lyapunov function for multimachine power system with transfer conductances," Int. J. Control, Vol. 21, No. 2, 1975, pp. 333-343.

5. Kakimoto, N., Y. Ohsawa, and M. Hayashi, "Transient stability analysis of electric power system via Lure type Lyapunov function," Parts I and II, Trans. IEE of Japan, Vol. 98, No. 5/6, May/June 1978.

6. Kakimoto, N., Y. Ohsawa, and M. Hayashi, "Transient stability analysis of multimachine power systems with field flux decays via Lyapunov's direct method," IEEE trans. on power apparatus and systems, Vol. PAS-99, No. 5, September/October 1980.

7. Hill, D.J. and A.R. Bergen, "Stability analysis of multimachine power networks with linear frequency dependent loads," IEEE trans. on circuits and systems, Vol. CAS-29, No. 12, December 1982.

8. Athay, Thomas M., and David J. Sun, "An Improved Energy Function for Transient Stability Analysis," IEE International Symp. on Circuits and Systems, 1981.

9. Musavi, M.T. and N. Narasimlanurthis, "A general energy function for transient stability analysis of power systems," IEEE trans. on CAS, No. 7, July 1984.

10. Moore, J.B. and B.D.O. Anderson, 1968, J. Franklin Int. 488-492.

11. Willems, J.L., "Improved Lyapunov function for transient power system stability," Proceedings of IEE, Vol. 115, No. 9, September 1968.

12. Desoer, C.A. and M.Y. Wu, "Stability of a nonlinear time-imminent feedback system under almost constant input," Automatica, Vol. 5, pp. 231-233, 1969.

13. Pai, M.A. and P.G. Murty, "New Lyapunov functions for power systems based on minimal realization, Int. J. Control 1974, Vol. 19, No. 2, pp. 401-415.

14. Anderson, B.D.O., "A system theory criterion for positive real matrices," SIAM J. Control. Vol. 5, No. 2, pp. 171-182, 1967.

15. Kakimoto, N., Y. Ohsawa, and M. Hayashi, "Transient stability analysis of large-scale power system by Lyapunov direct method," IEEE transaction on power apparatus and systems, July 1983.

16. Sastry, H.S.Y., "Application of topological energy functions for the direct stability evaluation of power systems, a Ph.D. thesis submitted to the Department of Electrical Engineering, University of California at Berkley, March 1984.

17. Rastgoufard, P., "Local energy function methods for power system transient stability," a Ph.D. thesis submitted to the Department of EE/SS, Michigan State University, December 1982.

18. Michel, Fouad, Vitall, "Power system transient stability using individual machine energy function," IEEE trans. on circuits and systems, Vol. 5, May 1983.

19. Vitall, Michel, "Stability and security assessment of a class systems caverned by Lagerange's with application multi-cavern system," IEEE trans. on CAS, November 1983.

20. Michel, Miller, "Qualitative Analysis of Large Scale Dynamical System," Academy Press, 1977.

21. Yazdankhah, A.S., "Power systems security assessment for faults using direct methods," a Ph.D. thesis submitted to the Department of EE/SS, Michigan State University, July 1984.

22. Chandroshekar, K.S., D.J. Hill, "Dynamic security dispatch: basic formulation," IEEE trans. on PAS, July 1983.

GENERAL REFERENCES

23. Kimbark, E.W., "Power System Stability," John Wiley and Sons, 1948.

24. Crary, S.B., "Power System Stability," John Wiley and Sons, 1945.

25. Anderson, P.M. and A.A. Fouad, "Power System Control and Stability," Iowa State University Press, Ames, Iowa, 1977.